Research Report

Mineral Resources and Petrol Engineering, Montanuniversität Leoben (MUL)
Civil and Environmental Engineering, Massachusetts Institute of Technology (MIT)

Numerical Methods for Tunneling using ABAQUS and Investigation of Long-Time-Effects of the Shotcrete Shell and its Impact on the Combined Support System

This Research Report is PART of a preliminary stage of my Master Thesis

The Master Thesis will be submitted at the

Chair of Subsurface Engineering
Montanuniversität Leoben/Österreich

Author:

Heiko Mödlhammer

Supervisor:

Robert Galler, MUL
Herbert H. Einstein, MIT

Cambridge, October 2010

Abstract

Since the finite element method is used for tunneling, a significant number of techniques and specific programs for the simulation of tunnel drifts have been developed. First, different methods to simulate a tunnel drift and the installation of a dual lining system (primary shotcrete shell / secondary cast-in-place concrete inner liner) using the general-purpose finite element program ABAQUS are discussed. The second aim of this study is to understand the influence of long-time deterioration processes around existing tunnels and its impact on the stability conditions of the combined support system (surrounding ground, shotcrete shell and inner liner). Based on a parameter study, different deterioration processes are simulated, coupled with elastic as well as elastic-plastic material behavior, under consideration of the tunnel drift, the interaction between the shotcrete shell and the ground, and the interaction between the shotcrete shell and the inner liner. The results interpret the main characteristics of the analyzed deterioration processes on the basis of the obtained stress distributions and displacements of the support elements.

Table of Contents

List of Figures

List of Tables

I. Introduction

Due to the increasing age of road and railway tunnels, maintenance and conservation practice become more important. Nowadays, the first tunnels with a dual lining system including shotcrete as primary liner are around 30 to 40 years old. As a result that the long-time behavior of shotcrete, considering deterioration processes, is not clearly known, assumptions are made from zero to a total deterioration of the shotcrete shell. To become clear about these processes, it is necessary to understand the characteristics and mechanisms of deterioration of shotcrete and to identify their causes and effects. Thus, this study categorized the deterioration into physical, chemical and other processes:

1. Physical processes are time-dependent changes of conditions and tectonic effects. Both, support elements and ground are affected. More often than not, the influence of ground water causes these processes and induces more stresses in the support elements.
2. Chemical processes change the chemical composition of support elements and ground with time. Aggressive ground water is usually the reason for these processes. Due to the fact, that the most tunnels with a dual lining system have a waterproofing membrane between shotcrete shell and inner liner, only the shotcrete shell is affected by these processes. The consequence of chemical processes is mostly a change of the stability conditions of the tunnel.
3. Other processes like ice- and frost-action and rare events such as fire and car-collisions may also change the equilibrium of a tunnel with time and should be considered.

Based on this classification, a tunnel constructed with a dual lining system is used for a numerical parameter study to analyze the long-time deterioration processes of the shotcrete shell and its impact on the on the combined support system – ground plus shotcrete shell plus inner liner. The results are discussed in terms of stresses and displacements of the support elements which evolve during deterioration.

II. Problem Statement

From today's perspective the dimensioning of the inner lining has to take into account that the shotcrete shell cannot permanently carry any loads. It is seen as a temporary support which loses its significance after the construction of the inner liner. (RVS 9.32, 2004)

There are two reasons for the deterioration of the shotcrete. On the one hand, there can be an increase of the ground pressure. This can occur by a sintering process in the tunnel drainage system which causes an increase of the water pressure and induces more stresses in the support elements. Pacher (1964) suggested that the load on the tunnel-crown may be estimated by simply considering the weight of the plastic zone. As a result of weathering processes, the plastic zone around the tunnel may grow and so does the load that the tunnel support has to bear.

On the other hand, deterioration of the shotcrete may occur through an attack of aggressive ground water (e.g. sulphates corrosion, calcium leaching, and more).

State of the art is that a back-calculation of the measured deflections of the shotcrete shell is used to determine the forces in the shotcrete shell. This is done by numerical or analytical methods. These forces from the shotcrete shell are considered as design loads for the inner liner.

The main aim of this thesis is to figure out a model, which considers the shotcrete shell and the inner liner in the dimensioning of the tunnel. The first step of the numerical calculation includes the excavation followed by the implementation of the shotcrete shell. After the shotcrete shell is loaded, the inner liner is installed. As next step, the deterioration of the shotcrete shell is simulated stepwise.

1 DETERIORATION OF TUNNELS

Structural and mechanical characteristics during the life-time of a tunnel change. There are many kinds of degradation processes, which may affect tunnels and reduce its safety and serviceability. Due to the increasing age of the tunnels in Europe an investigation of time effects becomes more important. Points which have to be considered are:

- Observation of the tunnel during construction and its life-time. This includes information such as material properties of support elements (initial support and final support) and ground, measurements of deformation, geology and ground water conditions.
- Investigation of the long-term degradation processes. This includes understanding their causes and their effects on the support elements and ground.

This thesis investigates degradation processes, which may affect the support elements. For a better overview these processes are divided into three categories:

- Physical processes
- Chemical processes
- Other processes

Physical processes

The properties of support elements and ground are affected by several aging processes. Sandrone & Labiouse (2009) recommended to calculate these effects by a stiffness reduction or a strain increase. Physical processes are time-dependent change of conditions and tectonic effects.

For example, time-dependent change of conditions can be caused by changes of the water-pressure and water-flow around the tunnel as well as over-consolidation. Change of conditions may lead to swelling or creeping of the ground. Subsequently, it is investigated in physical processes in detail:

Zachow (1995) argued that an increase of the water-pressure may be the result of sintering of the tunnel drainage system and causes higher stresses on the support elements.

For deep tunnels Pacher (1964) suggested the load on the tunnel crown by considering the weight of the plastic zone. According to the German guideline DS 853 (2007) water ingress may lead to a deterioration of ground around the opening by the fact that a tunnel which is built in an aquifer can act like a drainage system. As a result the ground is evaded and the plastic zone around the tunnel grows. Accordingly, the entire support elements receive additional load.

Marcher & Jiricny (2004) state that over-consolidation of highly cohesive soils may influence the load on tunnel support. As a result of the tunnel excavation in highly cohesive soils, negative pore water pressure may initially build up and loads the support to a small extent. Through reduction of the negative pore water pressure over time, the tunnel support elements are loaded. Also, considering the geological conditions, impacts from tectonic movements and viscoplastic deformations which lead to creep-displacements have to be taken into account. (Marcher & Jiricny, 2004)

The main physical processes can be summarized:

- Support elements:
  - Ageing
- Ground:
  - Change of water-pressure
  - Water-flow around the opening
  - Over-consolidation of highly cohesive soil
  - Swelling
  - Creeping
  - Tectonic movements

Chemical processes

Support elements as well as the surrounding ground are affected by chemical processes. More often than not aggressive water causes chemical reactions of the surrounding ground or of the support elements. The chemical composition of ground and support elements changes with time and in most instances leads to a change of the stability conditions. Sandrone & Labiouse (2009) recommended to simulate these effects by a reduction of the material's strength and by a reduction of the mechanical properties. Also a thickness reduction of the inner liner (final support) which may be caused by deterioration due to de-icing salt corrosion is discussed.

The main attention is paid to the exposed surfaces of the support elements. These surfaces may be affected first by aggressive groundwater (e.g. sulphates corrosion, calcium leaching, and so on). However, one has to distinguish between a tunnel system with and without sealing. When a waterproofing membrane is placed between the shotcrete shell (part of initial support) and the inner liner, only the initial support (shotcrete shell, rock bolts and anchors) and the inner liner intrados can be affected by chemical deterioration processes. Sandrone & Labiouse (2009) state that in case of a sealing, the deterioration of the shotcrete occurs much faster. This he based on the fact that between the shotcrete shell intrados and the sealing, the aggressive groundwater is concentrated.

One assumption for the long-term failure behavior of the support elements is based on the fact that the structural steel elements (rock bolts, anchors, wire mesh and steel ribs) are not perfectly protected against corrosion. A concrete cover is feasible during construction, but subsequent deformations of the ground may cause cracks in the shotcrete/concrete cover and as a result the protection effect is abolished. (Marcher & Jiricny, 2004)

The main chemical processes can be summarized:

- Support element:
  - Aggressive groundwater
  - De-icing salt corrosion affects inner liner intrados
  - Steel corrosion
- Ground:
  - Weathering

Other processes

Ice- and frost-action and rare events such as fire and car-collisions may also change the equilibrium of a tunnel with time and should be considered.

Research approach

Since a detailed description of all aspects (deterioration of support elements and ground caused by physical-, chemical- and other processes) would go beyond the size of this thesis, only the deterioration of the shotcrete shell caused by physical- and chemical processes is investigated.

Hence, to simulate the physical deterioration processes, a degradation of the Young's modulus is used and to simulate the chemical deterioration processes the compressive strength is reduced. For detailed values of the reduction of the Young's Modulus and the compressive strength see chapter 2.7.

2 NUMERICAL MODEL

The dimensioning of the numerical model is divided into three parts:

- Chapter 2.1 to 2.4: general
- Chapter 2.5 to 2.6: tunnel construction
- Chapter 2.7: deterioration of the shotcrete shell

The first part, general, deals with the model and model-parts, which include the mesh, the boundary conditions, material properties and material behavior. Contact formulations as well as sources of nonlinearity of the finite element (FE) method are also treaded.

The second part, tunnel construction, deals with the excavation progress and the installation of the shotcrete shell and inner liner. Several procedures for the 2D numerical simulation of tunnel excavation as well as several methods for the installation of support elements (shotcrete shell and inner liner) are discussed.

The third part, deterioration of the shotcrete shell, deals with the degradation of the material properties to simulate a deterioration of the shotcrete. The aim of this part is to determine the interaction between the shotcrete shell and inner liner during the deterioration progress.

2.1 Investigation of the FE model

The tunnel is assumed to have a circular shape with a diameter of 10 m and to be constructed at a depth of 250 m below the ground surface. The stress field around the tunnel is applied with uniform vertical and horizontal stresses.

Considering the symmetric conditions of the tunnel, a quarter portion of the tunnel is used for the numerical analysis. The thickness of the shotcrete shell is 20 cm and the thickness of the inner liner is 30 cm. The excavation method is simplified to a full-face excavation. The size of the FE mesh is chosen in such a way, that the boundary effects are minimized. This is the case when the horizontal mesh length is 4 to 5 times the tunnel diameter (Meißner, 1996). To simulate a quarter of the tunnel with a diameter of 10 m, an absolute mesh size of 55 m x 55 m is chosen (Fig. 1). The calculations are done using the ABAQUS 6.7-1 FE program (Hibbitt et al., 2007).

To consider the time dependent behavior of the shotcrete (creeping and hardening), two different Young's moduli are used. According to the guideline (RVS 9.32, 2004), for a short time after application of the so called "young" shotcrete, a Young's modulus of E_{S1} = 10,000 MN/m² is used, and to represent a "hardened" shotcrete, a Young's modulus of E_{S2} = 15,000 MN/m² is applied.

2.1.1 Boundary conditions

The model is bounded on the right vertical and the bottom side with roller supports. These axes are also planes of symmetry. The vertical earth pressure is applied on the top side and the horizontal earth pressure is applied on the left vertical side (Fig. 1).

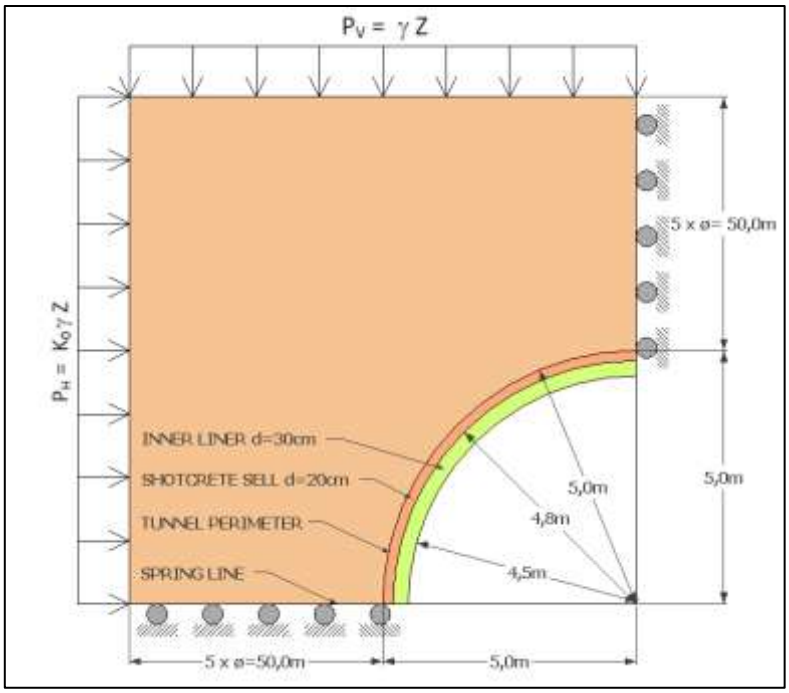

Fig. 1: Schematic representation of model size, boundary conditions, system load and model parts

2.1.2 Elements, nodes and mesh

The ground, the shotcrete shell and the inner liner are usually modeled with 4-node bilinear plane strain continuum elements (CPE4) (Fig. 2). For the parametric studies also 8-node biquadratic plane strain continuum elements with reduced integration (CPE8R) are used.

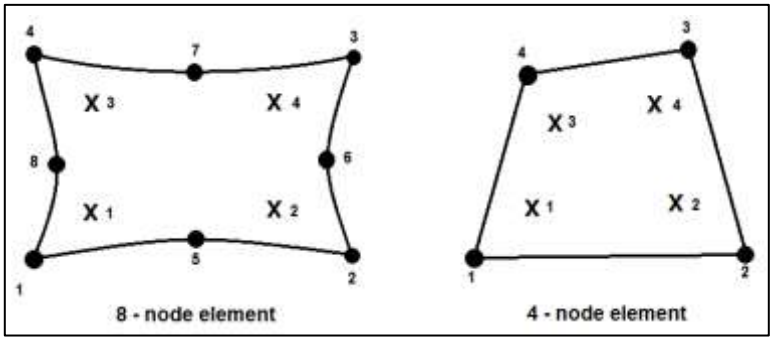

Fig. 2: Numbering of integration and node points for output; CPE8R (left) and CPE4 (right); Source: Hibbitt, Karlson, & Sorenson, 2007

4-node bilinear plane strain continuum elements:

Fig. 3 & Fig. 4 show the structured mesh, which was chosen according to Einstein et al. (1995). To model the ground, 624 elements are used. The shotcrete shell is modeled using 48 elements and the inner liner is modeled with 72 elements. The contact interface between the ground and the shotcrete shell, as well as between the shotcrete shell and inner liner are modeled using the same number of nodes (25).

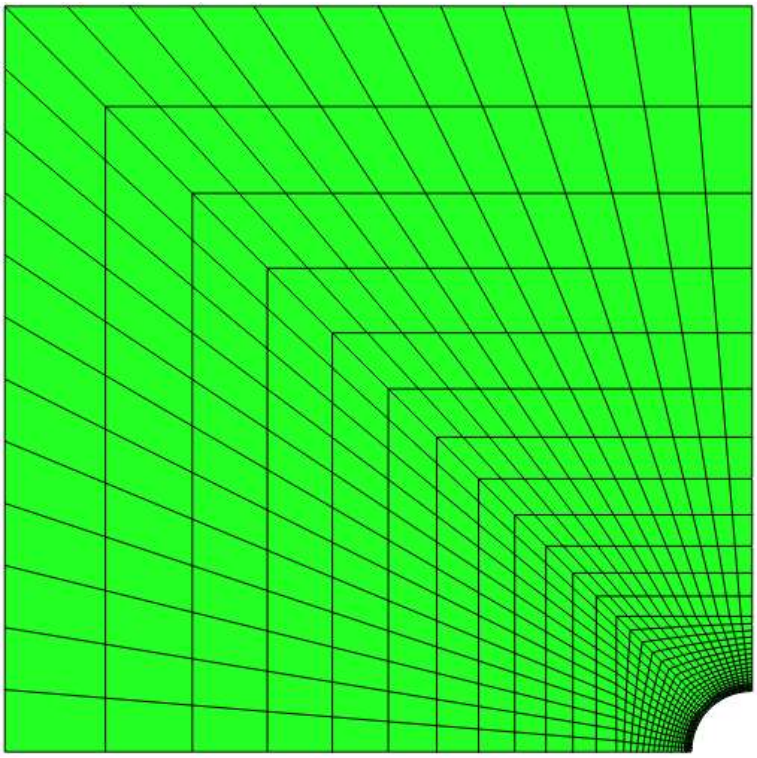

Fig. 3: FE mesh CPE4

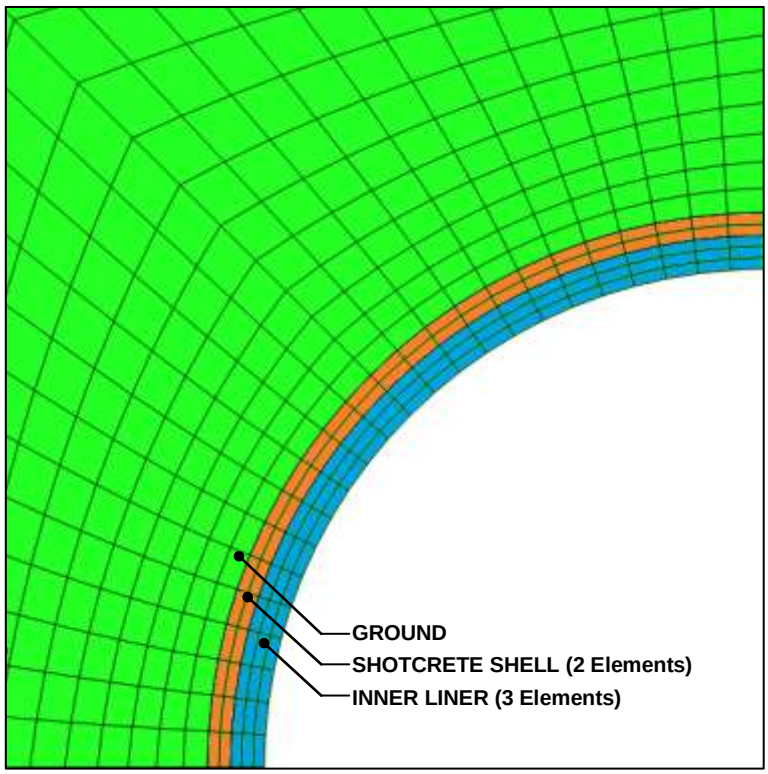

Fig. 4: mesh CPE4 – detail tunnel

8-node biquadratic plane strain continuum elements with reduces integration:

Based on a convergence study CPE8R elements are chosen. The convergence study investigates the use of 8-node biquadratic plane strain elements with and without reduced integration, using a mesh which can be created with so called FREE, STRUCTURED and SWEEP techniques. The best results were obtained with the FREE technique and the CPE8R elements. The element number around the tunnel is double that of the CPE4 elements. Accordingly, to model the ground, 1738 elements are used. The shotcrete shell is modeled using 96 elements and the inner liner is modeled with 144 elements. The contact interface between ground and shotcrete shell, as well as between shotcrete shell and inner liner are modeled using the same number of nodes (97). (Fig. 5 & Fig. 6)

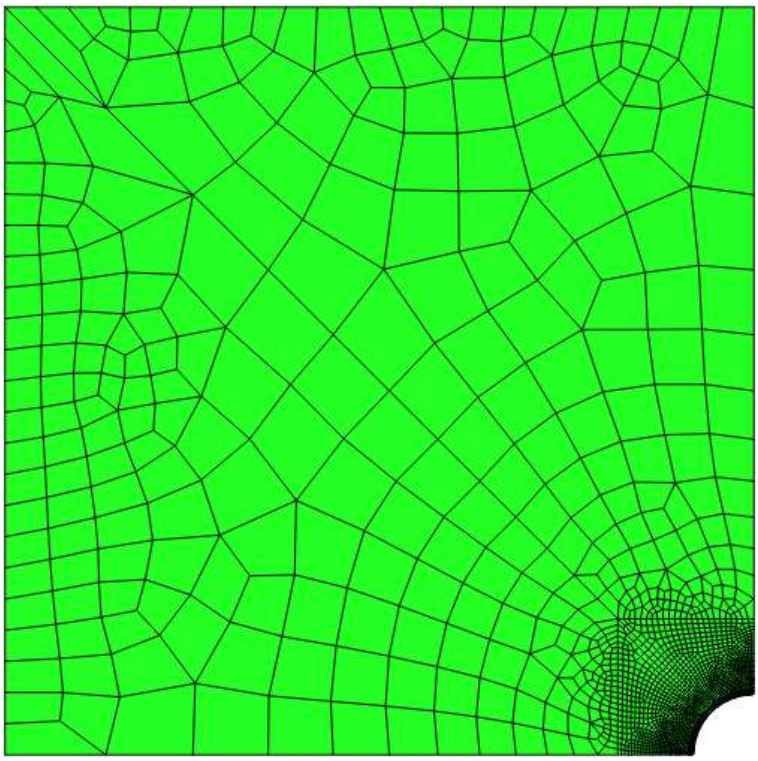

Fig. 5: FE mesh CPE8R

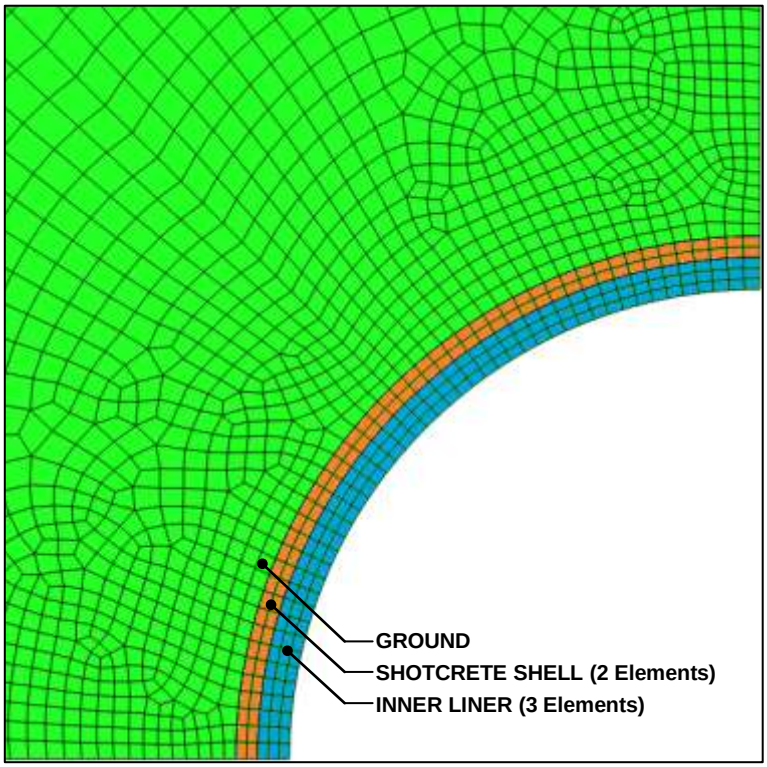

Fig. 6: mesh CPE8R – detail tunnel

2.2 Parameters for the numerical analysis

The model consists of different materials:

1. ground
2. “young” shotcrete (for: shotcrete shell)
3. “hardened” shotcrete (for: shotcrete shell)
4. concrete (for: inner liner)

The ground is assumed to be marl and is idealized homogenous and isotropic. The unit weight is assumed as γ = 27 kN/m³. The overburden above the crown of the tunnel is 250 m. Poisson’s ratios of ν = 0.5 and ν = 0.4 for the ground are assumed.

In the first part of this paper, the material behavior of the ground is assumed to be governed by a linear elastic relationship. Later on a linearly elastic – perfectly plastic relation based on the Coulomb criterion is investigated. The basic principle of this behavior is to separate the strains and stresses into an elastic and plastic part:

$$\varepsilon = \varepsilon^{e} + \varepsilon^{pl} \tag{2.1}$$

2.2.1 Investigation of dilatation of ground (soil and rock)

Dilatation is defined as volume-increase due to loosening of the ground.

The plastic strain increments are assumed to be normal to the yield surface, i.e. using the associated flow rule. However, for soil to use an associated flow rule with a Coulomb yield function leads to an overestimating of dilatation. Fig. 7 shows a non-associated flow rule with the Coulomb criterion.

Fig. 8 illustrates that the dilatation behavior only occurs in the plastic state. In short, the volume increase only occurs in the plastic state and concerns only the plastic strain ε^{pl}.

The friction-angle (φ) is defined by the angle of internal-friction (φ_i) and by the dilatation-angle (ψ):

$$\varphi = \varphi_i + \psi \tag{2.2}$$

Generally it can be assumed that cohesive soils, except very highly over-consolidated soils, have no dilatation behavior (ψ = 0).

The dilatation angle of non-cohesive soils is dependent on the friction angle as well as on the density of soil. It is possible to estimate the dilatation angle by subtracting a constant factor from the friction angle (Bolton, 1986; Brinkgreve & Veermeer, 2002):

$$\psi \cong \varphi - 30° \tag{2.3}$$

For friction-angles less than 30° the dilatation-angle is assumed to be zero.

For rock, the dilatation is defined as volume increase due to riding over asperities (Fig. 8). F_N, F_S, l and d are the normal-force, the shear-force, the shear-displacement and the dilatation. For the dilatation-angle of rock the notation (i) is used. (Brosch, 1990)

To limit the number of input variables for the parametric studies a dilatation-angle of $\psi = 0°$ is used.

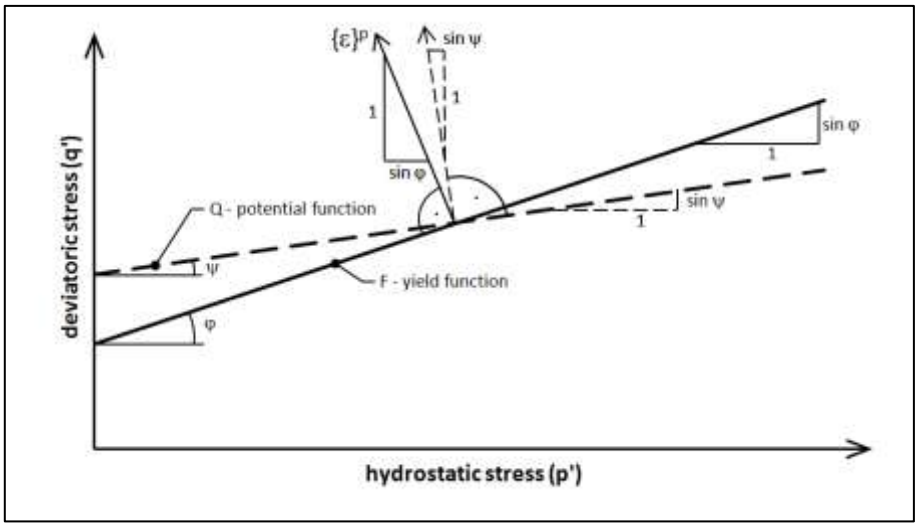

Fig. 7: Basic principle of a non-associated flow rule

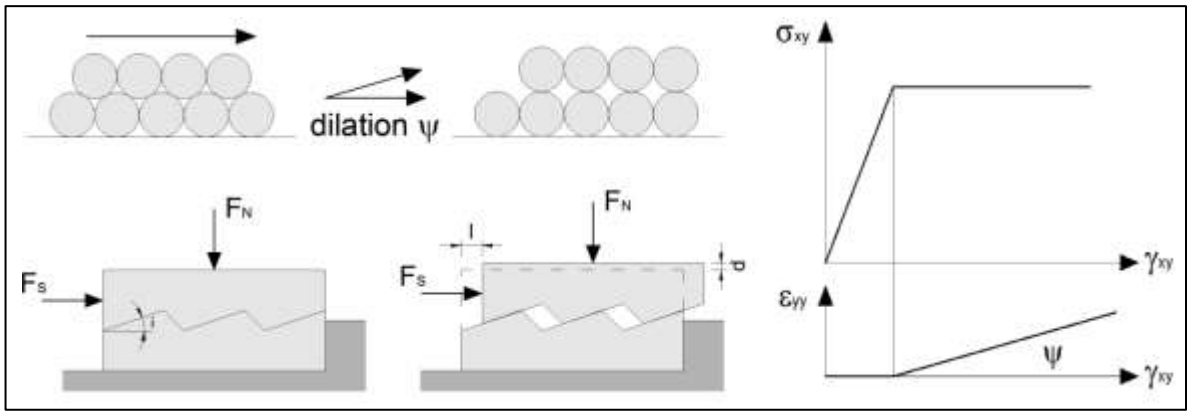

Fig. 8: Dilatation behavior of soil and rock

2.2.2 Material properties

Table 1 shows the main physical mechanical parameters, where E, ν, c, φ and ψ are the Young's modulus, the Poisson's ratio, the cohesion, the friction-angle and the dilatation-angle.

The material behavior of the ground is, as mentioned above, first assumed to be governed by a linear elastic relationship and in a second investigation by a linearly elastic – perfectly plastic relationship using the Coulomb constitutive law.

The material behavior of the shotcrete shell and inner liner are assumed to be governed by a linear elastic relationship. Furthermore for the shotcrete a yield stress of 20 MN/m² is assumed. All support elements (shotcrete shell and inner liner) are also assumed to be homogenous and isotropic. The shotcrete shell has a uniform thickness of 20 cm and the quality is assumed to be a SpC 25/30-J2 (MPa). The inner liner has a uniform thickness of 30 cm and the quality is assumed to be a C 25/30 (MPa).

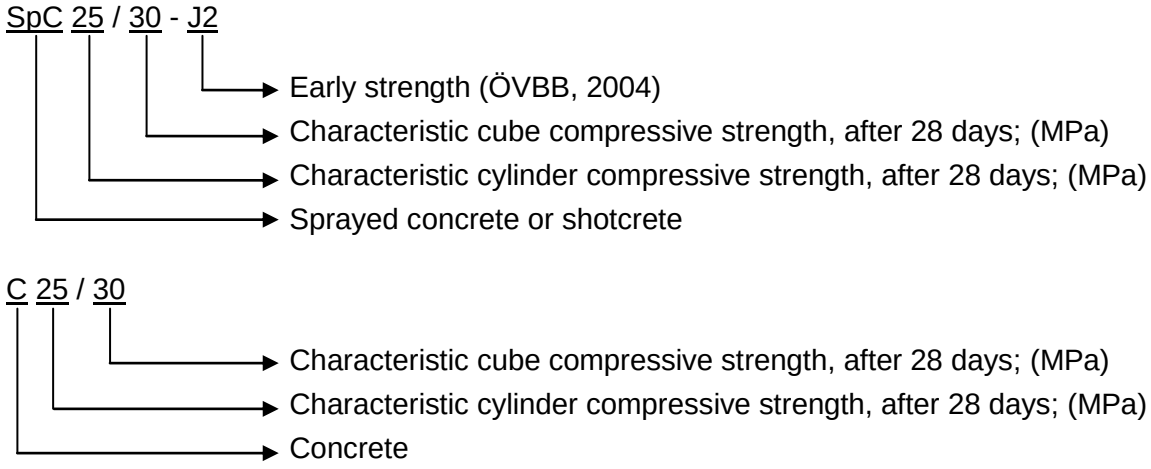

Table 1: Physical mechanical properties of ground, shotcrete shell and inner liner

Material	Material Detail	E (MN/m²)	ν (-)	c (MN/m²)	φ (deg)	ψ (deg)
GROUND	MARL	500	0.4 + 0.5	3.0	35	0
SHOTCRETE SHELL (YOUNG)	SpC 25/30-J2	10,000	0.2			
SHOTCRETE SHELL (HARDENED)		15,000	0.2			
INNER LINER	C25/30	30,500	0.2			

2.3 Contact formulation

For the numerical calculation, contact conditions have to be defined between all elements. An overview of possible contact conditions for the numerical model is provided below:

- ground and shotcrete shell (2.3.1)
- shotcrete shell and inner liner (2.3.2)

2.3.1 Contact formulation between ground and shotcrete shell

Tangential behavior:

- The Coulomb friction law is assumed with a friction coefficient of $\mu = 100$ ($\varphi = 89.43°$) and no cohesion. This value ($\mu = 100$) is recommended in the

ABAQUS User's Manual (Hibbitt, Karlson, & Sorenson, 2007) to simulate a contact with no slip. (Fig. 9 left)

- To achieve better conversion behavior an elastic slip of $\gamma_{elast.}$ = 1 mm is defined. In other words, the maximum transferable shear stress ($\tau_{crit.}$) is reached after a displacement of 1 mm. (Fig. 9 right)

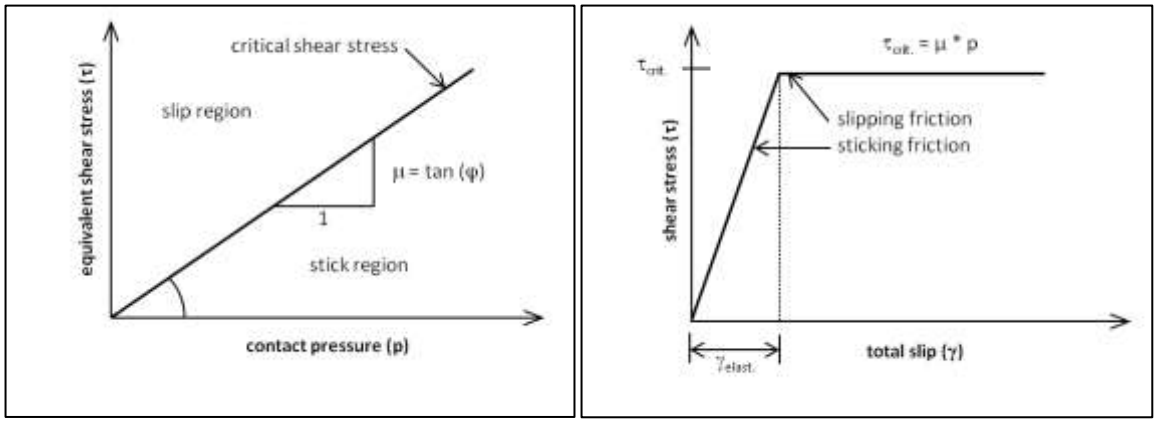

Fig. 9: Coulomb friction law (left) and elastic slip behavior (right)

Normal behavior:

- Separation of the two surfaces is prevented once contact has been established. In other words, a transfer of tensile stresses is possible.
- To ensure numerical convergence a so called "hard contact" is implemented. After the clearance between the two surfaces is closed a transfer of normal stresses (contact pressure or tensile stress) is possible. (Fig. 10)

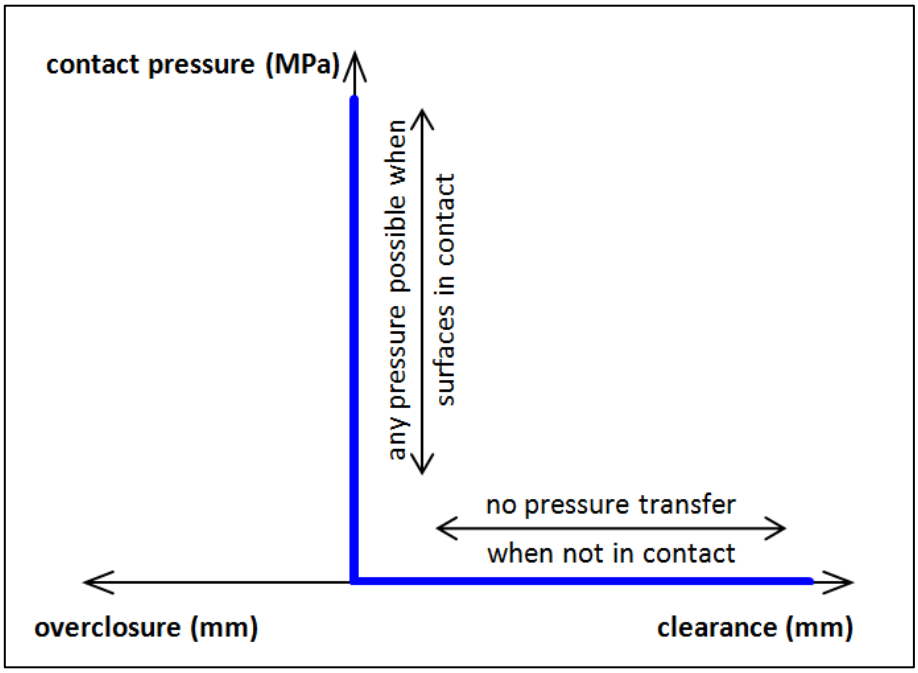

Fig. 10: Contact normal behavior: "hard contact"; tensile stresses are not considered; adapted from Hibbitt, Karlson, & Sorenson, (2007)

2.3.2 Contact formulation between shotcrete shell and inner liner

Tangential behavior:

- The Coulomb friction law is assumed with a friction coefficient of $\mu = 1$ and no cohesion. Hence, the possibility for slippage is provided. (Fig. 9 left)
- To achieve better conversion behavior an elastic slip of $\gamma_{elast.} = 1$ mm is defined. In other words, the maximum transferable shear stress ($\tau_{crit.}$) is reached after a displacement of 1 mm. (Fig. 9 right)

Normal behavior:

- Separation of the two surfaces is allowed once contact has been established. In other words, there is no possibility for a transfer of tensile stresses.
- To ensure numerical convergence a so called “hard contact” is implemented. After the clearance between the two surfaces is closed a transfer of normal stresses (contact pressure) is possible. (Fig. 10)

2.3.3 Removing and reactivation of elements and contact pairs

Removing of elements and contact pairs is a useful technique for uncoupling several parts (ground, shotcrete shell and inner liner) of a model until they should be brought together. This option is recommended in the ABAQUS User’s Manual (Hibbitt, Karlson, & Sorenson, 2007) when complicated processes with deformation are simulated:

After excavation, the tunnel perimeter moves inward until the shotcrete shell is installed and before the inner liner is installed, the ground and the shotcrete shell moves inward. To simulate the installation of the support elements (shotcrete shell and inner liner), the corresponding elements are removed in the first step of the calculation and reactivated later on. Hence, the contact pairs are also removed until the support elements get installed. (See Fig. 25 to Fig. 27)

This procedure is used for the two contact pairs:

- Ground – shotcrete shell
- Shotcrete shell – inner liner

Another advantage is that significant computational time can be saved by eliminating unnecessary calculations of a non-existing contact.

2.4 Sources of nonlinearities

There are three different kinds of nonlinearities occurring with finite elements simulations:

- Geometric nonlinearities

- Nonlinear material behavior
- Contact and friction

Geometric nonlinearities are introduced by displacements. Displacements and strains may not linear. The new equilibrium of the system is formulated on the deformed structure. In this study, the nonlinearity results from the excavation of the tunnel.

Nonlinear material behavior can occur for nonlinear elastic material, like rubber or plastic, for nonlinear plasticity or viscoplasticity in concrete or bitumen, for phase transformations or thermo-mechanic simulations.
However, this thesis deals mostly with linear elastic material behavior. Hence, nonlinearity of material behavior is not considered.

Contact and friction mostly occur together. Friction changes with contact pressure.
In this study contact and friction problems exist at the interfaces between the ground and shotcrete shell as well as between shotcrete shell and the inner liner.

The basic idea for the solution of nonlinear relationships of the displacement based FE-method is given by the incremental- iterative concept. Thereby the load is applied step-by-step (incrementally), and the tangent stiffness matrix is calculated from displacements and stresses of the last increment. (Bathe, 1996)

In ABAQUS the increments are defined by a “time period of one step”, an “initial time increment”, a “minimum time increment” and a “maximum time increment”. Assuming linearity, 1 step can be calculates using 1 increment (“time period of one step” = “initial time increment”). In case of nonlinearities, a smaller “initial time increment” should be chosen (“time period of one step” > “initial time increment”). If the chosen increment size is too large, the time increment is reduced to within the previously selected range (“minimum/maximum time increment”).

2.5 Simulation of the tunnel excavation

The excavation of a tunnel is a three dimensional problem. Here, the excavation is simulated in plane strain. To get more realistic results, operating with a two dimensional model, the so called “3D effect” can be simulated by two methods (Golser & Schubert, 2003; Schwartz & Einstein, 1980):

- Load reduction method (β-method) (2.5.1)
- Stiffness reduction method (α-method) (2.5.2)

As it is usual in tunneling, displacement occurs in the ground before the support can be applied. This displacement mobilizes the resistance of the ground and reduces the load, which the later installed support must carry.

2.5.1 Load reduction method (β-method)

In the load reduction method (Panet, 1978), an initial state is assumed, where the internal pressure (p_0) in this opening equals the external earth pressure (Fig. 11a). Before the shotcrete shell is included, this internal pressure is reduced by a β-factor (between 0 and 1; 0 = full internal pressure; 1 = no internal pressure). According to Fig. 11a, $\beta_0 = 0$, $\beta_1 > \beta_0$, $\beta_2 > \beta_1$, and so on.

Fig. 11a_1 shows the installation of the shotcrete shell with a Young's modulus (E_{S1}) of a "young" shotcrete. Before this is done, the unloading factor (β-factor) is set to β_1. Hence, the internal pressure is reduced and the ground moves radially inward. Subsequently, the shotcrete shell is installed.

Fig. 11a_2 illustrates a further reduction step of the internal pressure. Hence, the unloading factor is set to β_2. After the internal pressure is reduced a second time, the material property of the shotcrete is changed to a "hardened" (E_{S2}) one.

Fig. 11a_3 shows the installation of the inner liner with a Young's modulus of E_L. Before this is done, the unloading factor is set to β_3. Hence, the internal pressure is reduced a third time and the combined system, ground plus shotcrete shell, moves radially inward. Subsequently, the inner liner is installed.

Fig. 11a_4 illustrates the last reduction of the internal pressure. Hence, the unloading factor (β) is set to one and consequently the internal pressure is reduced to zero.

The magnitude of the β-factor that corresponds to reality must be obtained from measurements.

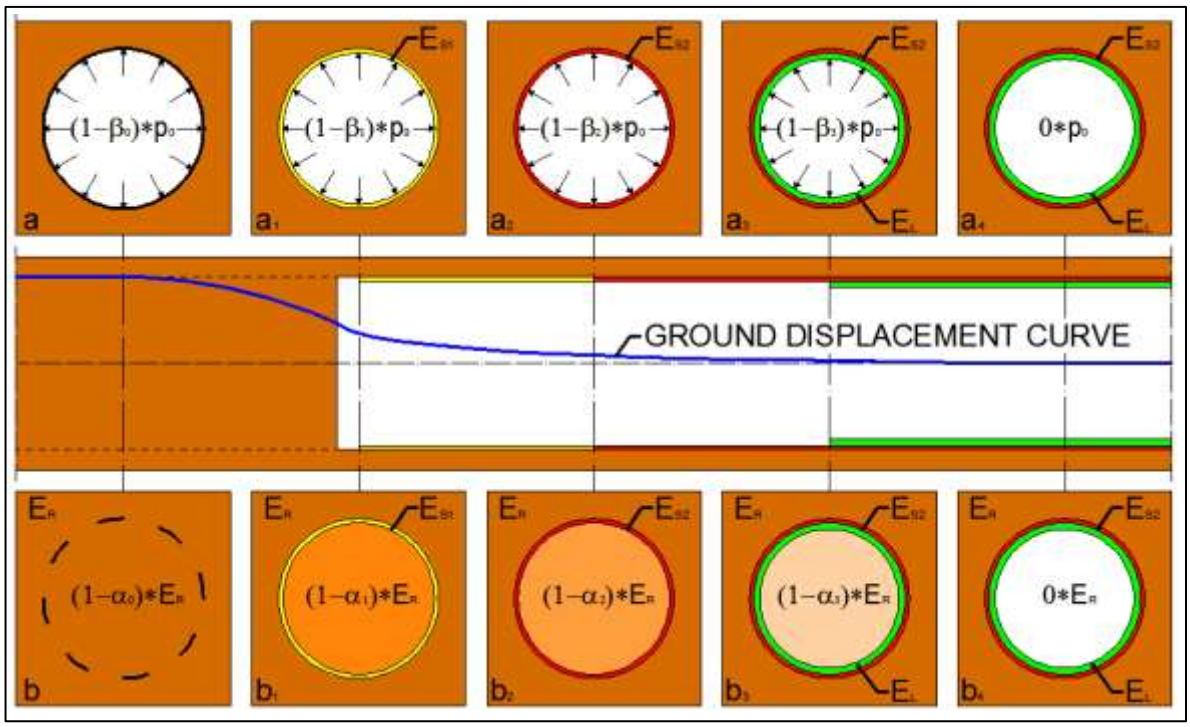

Fig. 11: Load and stiffness reduction method with implementation of shotcrete shell and inner liner

2.5.2 Stiffness reduction method (α-method)

In the stiffness reduction method (Fig. 11b) (Laabmayr & Swoboda, 1978), the tunnel construction simulation is conducted by reducing the stiffness of the material in the future opening gradually. Between these steps, the shotcrete shell and inner liner are installed similarly to the scheme of the load reduction method mentioned above.

The material in the future opening is reduced by an α-factor (between 0 and 1; 0 = same stiffness of material inside as around the outside of the opening zone; 1 = no stiffness of material in the opening). According to Fig. 11b, $\alpha_0 = 0$, $\alpha_1 > \alpha_0$, $\alpha_2 > \alpha_1$, and so on.

In the first excavation step (Fig. $11b_1$) a stiffness reduction factor of $\alpha = 50\%$ is recommended by Laabmayr & Swoboda, (1978).

The advantage of the stiffness reduction method is that it works well with all values of K. In comparison, the load reduction method, which assumes a uniform internal pressure applied at the tunnel perimeter, can only be used to calculate a uniform earth stress field with K = 1.

2.5.3 Evaluation and critique of the reduction factor

Nowadays it is very common to use 2D numerical analyses for the design of tunnels. One main advantage of this analysis, compared to 3D analyses, is that it saves time to build the model and to do the calculations. Nevertheless, assumptions have to be made to consider

the so called “3D effects”. Displacements occur in the ground before the tunnel is excavated. Furthermore, the support can often only be constructed with a delay behind the excavation face. Subsequently the tunnel perimeter deforms before shotcrete or other support material can be applied. Fig. 11 shows a schematic ground displacement curve for this pre-displacements[1] and support delay[2]. This behavior can be simulated with the load- or stiffness reduction method. However, assumptions concerning the unloading factor have to be made in both methods.

Several authors have suggested different values for pre-displacements and support delay, either based on measurements or engineering practice. Panet (1976) derives an unloading factor of β = 33% at the tunnel face, and β = 100% at a distance “four times the radius” behind the tunnel face. Laabmayr et al. (1978) determined based on measurements an unloading factor of β = 50% at the tunnel face. For partial excavation they come up with a factor between β = 20% and β = 50% for top heading excavation and with a factor between β = 40% and β = 80% for side drift excavation (Laabmayr & Swoboda, 1986). Golser (2008) simulated the Brenner base tunnel in rock with a very high overburden using an unloading factor of β = 95%. Möller et al. (2010) simulated a tunnel drift in a cohesive soil using a load reduction factor of β = 70% for the top heading and a load reduction factor of β = 50% for the bench and invert. Baudendistel, (1979) quoted in Möller, (2006) says that the unloading factor for full excavation of a horse-shoe profile dependents on the round length[3].

This short review makes it clear that the load reduction factor varies and that it is very difficult to come up with an exact value.

The load reduction factor is dependent on the opening size (S. Möller, 2006), the round length and the material behavior of the surrounding ground, the overburden, the advance method, and much more. Hence, assumptions of the load reduction factors have to be made for each separate case. The best way to do this is with dilatometer measurements ahead of the tunnel-face as well as displacement measurements at the tunnel wall after excavation. Another possibility is to compare the results with a three dimensional numerical analysis, in which the excavations are simulated step by step. Last but not least, a third way would be to calibrate the load reduction factor with the use of an analytical or empirical method. For instance it is possible to use the characteristic curve concept to determine the pre-excavation displacements as well as the support delay (Lombardi, 1973).

[1] Movement of ground (rock or soil) into the future opening before tunnel is excavated.
[2] Displacement on tunnel perimeter behind tunnel face and before initial support is installed.
[3] Length of one excavation cycle

This thesis does not consider measurements or use three dimensional numerical calculations. Hence, a calibration of the load reduction factor is done based on the characteristic curve concept.

2.5.4 Conclusion

For this investigation the load reduction method is used. This method is chosen on the basis of conceptual considerations of contact problems. Using the stiffness reduction method two parts are in contact with the ground's tunnel perimeter at the same time:

- Part of future opening
- Part of shotcrete shell

This would cause numerical problems. For this reason, the load reduction method is chosen.

To remove the above mentioned disadvantage of the load reduction method (not all values of K can be simulated), the internal pressure is simulated with reaction forces in the vertical and horizontal direction at each node of the tunnel perimeter. These reaction forces are obtained from an independent calculation, whereby all nodes at the tunnel perimeter are fixed. (See also chapter 2.6.4)

2.6 Simulation of the tunnel construction

Different methods have been proposed in the literature (Einstein, Bobet, & Aristorenas, 1995; Hibbitt, Karlson, & Sorenson, 2007) to simulate in ABAQUS the implementation of support elements (i.e. shotcrete shell and inner liner) during the calculation.

- Model Change Method (2.6.1)
- Dummy Node Method (2.6.2)
- Changing Stiffness Method (2.6.3)
- Four Calculation Method (2.6.4)

The task of this chapter is to determine a method, which provides a stress-free activation of support elements and the possibility to simulate contact conditions. This is not straight forward in ABAQUS by the fact that displacements occur before the support elements are included. Each of these methods involves a different approach to deal with this task.

Each of these methods required either the stiffness reduction method or the load reduction method (see chapter 2.5) to simulate pre-displacements, support delay and the loading on the support elements (shotcrete shell and inner liner).

For the Model Change Method (2.6.1) and the Dummy Node Method (2.6.2), only the implementation of the shotcrete shell is discussed. This simplification ensures clarity.

For the Changing Stiffness Method (2.6.3) and the Four Calculation Method (2.6.4), the implementation of the shotcrete shell and the inner liner are discussed, including detailed description of the calculation steps.

The conclusion (2.6.5) provides an overview of properties and behaviors which can be simulated using the several methods. The task is to determine a method, which provides a stress-free activation of support elements and the possibility to simulate contact conditions. For further investigations one of the four methods is chosen. The reasons for this decision are given.

2.6.1 Model Change Method

This method is recommended in the ABAQUS Example Problems Manual (Hibbitt, Karlson, & Sorenson, 2007).

A half circle for the tunnel is simulated. The tunnel is situated at the left hand side of the model (Fig. 12). The excavation and construction of the tunnel are simulated in four steps.

In the initial step a geostatic stress field is applied. It is assumed that the stress increases linearly with the depth. Moreover, the vertical stress is two times the horizontal stress. Ground and shotcrete shell are implemented in this step. The load reduction method is provided by the function AMPLITUDE, which allows one to decrease the reaction forces at the tunnel perimeter during several calculation steps. Additionally the interaction between ground and shotcrete shell is defined as a so called TIE contact, where no slippage is allowed.

Fig. 15a shows in detail a section of the ground and the shotcrete shell. Fig. 15b shows the same as Fig. 15a, only with more details on the connection between ground and shotcrete shell. Note that the nodes at the tunnel perimeter have the same coordinates as the nodes on the outside of the shotcrete shell and are connected during the entire calculation. Fig. 13a illustrates the FE-mesh around the tunnel.

In the first step the shotcrete shell is removed with the method MODEL CHANGE (Fig. 15c & Fig. 13b). A gravity field is activated with a predefined unit weight. The degree of freedom 1 (Fig. 18) is fixed at every node at the entire left vertical side of the model. Moreover, vertical and horizontal reaction forces are set at the nodes at the tunnel perimeter to ensure no displacement.

The reaction forces were obtained from an independent analysis where the displacements on the tunnel perimeter were constrained. In short, the first and second degrees of freedom at the tunnel perimeter are fixed. After full loading of the model the reaction forces were obtained at each node at the tunnel perimeter. (See also chapter 2.6.4)

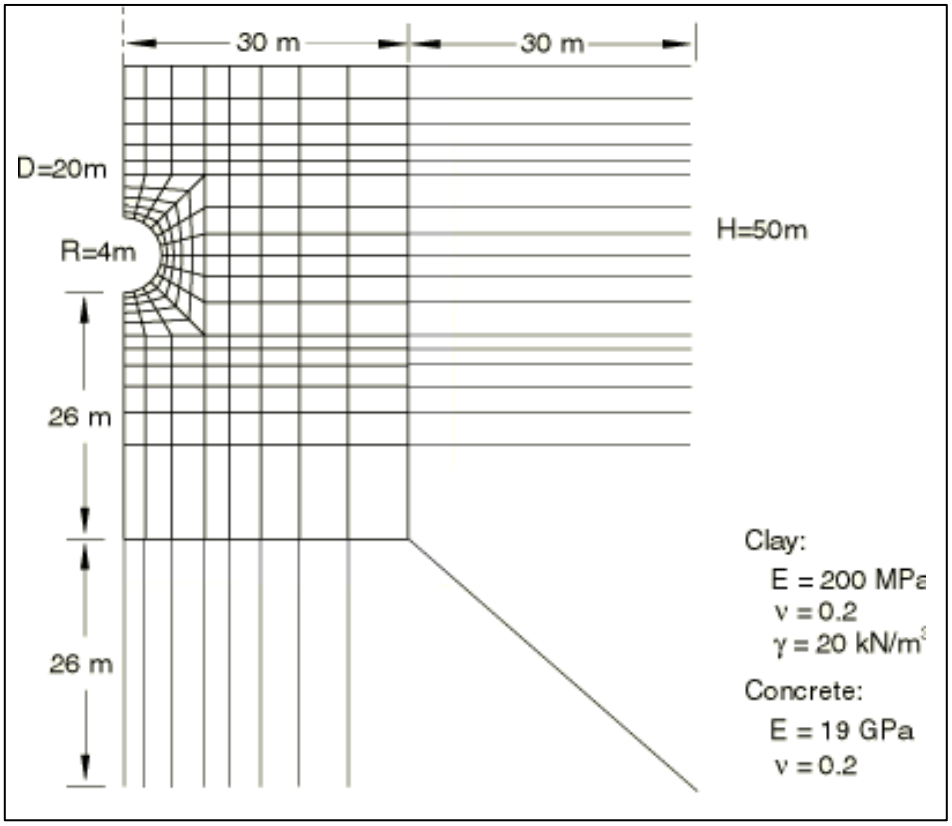

Fig. 12: Geometry and finite element discretization; Source: Hibbitt, Karlson, & Sorenson, 2007

In the second step the internal pressure was reduced to 60% of its initial value. As a result the ground moved inward (Fig. 13c). Fig. 15d illustrates the movements which occurred at the ground-tunnel interface. The hatching shows the undeformed geometry. Note that the nodes of the tunnel perimeter and the outside of the shotcrete shell were connected by the TIE contact, even when the shotcrete shell was deactivated. It can be seen that the original thickness of the shotcrete shell changes during this step (Fig. 14).

In the third step the shotcrete shell was reactivated in a stress-free state. Fig. 15e shows again that the thickness of the now activated shotcrete shell (solid-part) changed in comparison with its original geometry (hatched-part).

In the fourth step the internal pressure was reduced to zero (Fig. 15f & Fig. 13d). As a result, the combined system, ground plus shotcrete shell, moves inward.

Between Fig. 13b and Fig. 13c which corresponds to the first load reduction step, the bottom part of the tunnel moved significantly upwards (see marked areas). Comparing the thickness of the shotcrete shell, at the tunnel-crown and the bottom, one can see that the thickness is different. Note: The shotcrete shell, represented in white, is not included (activated) at this calculation step.

To sum up, the tunnel moves radially inward before the shotcrete shell can be constructed (see chapter 2.5). During this first load reduction step, the nodes at the outer edge of the shotcrete shell are connected to the nodes at the tunnel perimeter. Since all other deactivated nodes of the shotcrete shell stay at their initial coordinates during this reduction step, the thickness of the shotcrete shell is reduced by the amount of displacements which occur on the tunnel perimeter. By reactivation of the deformed shotcrete shell and further unloading, all nodes of the shotcrete shell deform together. However, given that the shotcrete shell is thinner than it should be, less support-resistance can be activated, and as a result of this, more deformation of the combined system occurs.

In short, the disadvantages of this method are that:

- a constant thickness of the shotcrete shell cannot be ensured
- realistic displacements of the shotcrete shell cannot be achieved
- no other contact formulation than a TIE contact can be realized

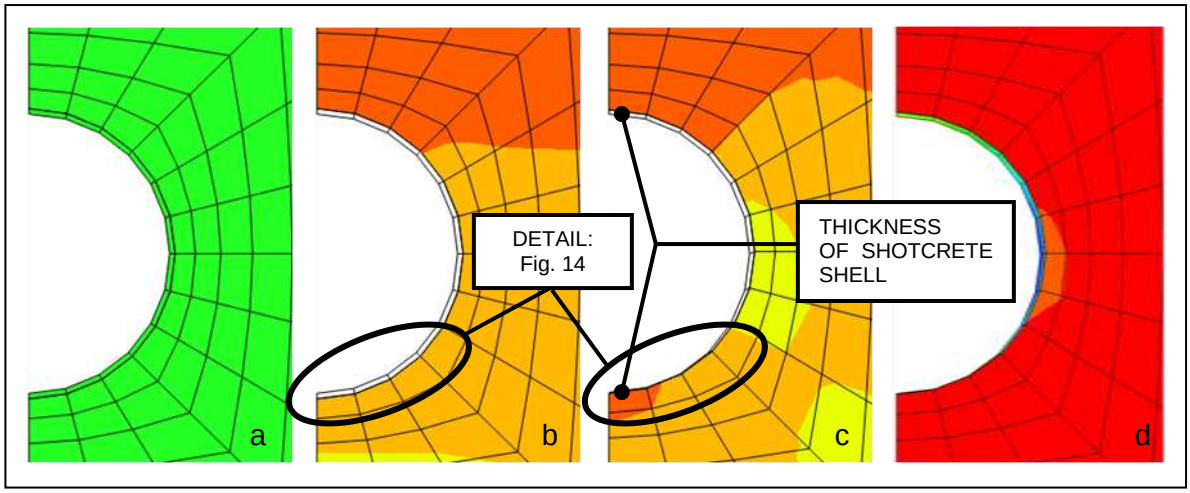

Fig. 13: Vertical stress and displacements; a) model; b) initial step, the shotcrete shell is not activated; c) first load reduction step, the shotcrete shell is not activated, deformation on deactivated the shotcrete shell; d) reactivation of the shotcrete shell and subsequently second load reduction step

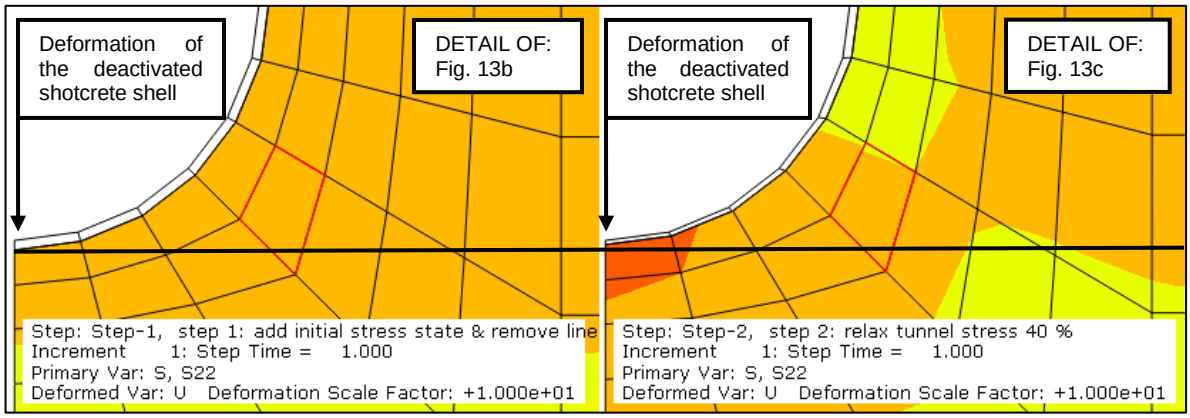

Fig. 14: Comparison: Fig. 13b and Fig. 13c; contours of vertical stresses and displacement; white part = deactivated shotcrete shell, colored part = ground; Note: displacement – bottom of tunnel moves up,

thickness – thickness of deactivated shotcrete shell gets reduced, stress – decrease of vertical stress at bottom;

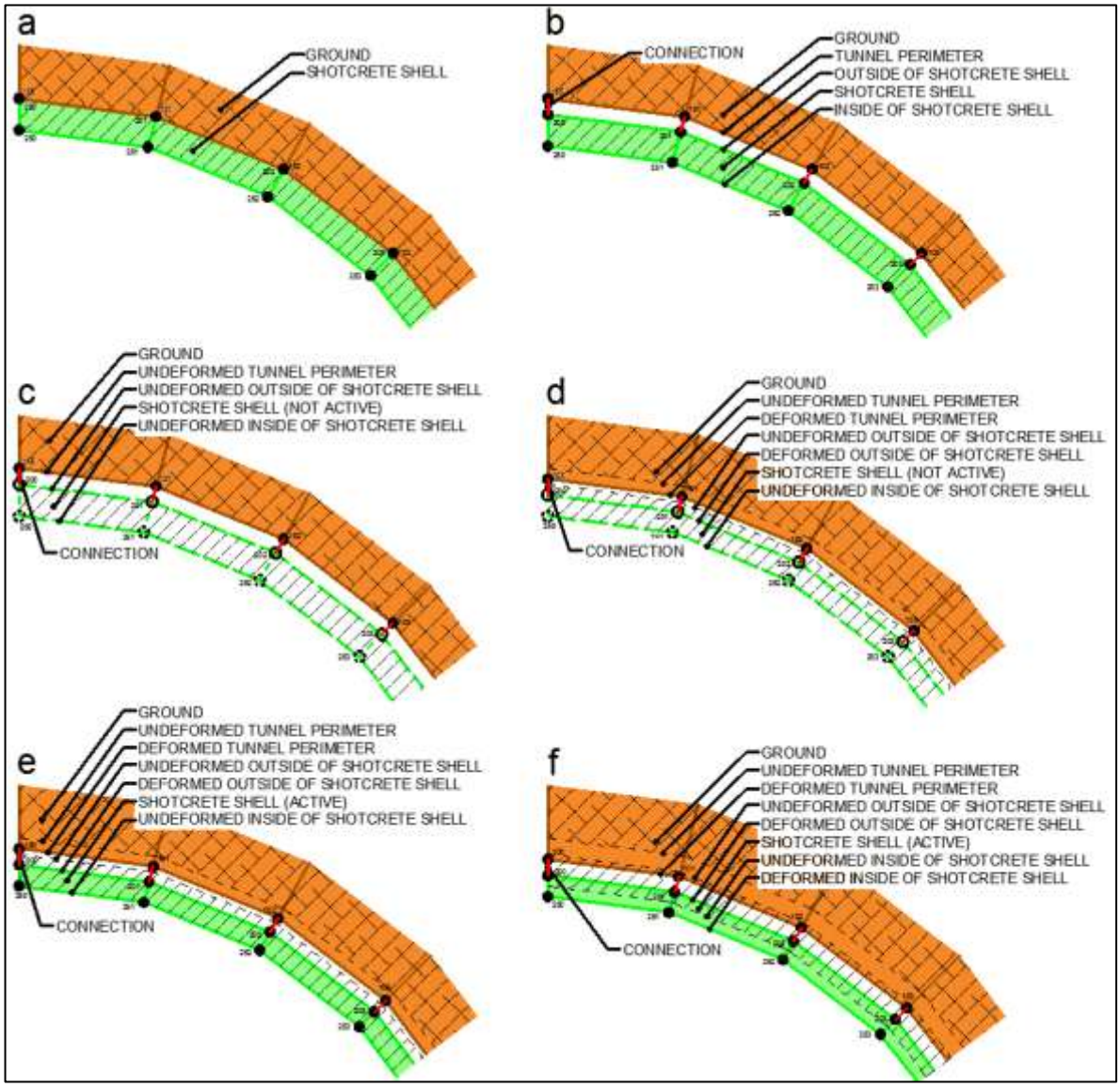

Fig. 15: Steps of the construction process using the Model Change Method; only a simple shotcrete shell is considered (no inner liner)

2.6.2 Dummy Node Method

Dummy Nodes can be used to connect the deformed tunnel perimeter with the corresponding nodes of the shotcrete shell using equation (2.4) (Einstein, Bobet, & Aristorenas, 1995). Therefore, it is necessary that in the initial step, three sets of different nodes, but with the same node coordinates are defined (Fig. 16). The first node set is for the ground-interface, the second node set is for the shotcrete shell-interface and the third node set is for the dummy nodes. The equation is set up in terms of displacement:

$$ground\_interface\ nodes = shotcrete\ shell\_interface\ nodes + dummy\ nodes \quad (2.4)$$

In the initial step the shotcrete shell is removed (Fig. 17a). Hence, displacements of the ground-interface nodes are equal to those of the dummy nodes. The load reduction method can be simulated in the same way as described in chapter 2.5.1. As a result, the ground-interface and the dummy nodes move inward ($\Delta 1$), while the shotcrete shell stays at its initial position (Fig. 17b).

Subsequently, the shotcrete shell gets reactivated and the dummy nodes are fixed (D.O.F. 1 and 2; (Fig. 18)) in their positions. According to equation

(2.4), the further displacements of the ground-interface are equal to those of the shotcrete shell-interface. Fig. 17c shows as result of the displacement of the ground-interface, which occurred before, an overlapping of the ground with the shotcrete shell. (Note that an overlapping of the ground with the shotcrete shell is also shown in Fig. 17b. This is not mentioned because the shotcrete shell is not activated)

Fig. 17d illustrates further reduction of the internal pressure and inward movement ($\Delta 2$). The nodes of the ground-interface are still connected with the nodes of the shotcrete shell-interface. Consequently the overlapping of the ground and the shotcrete shell-interface still exists.

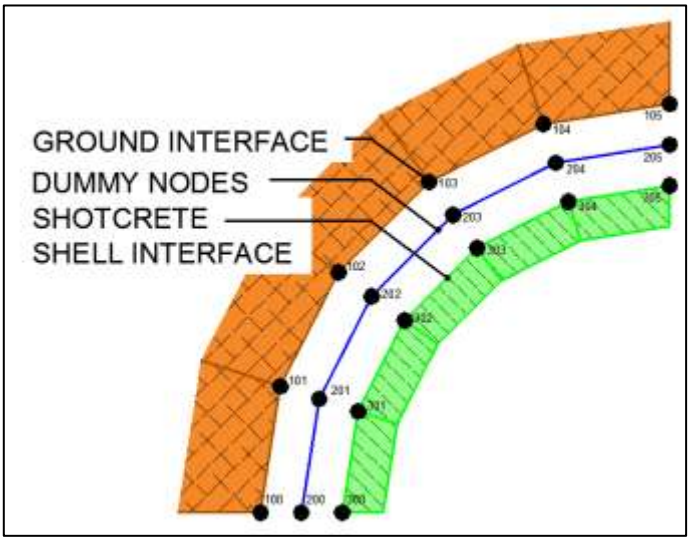

Fig. 16: Dummy Node Model; only a simple liner is considered

The advantage compared of the Dummy Nodes Method to the Model Change Method (2.6.1) is that a constant thickness of the liner can be maintained. A disadvantage of this method is that no contact formulation can be set.

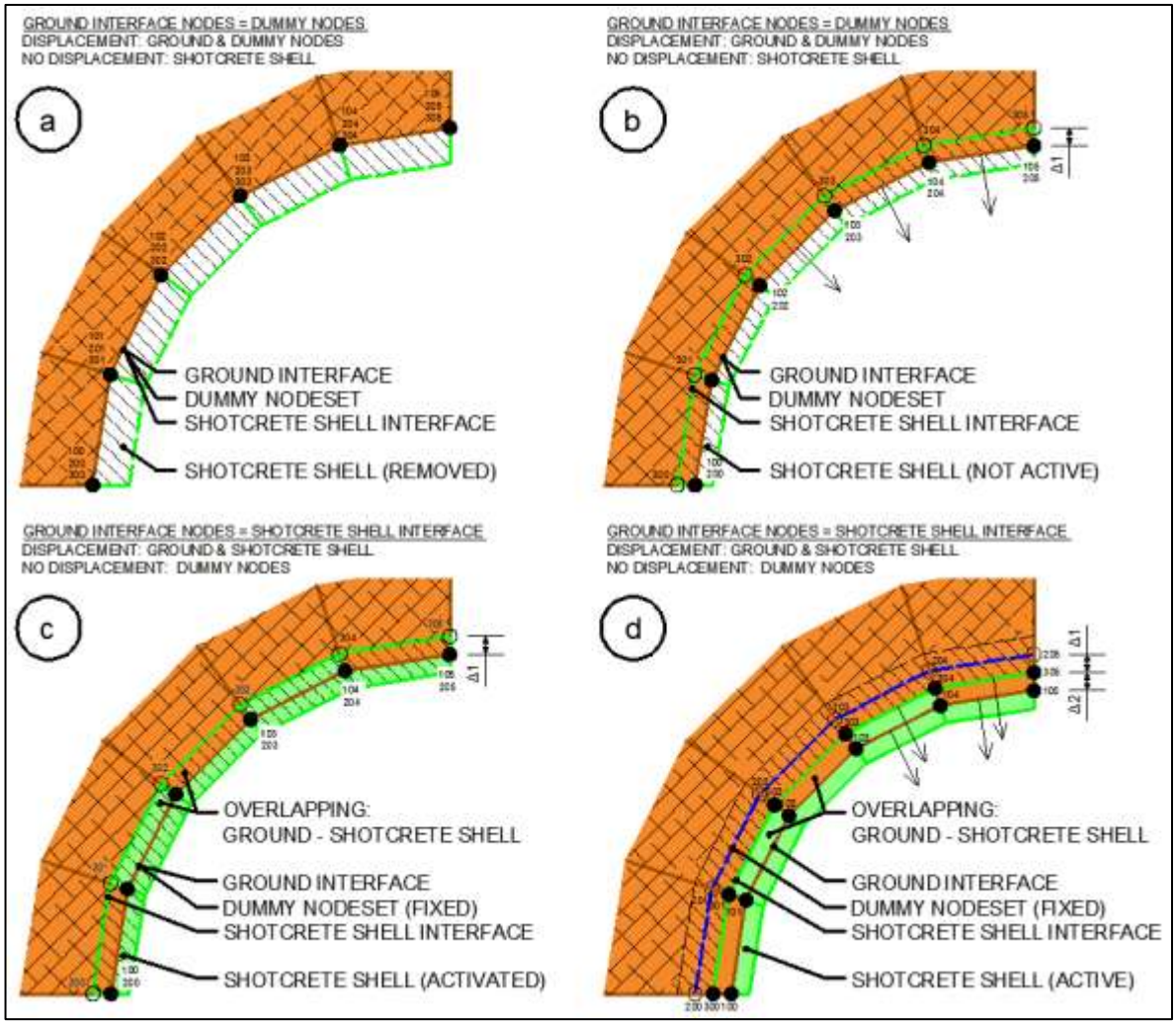

Fig. 17: Steps of the construction process using the Dummy Node Method; only a simple liner is considered; hatching symbolized initial geometry of ground and shotcrete shell (no changing of hatching in all four figures for a compare with displacements of activated – colored – parts);
Ad a: the shotcrete shell is removed; according to equation (2.4) the ground interface and the dummy nodes are connected;
Ad b: inward movement of ground and dummy nodes (Δ1); no displacement of deactivated shotcrete shell;
Ad c: the shotcrete shell is activated and the dummy nodes are fixed; hence, according to equation (2.4) the ground interface and the shotcrete interface are connected; note an overlapping of the ground and the shotcrete shell as a result of the displacements (Δ1) which occur on the ground in step b;
Ad d: inward movement of ground and shotcrete shell (Δ2); no displacement of fixed dummy nodes;

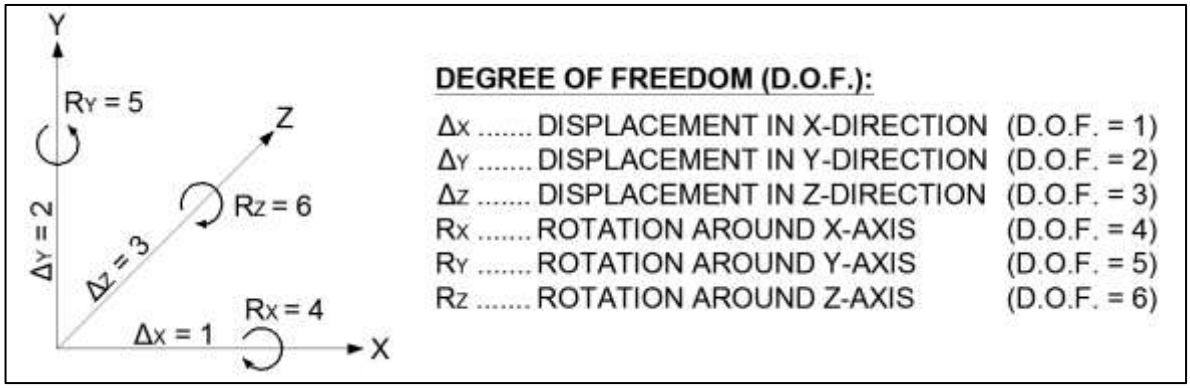

Fig. 18: Degree of freedom formulation in ABAQUS

2.6.3 Changing Stiffness Method

This method should ensure that no geometrical problems occur. The basic idea is to make material properties dependent on field variables. Therefore, in the initial step the shotcrete shell and inner liner have a Young's modulus of 50 N/m² (i.e. very low). Accordingly, they do not influence the displacement of the tunnel perimeter during a decrease of the internal pressure by the load reduction method. To avoid numerical problems, the Young's modulus is not set to zero.

After a first reduction with the β-factor, the shotcrete shell is activated by setting the Young's modulus to E_{S1} = 10,000 MN/m². After a second reduction of the internal pressure the Young's modulus of the shotcrete shell is set to E_{S2} = 15,000 MN/m². To ensure a loading on the inner liner, the inner liner is activated after a third load reduction step. Finally the internal pressure is set to zero in a last reduction step.

Changing material properties (i.e. stiffnesses) during the calculation is not straightforward in ABAQUS. First the material properties have to be dependent on field variables. To call them in later steps, the user subroutine USER DEFINED FIELD is used.

The calculation steps for the simulation of the construction progress are listed below:

INITIAL: Imposing of the initial stress field; fix degree of freedom (D.O.F.) 1, 5, 6 (Fig. 18) for the right vertical boundary; fix D.O.F. 2, 4, 6 for the bottom boundary; Young's modulus of shotcrete shell (E_{S0}) and inner liner (E_{L0}) is initialized with 50 N/m²; the load reduction method is implemented by the function AMPLITUDE, which allows one to decrease the reaction forces at the tunnel perimeter during the calculation; additionally the interaction between ground and shotcrete shell as well as between shotcrete shell and inner liner are defined by a Coulomb friction law with a friction coefficient of μ = 100 (φ = 89,43°) and μ = 1.0.

STEP 1: Apply σ_V at the top boundary; apply σ_H at the left vertical boundary; apply $p_0 * (1-\beta)$ at the tunnel perimeter; set β to zero; (Fig. 19a)

STEP 2: Set β to 20%; (Fig. 19b)

STEP 3: The shotcrete shell is included. Therefore, D.O.F. 1, 2 at the tunnel perimeter are fixed and the Young's modulus of shotcrete is set to E_{S1} = 10,000 MN/m².

STEP 4: D.O.F. 1, 2 at the tunnel perimeter are released; (Fig. 19c shows step 3 and 4)

STEP 5: Set β to 40%; (Fig. 19d)

STEP 6: Idle step

STEP 7: Changing material behavior of the shotcrete from a "young" to a "hardened" one. Therefore, D.O.F. 1, 2 at the tunnel perimeter are fixed and the Young's modulus of shotcrete is set to E_{S2} = 15,000 MN/m². (Fig. 19e)

STEP 8: D.O.F. 1, 2 at the tunnel perimeter are released; set β to 60%; (Fig. 19f)

STEP 9: The inner liner is activated; Therefore, D.O.F. 1, 2 at the tunnel perimeter are fixed and E_L is set to 30,500 MN/m². (Fig. 19g)

STEP 10: D.O.F. 1, 2 at the tunnel perimeter are released; set β to 80%; (Fig. 19h)

STEP 11: β is set to 100%; end of tunnel construction; (Fig. 19i)

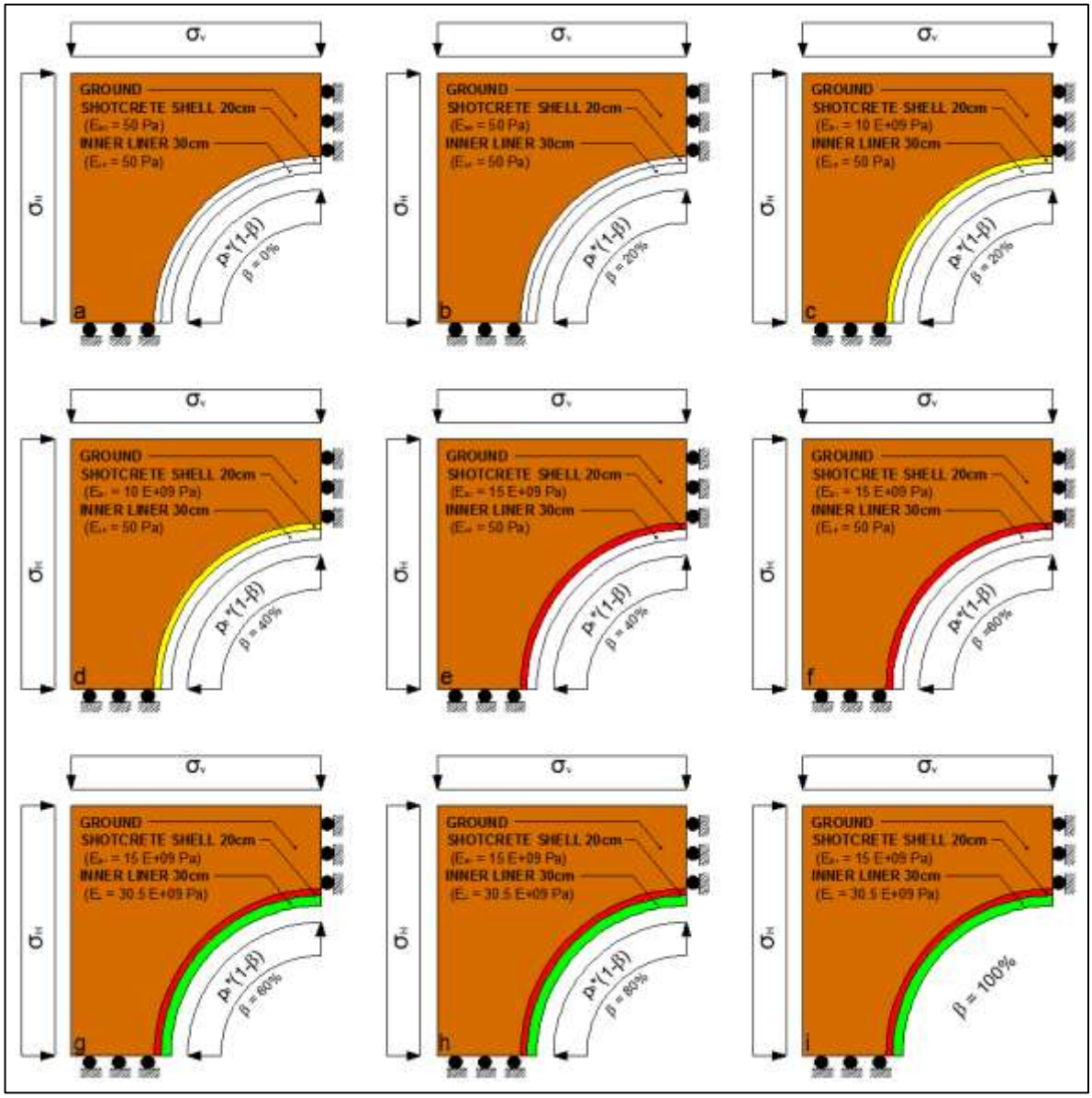

Fig. 19: Changing Stiffness Method – construction process; (Note: figure sub-numbering in left lower corner)

Fixing the boundary at the tunnel perimeter during installation of the support elements (shotcrete shell and inner liner) was done by Einstein et al., (1995). It should ensure that no numerical problems during changing of the material properties occur. Fig. 20 shows a plot of tangential stresses (S22) in the support elements as well as the radial displacements (U1) of the tunnel perimeter during the above mentioned calculation steps. All results are obtained at the spring-line (Fig. 1).

In the third step (Fig. 20) a significant increase of the stresses in the shotcrete shell occurs. In the fourth step a significant decrease of those stresses occurs. To investigate this behavior, a comparison with a calculation in which D.O.F. 1, 2 at the tunnel perimeter

are not fixed during the modification of the material properties is done. (Note that D.O.F. 1, 2 are fixed for step-3, step-7 and step-9 in Fig. 20)

Fig. 21 shows this comparison: The first calculation in which D.O.F. 1, 2 at the tunnel perimeter are fixed during the modification of material properties (same as in Fig. 20; black dashed lines) is compared with a second calculation in which D.O.F. 1, 2 at the tunnel perimeter are not fixed during the modification of material properties (colored solid lines).

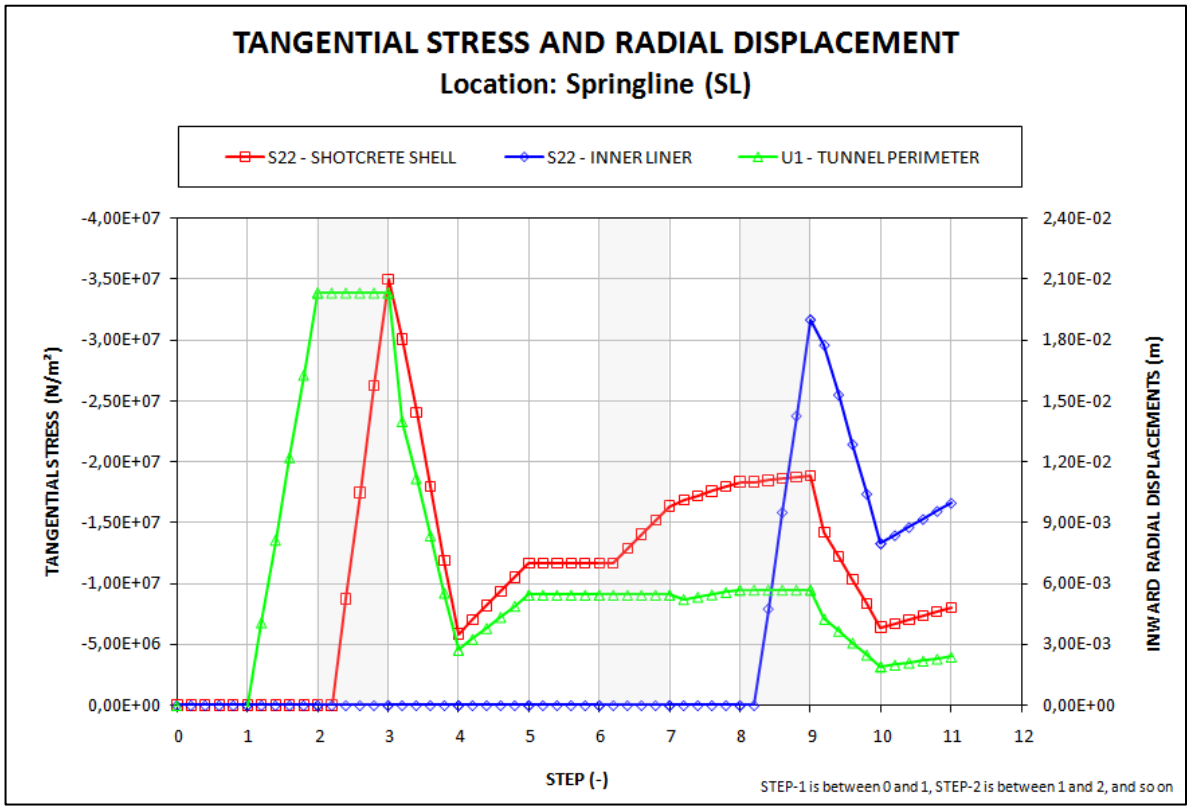

Fig. 20: Result of Changing Stiffness Method; in the gray marked steps 3, 7 and 9 the D.O.F. 1, 2 at the tunnel perimeter are fixed;

With regards to Fig. 20 and Fig. 21 the squared (□) curves are the averaged stresses of the shotcrete shell, the diamond (◊) curves are the averaged stresses of the inner liner and the triangular (Δ) curves are the radial displacements (positive = inward) of the tunnel perimeter at the spring-line. Regarding the simulation steps which are mentioned above, step one is shown on the horizontal axis between 0 and 1, step two is between 1 and 2, and so on.

Table 2 gives a detailed description of Fig. 21, providing a comparison of tangential stresses in the shotcrete shell and the inner liner, and of the radial displacements of the tunnel perimeter at the spring-line.

Parentheses are used in Table 2 to make comments about the real behavior. Square brackets are used to insert notes. Note that the only difference between these two calculations is that D.O.F. 1 and 2 are fixed or not fixed in step-3, -7 and -9.

Looking at the values at step-11 (end of tunnel construction progress) it is obvious that the stresses and displacements of the two calculations (with and without fixed D.O.F. 1 and 2 in step-3, -7 and -9) are exactly the same. (Fig. 21)

A comparison with another calculation in which all support elements are simulated with its final material parameters from the beginning, shows the same values of stresses and displacements at step-11 as the two discussed calculation which are shown in Fig. 21. This makes it clear that displacements, which occur till step-10, are considered by changing material properties.

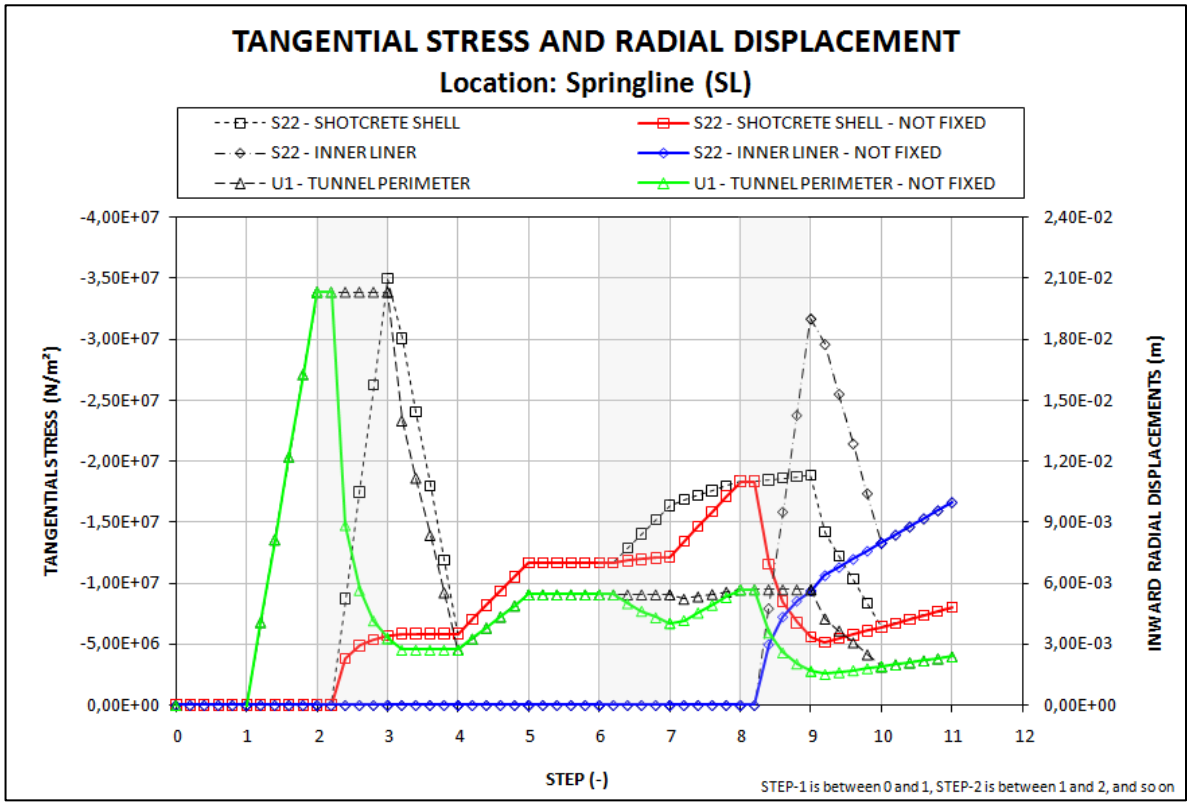

Fig. 21: Comparison: Changing Stiffness Method with and without fixed D.O.F. 1 and 2 at the tunnel perimeter during the change of properties;

Table 2: Interpretation Fig. 21; distribution of stresses and displacements; Comparison: Changing Stiffness Method with and without fixed D.O.F. 1, 2 at tunnel perimeter;

	TANGENTIAL STRESSES SHOTCRETE SHELL		TANGENTIAL STRESSES INNER LINER		RADIAL DISPLACEMENTS TUNNEL PERIMETER	
	FIXED D.O.F.	D.O.F. NOT FIXED	FIXED D.O.F.	D.O.F. NOT FIXED	FIXED D.O.F.	D.O.F. NOT FIXED
STEP-1	no change	no change	no change	no change	no change	no change
STEP-2	no change	no change	no change	no change	Tunnel perimeter moves 2cm radially inward	Tunnel perimeter moves 2cm radially inward
STEP-3	Stresses go up to 35MPa; (Reality: no stresses)	Stresses go up to 6MPa; (Reality: no stresses)	no change	no change	no change; [Note: fixed D.O.F.]	Tunnel perimeter moves 1.7cm radially outward; (Reality: no change)
STEP-4	Stresses go down to 6MPa; (Reality: no stresses)	no change	no change	no change	Tunnel perimeter moves 1,7cm radially outward; (Reality: no change)	no change
STEP-5	Stresses go up	Stresses go up	no change	no change	Tunnel perimeter moves radially inward	Tunnel perimeter moves radially inward
STEP-6	no change	no change	no change	no change	no change	no change
STEP-7	Stresses go up; (Reality: no change)	almost no change; (Reality: no change)	no change	no change	no change; [Note: fixed D.O.F.]	Tunnel perimeter moves radially inward; (Reality: no change)
STEP-8	Stresses go up; (Reality: greater increase)	Stresses go up	no change	no change	almost no change; (Reality: Tunnel perimeter moves radially inward)	Tunnel perimeter moves radially inward
STEP-9	almost no change; (Reality: no change)	stresses go down to 5MPa; (Reality: no change)	Stresses go up to 32MPa; (Reality: no stresses)	Stresses go up to 9MPa; (Realistic: no stresses)	no change; [Note: fixed D.O.F.]	Tunnel perimeter moves radially outward; (Reality: no change)
STEP-10	Stresses go down; (Reality: stresses go up)	Stresses go up	Stresses go down; (Reality: stresses go up)	Stresses go up	Tunnel perimeter moves radially outward; (Reality: Tunnel perimeter moves radially inward)	Tunnel perimeter moves radially inward
STEP-11	Stresses go up	Stresses go up	Stresses go up	Stresses go up	Tunnel perimeter moves radially inward	Tunnel perimeter moves radially inward

In short, the advantages of this method are:

- a constant thickness of the support elements (shotcrete shell and inner liner) can be maintained
- the possibility for contact formulation (i.e. Coulomb friction) exists

However, the disadvantages of this method are:

- real displacements of the support elements cannot be achieved
- real stresses of the support elements cannot be achieved

2.6.4 Four Calculations Method

This method uses four separate calculations to simulate the construction of a tunnel:

- calculation to obtain reaction forces (at tunnel perimeter)
- calculation to obtain coordinates to construct the shotcrete shell
- calculation to obtain coordinates to construct the inner liner
- Final calculation of tunnel construction

With ABAQUS it is not possible to run a calculation stepwise. All steps of a simulation have to be defined before the calculation is submitted. This is the major reason for having four separate calculations. The calculations are formulated such that the preceding one is always included into the following. The only exception to this rule is in the first calculation, calculation to obtain the reaction forces, in which boundary conditions are applied to the tunnel perimeter by fixing D.O.F. 1 and 2 at the tunnel perimeter and reducing the reaction forces to zero without installation of support elements (shotcrete shell and inner liner).

The following will give an overview of these four separate calculations. At the end an overview of all steps is represented.

The first calculation is to obtain reaction forces at each node of the tunnel perimeter (Fig. 24). In case of a uniform earth pressure (K = 1) this calculation can be omitted and a pressure ($p_0 = \sigma_v = \sigma_H$) can be applied at the tunnel perimeter. However, in all other cases the D.O.F. 1 and 2 of all nodes at the tunnel perimeter are fixed. Furthermore, in the initial step, a geostatic stress field is introduced and boundary conditions, roller support, are applied at the bottom and the right side of the model (see chapter 2.1.1). In the first step the vertical and horizontal earth pressure are applied at the top and the left side of the model. After full loading of the model, the reaction forces can be obtained at each node.

The second calculation is to simulate the pre-displacements and support delay. For this purpose, the previously determined reaction forces are applied at the tunnel perimeter (Fig. 24). These reaction forces are reduced with the load reduction method. Upon

reaching the load reduction factor at which the shotcrete shell is to be installed, the calculation is terminated and the node-coordinates of the deformed tunnel perimeter can be read out.

The third calculation is to include the shotcrete shell. The previously determined node-coordinates are used to model and apply the shotcrete shell. At the start of the calculation the outer edge of the shotcrete shell has a smaller radius than the tunnel perimeter. Consequently there is no contact between tunnel perimeter and shotcrete shell. Subsequently, the reaction forces are reduced with the load reduction method. As a result, the tunnel perimeter moves radially inward. Upon reaching the load reduction factor at which the node-coordinates were obtained in the second calculation, the contact between tunnel perimeter and shotcrete shell is closed. Subsequently, the reaction forces on the combined system, ground plus shotcrete shell, are reduced till the node-coordinates to construct the inner liner can be obtained.

A brief discussion of contact formulations is necessary:

An accurate formulation of contacts is very important to avoid numerical nonlinearities. (See chapter 2.4). Contact formulations have to be set in ABAQUS when two parts are interacting. For instance, a contact formulation has to be set between the tunnel perimeter of the ground and the outer edge of the shotcrete shell. Let's call the tunnel perimeter master-surface and the outer edge of the shotcrete shell slave-surface. The general definition of surfaces in ABAQUS is as follows:

Nodes of the master-surface can penetrate into the slave-surface, but nodes of the slave-surface cannot penetrate into the master-surface (node-to-surface contact) (Fig. 23_{LEFT}).

A node on the slave-surface cannot penetrate into a node on the master-surface (Fig. 23_{RIGHT}). Nodes on the tunnel perimeter have the same position as nodes on the outer edge of the shotcrete shell. Also nodes on the inner edge of the shotcrete shell have the same position as nodes on the outer edge of the inner liner.

Now the question arises: Are the nodes of these interfaces in the same position, or is an interface thickness to consider? For this purpose, CPE8R and CPE4 elements are investigated.

Regarding CPE8R elements a thickness of the interface cannot be considered. Consequently, two nodes (one on the master- and one on the slave-surface) have the same coordinates once contact has established.

Regarding CPE4 elements a thickness of the interface can be considered. Consequently, two nodes (one on the master- and one on the slave-surface) have not the same coordinates once contact has established. As a result, the interface has a finite thickness.

Fig. 22 shows how to consider the finite interface thickness (z) during the construction of the shotcrete shell. The new coordinates of the nodes on the outer edge of the shotcrete shell, considering a finite interface thickness, are extrapolated from the node-coordinates of the undeformed initial tunnel perimeter and the deformed the tunnel perimeter:

$$y_3 = y_2 + z * \sin\left[\tan^{-1}\left(\frac{y_1 - y_2}{x_1 - x_2}\right)\right] \tag{2.5}$$

$$x_3 = x_2 + z * \cos\left[\tan^{-1}\left(\frac{y_1 - y_2}{x_1 - x_2}\right)\right] \tag{2.6}$$

Note that the node-coordinates of the undeformed initial tunnel perimeter can be obtained at beginning of each calculation. The node coordinates from the deformed calculation are calculated by adding or subtracting the vertical (ΔY) and horizontal (ΔX) displacements.

A finite interface thickness can be considered to construct the shotcrete shell and inner liner.

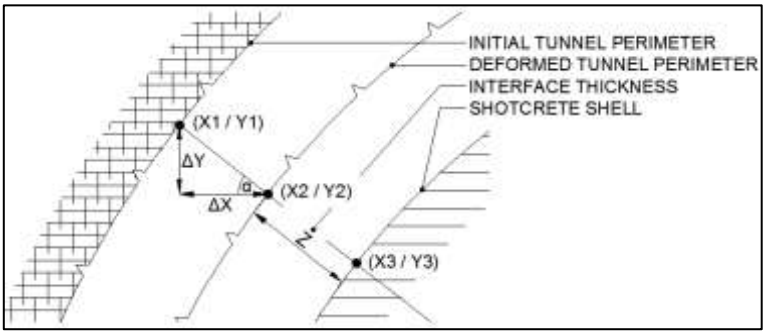

Fig. 22: Establish node-coordinates of shotcrete shell under consideration of interface thickness

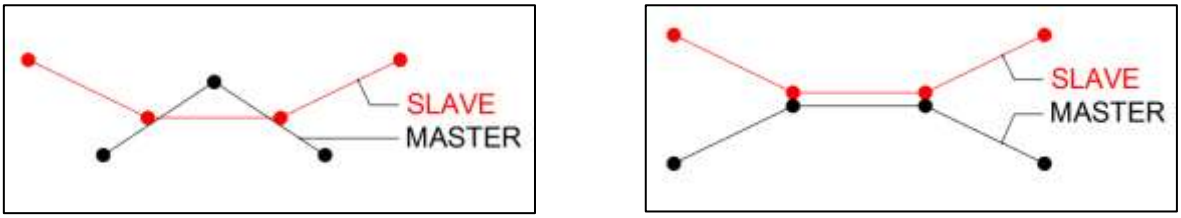

Fig. 23: node to surface (left) and node to node contact (right) of MASTER and the SLAVE surface

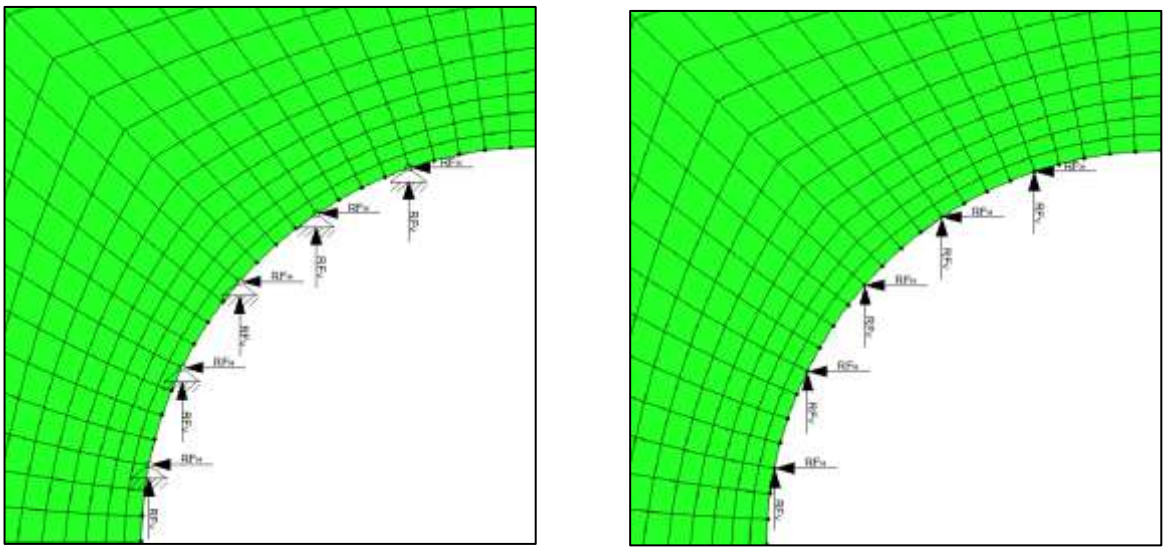

Fig. 24: Obtaining reaction forces for fixed D.O.F. 1 and 2 (left), and applying reaction forces at the tunnel perimeter (right)

The fourth calculation is to include the inner liner. For this purpose, the determined node-coordinates from the third calculation are used to model and apply the inner liner in the fourth calculation. At the start of the calculation, the outer edge of the shotcrete shell has a smaller radius than the tunnel perimeter, and the outer edge of the inner liner has a smaller radius than the inner edge of the shotcrete shell. This can be also seen as gaps (Fig. 25_{LEFT}). First the gap between tunnel perimeter and shotcrete shell is closed in the same way as in calculation three. Subsequently, the gap between shotcrete shell and inner liner is closed as well. Finally the reaction forces, which are still applied at the tunnel perimeter, are reduced to zero.

In order to provide an overview, all calculation steps are now listed in detail:

INITIAL: INITIAL CONDITIONS (PART ONE):

The calculation starts with a gap between tunnel perimeter and shotcrete shell (SHOT) as well as between shotcrete shell and inner liner (LINER) (Fig. 25). Contact formulations in terms of normal and tangential behavior are defined and applied to these interfaces. The D.O.F. 1, 5, 6 are fixed for all three parts (GROUND, SHOT, LINER) of the model at the right vertical boundary and the D.O.F. 2, 4, 6 are fixed for all three parts of the model at the bottom (Fig. 18). Furthermore, an initial stress field is applied to the GROUND (Fig. 28). The initial stress field is defined by a uniform vertical stress and a horizontal stress, which is defined by the vertical stress and the lateral stress coefficient (K). The initial stress field is to prevent displacement on the model in the first step, when the external vertical and horizontal stresses are applied. The external stress field is to maintain a constant stress in the GROUND during the excavation process. Note that the external stress field is applied in step-1. Finally the load

reduction method is implemented using the function AMPLITUDE, which allows one to decrease the reaction forces at the tunnel perimeter during the calculation.

STEP 1: INITIAL CONDITIONS (PART TWO):
The vertical stress σ_V is applied at the top boundary of the model and the horizontal stress σ_H is applied at the left vertical side of the model (Fig. 28). The reaction forces are applied at the tunnel perimeter (Fig. 24). The function AMPLITUDE is applied to the reaction forces, to reduce them over several calculation steps. The support elements are removed by using the method MODEL CHANGE (Fig. 25_{right}). Simultaneously the contact formulations between tunnel perimeter and SHOT as well as between SHOT and LINER are removed.
[Notes regarding the first calculation: Reaction forces are not applied; D.O.F. 1 and 2 are fixed at tunnel perimeter]

STEP 2: OBTAIN REACTION FORCES [Note: End of first calculation]:
At this step, the first calculation is terminated and the reaction forces at each node of the tunnel perimeter are obtained.

EXCAVATION (UNLOADING FACTOR β = 85%):
Here, the support delay is simulated. Hence, the reaction forces are reduced using the load reduction method until the point is reached at which the SHOT is to be installed (Fig. 11).

STEP 3: OBTAIN NODE COORDINATES SHOT [Note: End of second calculation]:
At this step the second calculation is terminated and the node coordinates on the deformed tunnel perimeter are obtained.

CONTACT TO YOUNG SHOT:
The contact formulation between tunnel perimeter and SHOT is reactivated (See chapter 2.3). Moreover, the SHOT is included with a Young's modulus of E_{S1} = 10,000 MN/m² (Fig. 26_{left}).

STEP 4: EXCAVATION (UNLOADING FACTOR β = 90%):
This step is to simulate the displacement of the combined system, GROUND plus "young" SHOT. Therefore, the reaction forces are reduced, using the load reduction method, till the point is reached at which the material behavior of shotcrete is changed to a hardened one (Fig. 11).

STEP 5: CHANGE PROPERTIES FROM YOUNG TO HARDENED SHOTCRETE:
The Young's modulus of shotcrete is changed from a "young" shotcrete to a

"hardened" one (E_{S2} = 15,000 MN/m²). This is done using the user subroutine USER DEFINED FIELD. This is done in the same way as in the Changing Stiffness Method (2.6.3).

STEP 6: EXCAVATION (UNLOADING FACTOR β = 95%):
This step is to simulate the displacements of the combined system, GROUND plus "hardened" SHOT. Therefore, the reaction forces are reduced, using the load reduction method, till the point is reached at which the LINER is to be installed (Fig. 11).

STEP 7: OBTAIN NODE COORDINATES LINER [Note: End of third calculation]:
At this step the third calculation is terminated and the node coordinates on the inner edge of the deformed SHOT are obtained.

CONTACT TO INNER LINER:
The contact formulation between SHOT and LINER is reactivated. Moreover, the LINER is included with a Young's modulus of E_{S1} = 30,500 MN/m² (Fig. 26_{right}).

STEP 8: EXCAVATION (UNLOADING FACTOR β = 100%):
In practice when all displacements, which occur on the combined system, GROUND plus SHOT, have occurred, the LINER is to be installed. As a result, no load will be carried by the LINER. The loading on the LINER is mostly done by assuming full deterioration of the SHOT. Consequently the LINER has to carry the load which was taken before by the SHOT. However, to ensure a load on the combined system, GROUND plus SHOT plus LINER, the reaction forces which appear at the tunnel perimeter are set to zero in the last step (step 8) of the calculation (Fig. 11).

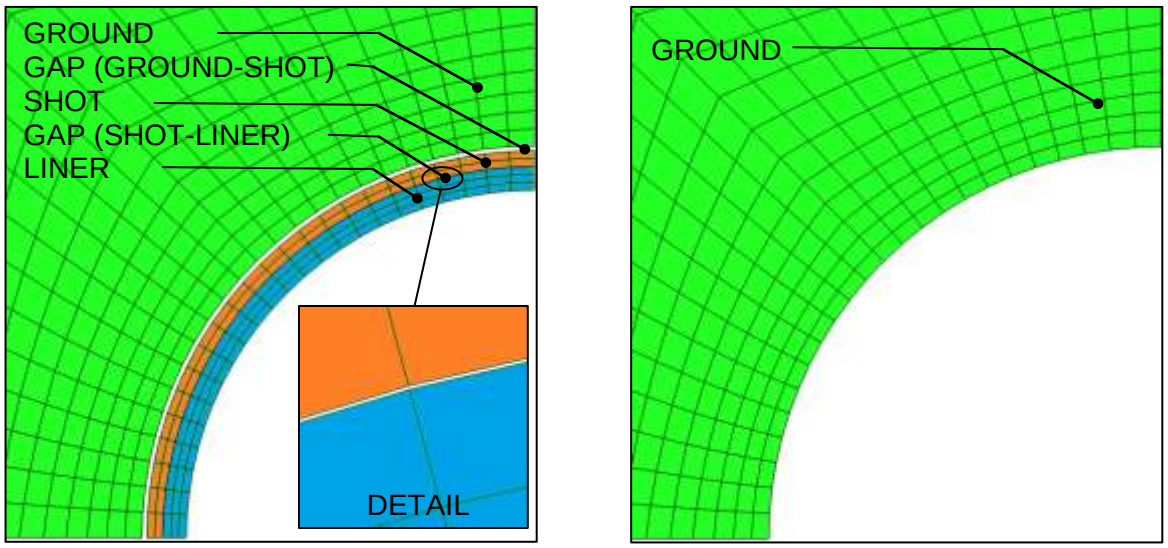

Fig. 25: Initial (left) and first step (right) of four calculation method. Supports elements (shotcrete shell and inner liner) are removed in first step.

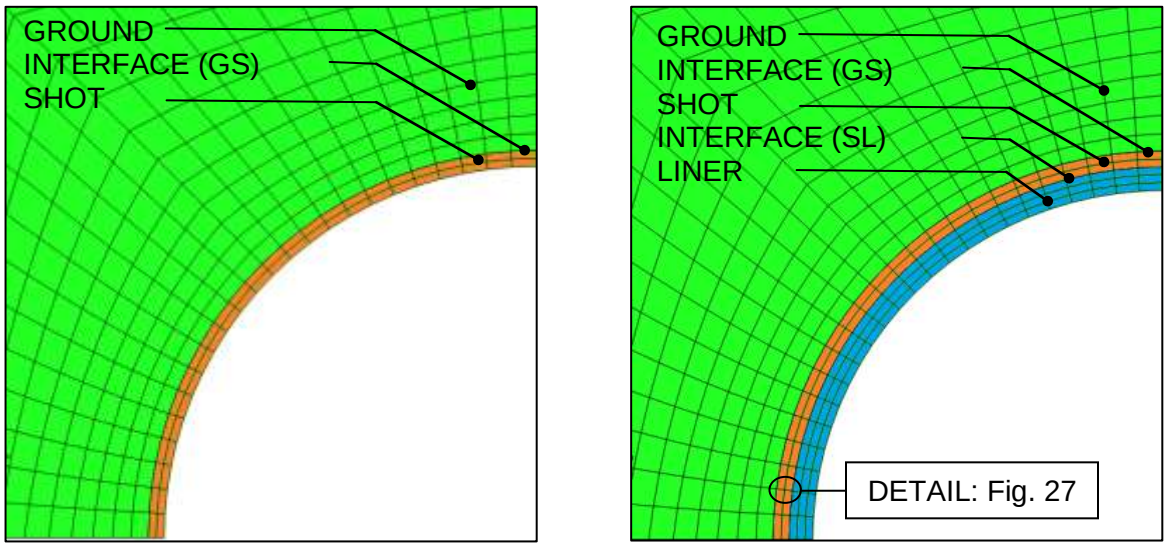

Fig. 26: Activation of shotcrete shell as well as the contact formulations at the ground – shotcrete shell (GS) interface at step 3 (left) and activation of inner liner as well as the contact formulations at the shotcrete shell – inner liner (SL) interface at step 7 (right).

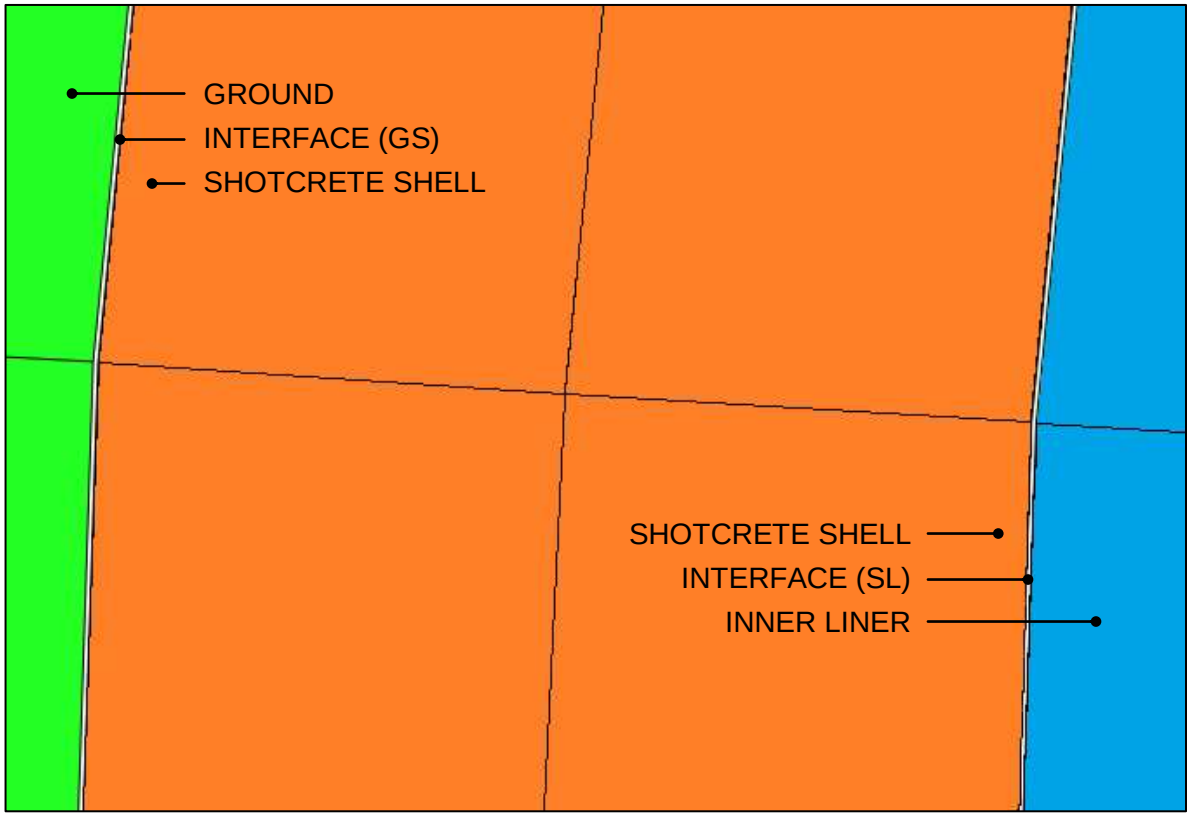

Fig. 27: Detail; Interfaces between ground (G), shotcrete shell (S) and inner liner (L)

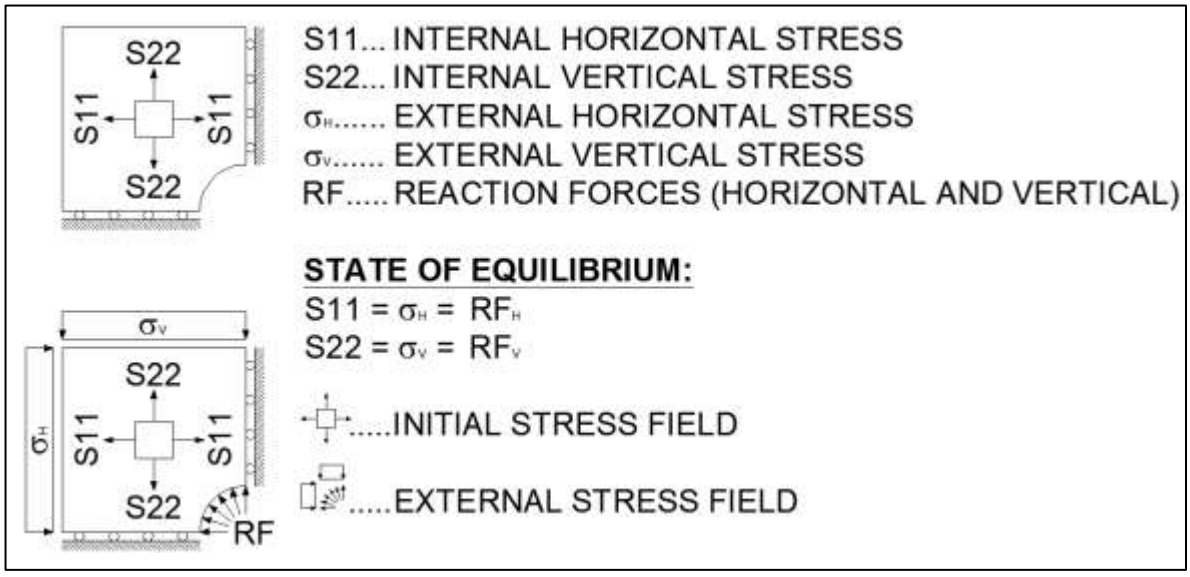

Fig. 28: Initial stress field (upper figure) and initial stress field with external stress field in equilibrium (lower figure); reaction forces are separated into horizontal and vertical direction;

The advantages of this method are that:

- a constant thickness of the support elements (shotcrete shell and inner liner) can be maintained
- the possibility for contact formulation (i.e. Coulomb friction) exists
- realistic displacements of the support elements can be achieved
- realistic stresses of the support elements can be achieved

2.6.5 Conclusion

Different methods to simulate a tunnel construction with a 2D numerical analysis, using ABAQUS, were discussed:

- Model Change Method
- Dummy Node Method
- Changing Stiffness Method
- Four Calculation Method

Depending on the aim and accuracy of the investigation, the best method for each case has to be figured out. Table 3 presents a brief overview of the discussed methods. One aim of this research is to have a method which considers contact formulations. This is possible using the Changing Stiffness Method or the Four Calculation Method. However, changing material properties during the calculation, as needed for the Changing Stiffness Method, is not straightforward in ABAQUS.

One possibility to simulate the change on material properties is given by the user subroutine USER DEFINED FIELD. This is done in the Changing Stiffness Method to simulate the construction or activation of support elements (shotcrete shell and inner liner). First, the support elements are included in the numerical model with a very low Young's Modulus. They can be seen as deactivated. On basis of this very low Young's Modulus, nearly no stresses exists in the support elements during the first reduction of the reaction forces. In other words, the support elements can deform without taking stresses. The activation of the support elements is simulated by changing their Young's Moduli. This change leads to stresses on the support. Displacements of support elements which occur with a very low Young's Modulus are considered. As a result of this behavior, a stress-free activation of the support elements cannot be performed.

This thesis is based on the Four Calculation Method. It is not the purpose of this thesis to investigate complex material formulations. Indeed, the aim of this thesis is to simulate a deterioration of the shotcrete shell under consideration of the combined system, ground plus support elements. Furthermore, contact formulation between ground and support

elements, as well as between the support elements should be provided. All these requirements are fulfilled by the Four Calculation Method.

Table 3: Overview tunnel construction methods; 1) Model Change Method; 2) Dummy Node Method; 3) Changing Stiffness Method; 4) Four Calculation Method; X = possible, O = partly possible;

PROPERTIES AND BEHAVIOR	1	2	3	4
Constant thickness of the support elements can be maintained		X	X	X
Contact formulation can be set (i.e. Coulomb friction)			X	X
Accurate geometrical definition of the boundaries of the parts (ground; support elements) is possible. (i.e. no overlapping of several parts)	X		X	X
Realistic behavior in terms of displacement (e.g. pre-displacements, support delay, deformation of the combined system)	O	O		X
Realistic behavior in terms of tangential stresses of the support elements (inner liner; shotcrete shell)	O	O		X
Divergent deformation behavior of tunnel shape can be simulated	X	X	X	

2.7 Simulation of deterioration of the shotcrete shell

The deterioration of the shotcrete is investigated. In addition, also investigated are the effects of different Poisson's ratios (ν), element types (CPE4 and CPE8R) as well as simulations with and without the Coulomb (C) constitutive law. The numerical model consists of three parts, the ground (GROUND), the shotcrete shell (SHOT), and the inner liner (LINER). The variation of the Poisson's ratio and the Coulomb constitutive law applies only to the material parameters of the GROUND, whereas the variation of the element type applies to all three parts (GROUND, SHOT and LINER).

The degradation of material properties is simulated using the user subroutine USER DEFINED FIELD. Thereby, material properties are linked to field variables. These field variables are related to the calculation steps:

- STEP-1 to STEP-8: Simulation of the tunnel construction
- STEP-9: Idle step between construction and deterioration part
- STEP-10 to STEP-18: Simulation of the deterioration of the shotcrete shell

The deterioration is assumed to be linear. Accordingly, the material properties are reduced by 10% in each step of the calculation, beginning with step-10. For this investigation the deterioration of the Young's modulus (E) and the deterioration of the compressive strength (f_C) are simulated.

The following is an overview of the applied deterioration methods shown:

- Young's Modulus (E)
- Compressive strength (f_C)
- Young's Modulus plus compressive strength (E & f_C) simultaneously

Table 4 shows the applied values of E and f_C related to the several calculation steps.

When the deterioration is simulated by reducing the compressive strength, a linearly elastic – perfectly plastic (LE-PP) material behavior for the shotcrete is assumed. The deterioration of the Young's Modulus is simulated based on a linear elastic (LE) material behavior. In a third case, the degradation of the Young's Modulus simultaneous with the degradation of the compressive strength is analyzed. This is based on a linearly elastic – perfectly plastic material behavior.

Table 4: Deterioration of Young's Modulus (E) and compressive strength (f_C) of the shotcrete shell; 10% reduction of E and f_c per step; this table is valid for three cases; note that in Case 1 only the Young's modulus, in Case 2 only the compressive strength and in Case 3 the Young's modulus and the compressive strength are degraded simultaneously;

STEPS	DETERIORATION	E (GPa)	f_C (MPa)
STEP-9	0%	15.0	20.0
STEP-10	10%	13.5	18.0
STEP-11	20%	12.0	16.0
STEP-12	30%	10.5	14.0
STEP-13	40%	9.0	12.0
STEP-14	50%	7.5	10.0
STEP-15	60%	6.0	8.0
STEP-16	70%	4.5	6.0
STEP-17	80%	3.0	4.0
STEP-18	90%	1.5	2.0

Table 5 shows an overview of the combinations. The first column shows a numbering of the combinations which is quoted in subsequent chapters. The second column shows the applied deterioration method. Either the Young's modulus or the compressive strength or both material properties are degraded simultaneously. The third column shows the applied element type. The fourth column shows the applied Poisson's ratio. Either a uniform stress state with a Poisson's ratio of $\nu = 0.5$ or a Poisson's ratio of $\nu = 0.4$ are investigated. The last three columns, at the right side, show the applied material behavior and if a Coulomb constitutive law is used or not.

Table 5: Combinations of numerical calculations – investigation in deterioration behavior of shotcrete; E – Young's Modulus, f_c – compressive strength, CPE4 – 4-node plane strain elements, CPE8R – 8-node plane strain elements with reduced integration, LE – linear elastic, LE-PP – linearly elastic – perfectly plastic, (C) – Coulomb constitutive law

Combination	Deterioration	Element Type	Poisson's ratio (ν)	Material Behavior & Constitutive Law		
				GROUND	SHOT	LINER
C01	E	CPE4	0.5	LE	LE	LE
C02	E	CPE4	0.4	LE	LE	LE
C03	f_C	CPE4	0.5	LE	LE-PP	LE
C04	f_C	CPE4	0.4	LE	LE-PP	LE
C05	E & f_C	CPE4	0.5	LE	LE-PP	LE
C06	E & f_C	CPE4	0.4	LE	LE-PP	LE
C07	E	CPE8R	0.5	LE	LE	LE
C08	E	CPE8R	0.4	LE	LE	LE
C09	f_C	CPE8R	0.5	LE	LE-PP	LE
C10	f_C	CPE8R	0.4	LE	LE-PP	LE
C11	E & f_C	CPE8R	0.5	LE	LE-PP	LE
C12	E & f_C	CPE8R	0.4	LE	LE-PP	LE
C13	E	CPE4	0.5	LE-PP (C)	LE	LE
C14	E	CPE4	0.4	LE-PP (C)	LE	LE
C15	f_C	CPE4	0.5	LE-PP (C)	LE-PP	LE
C16	f_C	CPE4	0.4	LE-PP (C)	LE-PP	LE
C17	E & f_C	CPE4	0.5	LE-PP (C)	LE-PP	LE
C18	E & f_C	CPE4	0.4	LE-PP (C)	LE-PP	LE

3 RESULTS

This chapter shows the results. The interpretation and comments of the results can be obtained from chapter 4.

The stresses in the inner liner during the deterioration of the shotcrete shell are the main focus of this research. In addition, radial displacements of the tunnel are investigated. Fig. 29 shows the stresses in the support elements (shotcrete shell and inner liner) as well as radial displacements at the spring-line.

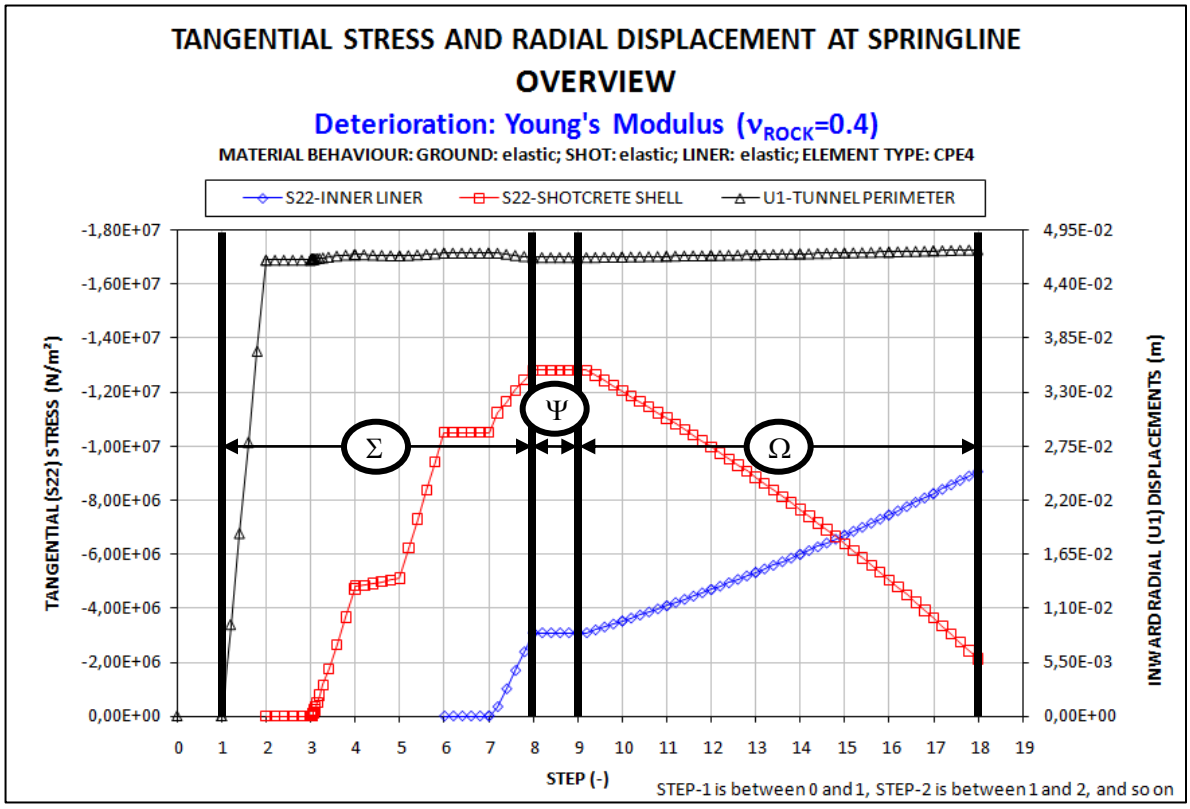

Fig. 29: Overview stresses in inner liner and shotcrete shell as well as radial displacements, all results are obtained at the spring-line; results based on (C02); Zone Σ, Ψ & Ω; [(C02) relates to the specific calculation used to develop this plot – deterioration: Young's modulus, element-type: CPE4, Poisson's ratio: 0.4, material behavior of ground, shotcrete shell and inner liner: linear-elastic; see Table 5]

Zone Σ, step-2 to step-8, represents the tunnel construction. Zone Ψ, step-9, represents an idle step between tunnel construction and the deterioration (No process changes occur in this part) and zone Ω, step-10 to step-18, represents the deterioration of the shotcrete shell and its effects on the inner liner.

Zone Σ & Ω are discussed in subsequent chapters:

- Zone Σ: Tunnel construction (chapter 3.1)
- Zone Ω: Deterioration of the shotcrete shell (chapter 3.2)

Regarding Fig. 29, the stresses were averaged over the liner thickness. The red square (□) line shows the averaged stress in the shotcrete shell. The averaged stresses in the inner liner are shown by the blue diamond (◊) line. The black triangular (Δ) line shows the radial displacements of the tunnel perimeter at the spring-line. All results are based on the combined system, ground plus shotcrete shell plus inner liner. Table 5 provides an overview of all combinations of calculations.

Also, considering Table 5, one can note that every combination of material behavior, finite element type and deterioration is done with a Poisson's ratio of the ground of $\nu = 0.5$ and $\nu = 0.4$.

Subsequently, only results regarding a Poisson's ratio of $\nu = 0.4$ are discussed. Other results can be seen in the appendix.

3.1 Tunnel construction

Fig. 30 shows the averaged stresses in the shotcrete shell and inner liner. The calculations can be divided into three cases:

- Case A: Linear elastic material behavior using CPE4 elements
- Case B: Linearly elastic – perfectly plastic material behavior using CPE4 elements
- Case C: Linear elastic material behavior using CPE8R elements

Note that the linearly elastic – perfectly plastic material behavior is based on the Coulomb failure criterion.

CPE4	4-node bilinear plane strain continuum elements
CPE8R	8-node biquadratic plane strain continuum elements with reduced integration
LE-PP (C)	linearly elastic – perfectly plastic material behavior based on the Coulomb failure criterion
LE	linear elastic material behavior
S22	tangential stress in shotcrete shell and inner liner
U1	radial displacement of tunnel perimeter at spring-line; positive = inward-movement (Fig. 31);

Generally, for all three cases, very similar stress-distributions could be obtained for the shotcrete shell and inner liner. Nevertheless, higher stresses occur, using linearly elastic – perfectly plastic material behavior and the Coulomb failure criterion (Case B), than using a linear elastic material behavior (Cases A and C). Changing the element types (Case A vs. Case C) did not bring any significant changes of the stresses.

Fig. 30 shows the stresses in the shotcrete shell and in the inner liner of all three cases. More iteration steps are needed in step-4 in Case C (see Fig. 30). Smaller iteration steps than usual, are caused by effects of nonlinearities (see also chapter 2.4).

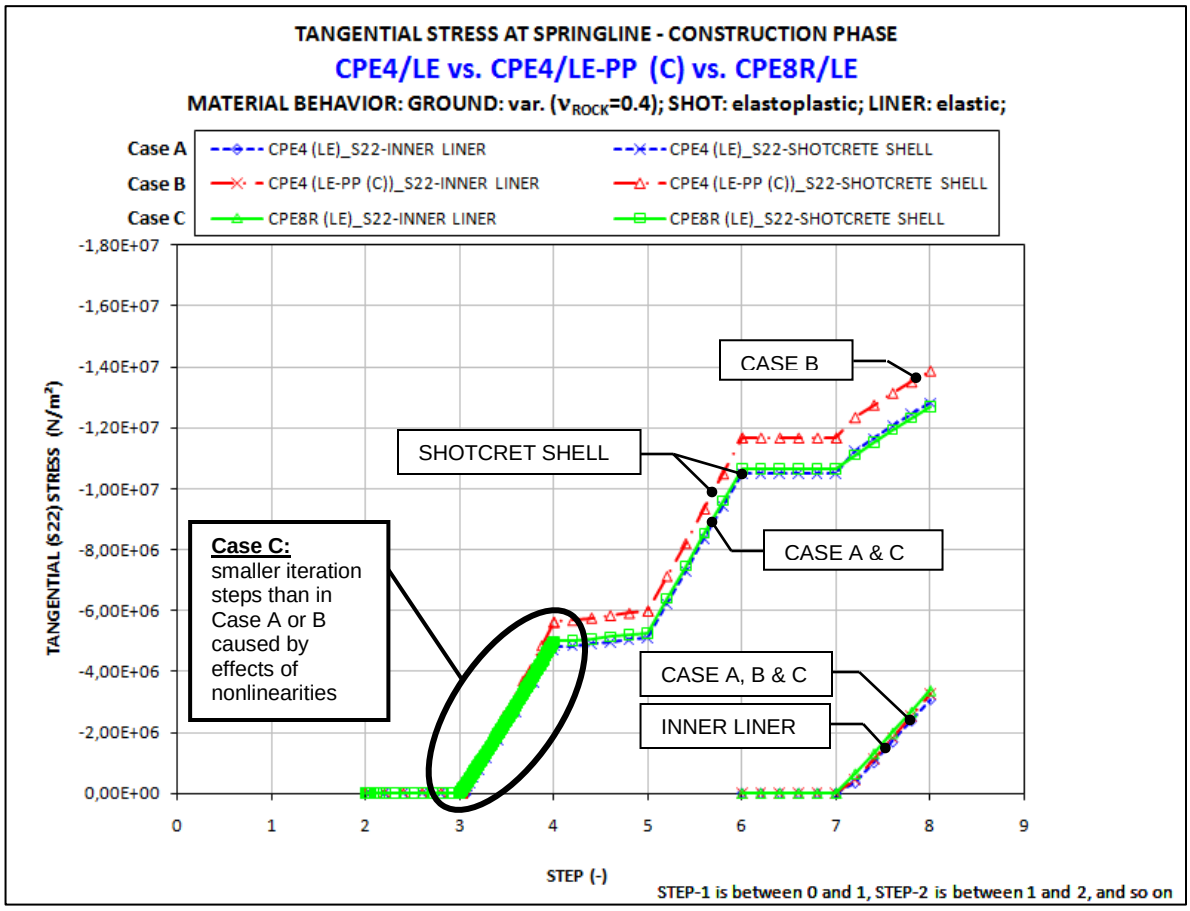

Fig. 30: Comparison of Case A (CPE4 elements & LE material behavior), Case B (CPE4 elements & LE-PP material behavior) and Case C (CPE8R elements & LE material behavior); tangential stresses at spring-line in shotcrete shell and inner liner are shown; Case C: smaller iteration steps than in Case A or B, caused by effects of nonlinearities, explanation of symbols see chapter 3.1; results based on (C06+C12+C18);

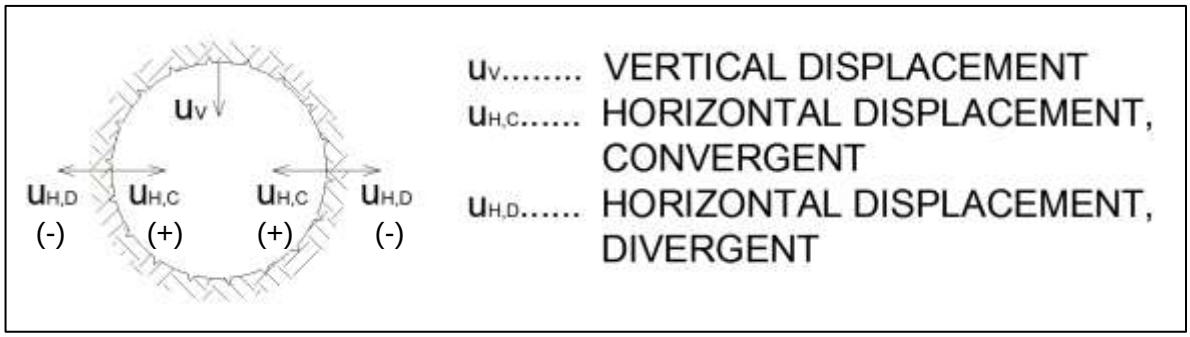

Fig. 31: Convergent and divergent deformation behavior

Fig. 32 shows the radial displacements. The linearly elastic – perfectly plastic investigation considers plastic strains. (See equation (2.1)) As a result, the displacements are larger

than in the linear elastic case. The investigations using different element types brought no significant changes.

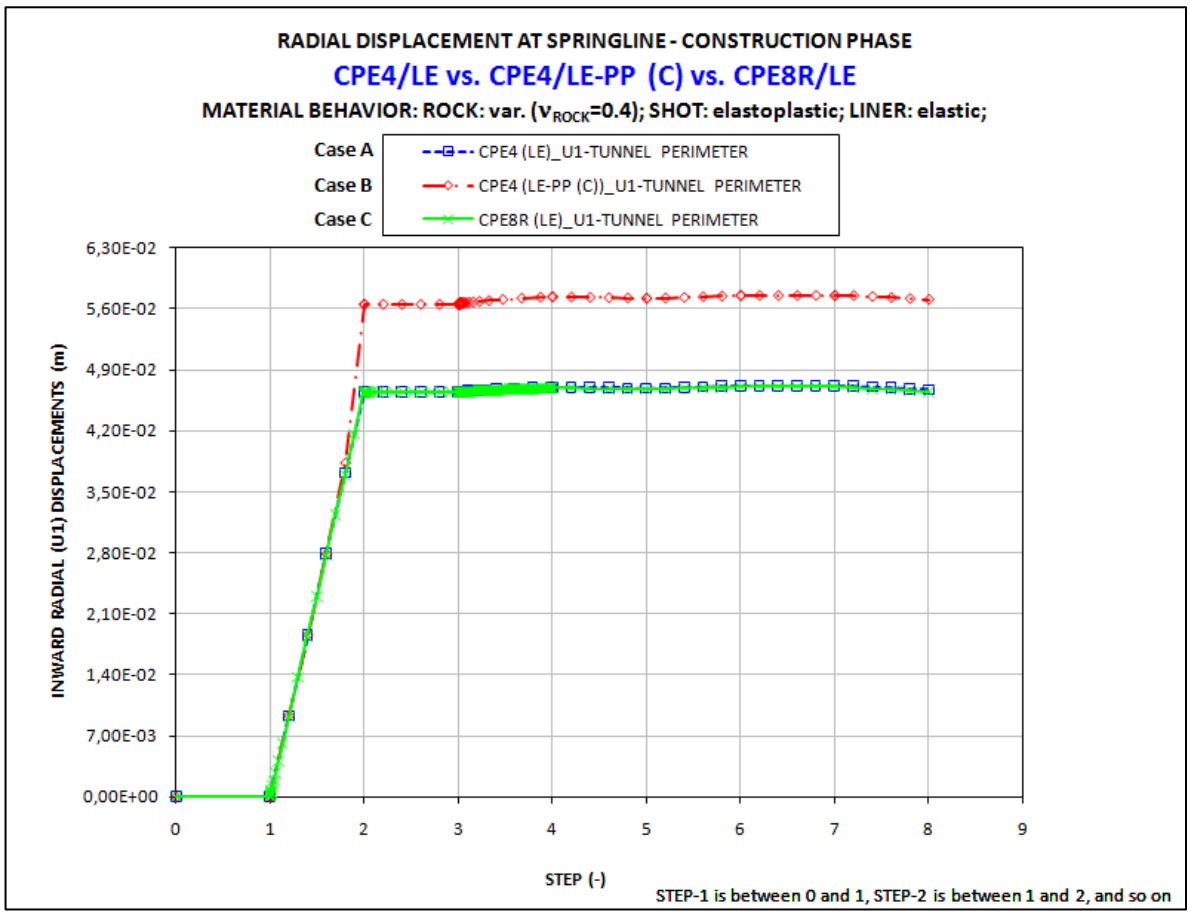

Fig. 32: Comparison of case A (CPE4 elements & LE material behavior), case B (CPE4 elements & LE-PP (C) material behavior) and case C (CPE8R elements & LE material behavior); radial displacements of tunnel perimeter at spring-line; results based on (C06+C12+C18);

Table 6 shows the values of the radial displacements at the spring-line at significant points for the Cases A, B and C. The column “STEP-2”, “STEP-4”, “STEP-7” and “STEP-8” shows the absolute horizontal displacements of the calculation-steps and the columns “Δ” shows the relative displacements between the steps.

There are two points of interests which can be observed from Table 6:

- No plastic deformations of the ground occur after “STEP-4” (after first load reduction with shotcrete shell – see chapter 2.6.4). (Note that plastic deformations can only occur in Case B)
- After including the inner liner (“STEP-7”), the tunnel perimeter at the spring-line moves radially outward (see Fig. 31).

Concerning plastic deformations:

One can observe from the column “Δ” between “STEP-2” and “STEP-4” that the greatest

radial displacements occur in Case B (CPE4 & LE-PP (C)). This is caused by plastic deformations. The column "Δ" between "STEP-4" and "STEP-7" shows that all values are approximately equal and so one can conclude that no plastic deformations occur after "Step-4".

Concerning relative displacements after the inner liner is included ("Step-7"):

One can see in the column "Δ" between "STEP-7" and "STEP-8" that all relative displacements have a negative sign. This means that the tunnel perimeter at the spring-line moves radially outward (divergent deformation behavior – see Fig. 31). Note that this divergent deformation behavior is only relative and occurs only between "Step-7" and "STEP-8". The absolute displacements of the tunnel perimeter at the spring-line at the end of the calculation of the tunnel construction ("STEP-8") are positive and so convergent.

Table 6: Comparison: Radial displacements at the spring-line at several steps – tunnel construction

ν_{GROUND} = 0.4	DISPLACEMENT AT TUNNEL PERIMETER - U1 (m)						
	STEP-2	**Δ**	**STEP-4**	**Δ**	**STEP-7**	**Δ**	**STEP-8**
Case A: CPE4 (LE)	0.046439	*5.59E-04*	0.046999	*1.67E-04*	0.047166	*-4.58E-04*	0.046707
Case B: CPE4 (LE-PP (C))	0.056509	*8.68E-04*	0.057377	*1.49E-04*	0.057526	*-4.64E-04*	0.057063
Case C: CPE8R (LE)	0.046425	*4.88E-04*	0.046912	*1.59E-04*	0.047071	*-5.73E-04*	0.046499

Fig. 33 shows the plastic zone around the tunnel at the end of step-2. Note that the plastic zone is only around spring-line.

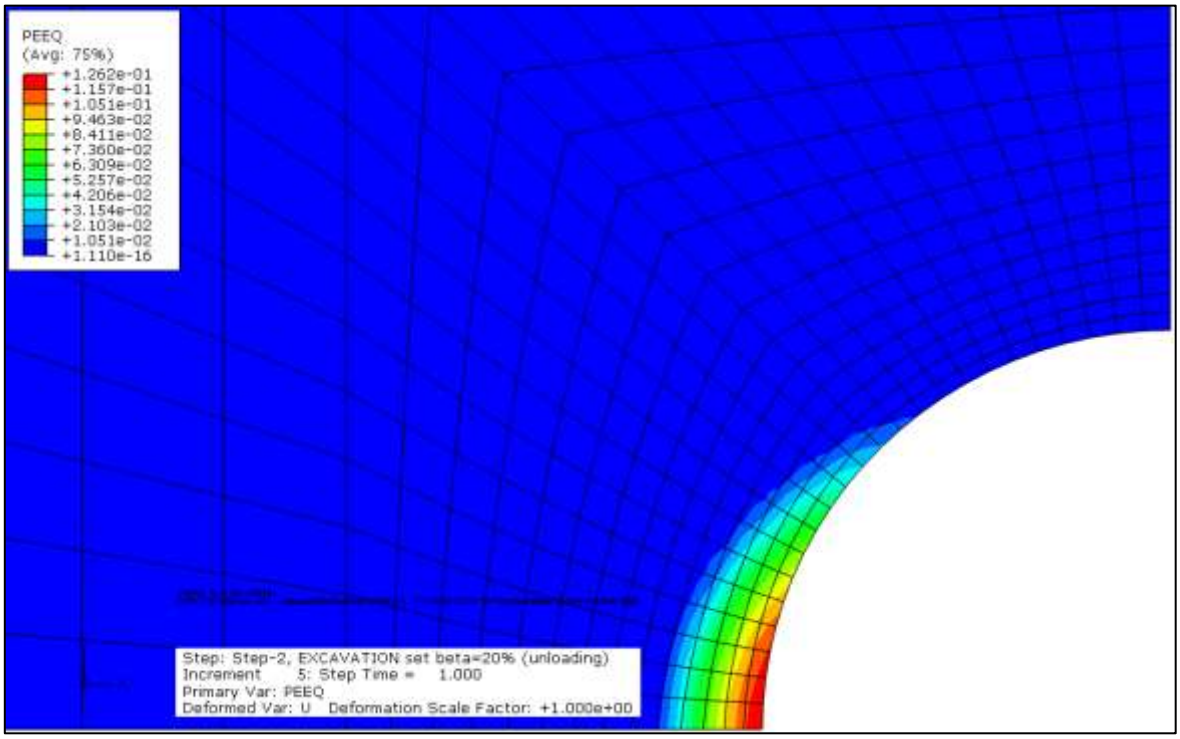

Fig. 33: Equivalent plastic strain at integration points – end of step-2, the plastic zone is only around the spring-line; result based on (C12)

3.2 Deterioration of the shotcrete shell

The evaluation of the deterioration of shotcrete is divided into three parts:

- Stress transfer from the shotcrete shell to the inner liner during the deterioration of shotcrete
- Investigation of the effects of element types (CPE4, CPE8R) and of material behavior (LE, LE-PP (C))
- Investigation of the effects of different deterioration processes of shotcrete

First, the effects of different element types and material behavior are investigated. The calculation can be divided into the same three cases as in chapter 3.1:

- Case A: Linear elastic material behavior using CPE4 elements
- Case B: Linearly elastic – perfectly plastic material behavior using CPE4 elements
- Case C: Linear elastic material behavior using CPE8R elements

The explanation of the abbreviations which are used in the text or in the figures and not following listed can be obtained from chapter 3.1.

SCC	support characteristic curve – stresses in shotcrete shell; inner liner is not included in the calculation of these stresses; no deterioration simulated; only used for a comparison in Fig. 35;
SHOT	shotcrete shell
LINER	inner liner

Table 4 shows the values of the deterioration parameters and their value at each step.

3.2.1 Stress transfer from the shotcrete shell to the inner liner during the deterioration of shotcrete

Fig. 34 illustrates the stress distribution in the shotcrete shell and in the inner liner during deterioration of the shotcrete shell. The deterioration is simulated by a degradation of the Young's modulus. The stress distributions in Fig. 34 are calculated using a linear elastic material behavior and 4-node continuum plane strain elements (Case A).

Following the description of Fig. 34 in detail:

- Blue diamond (◊) curve: Stress distribution in the inner liner during degradation of the shotcrete.
- Red squared (□) curve: Stress distribution in the shotcrete shell during degradation of the shotcrete.
- Green crossed (x) curve: Based on a separate calculation where the inner liner is not included and the shotcrete is not deteriorated. All stresses are carried by the

shotcrete shell. In other words, the stresses of this support characteristic curve are the sum of the stresses in the shotcrete shell and the inner liner after tunnel construction.

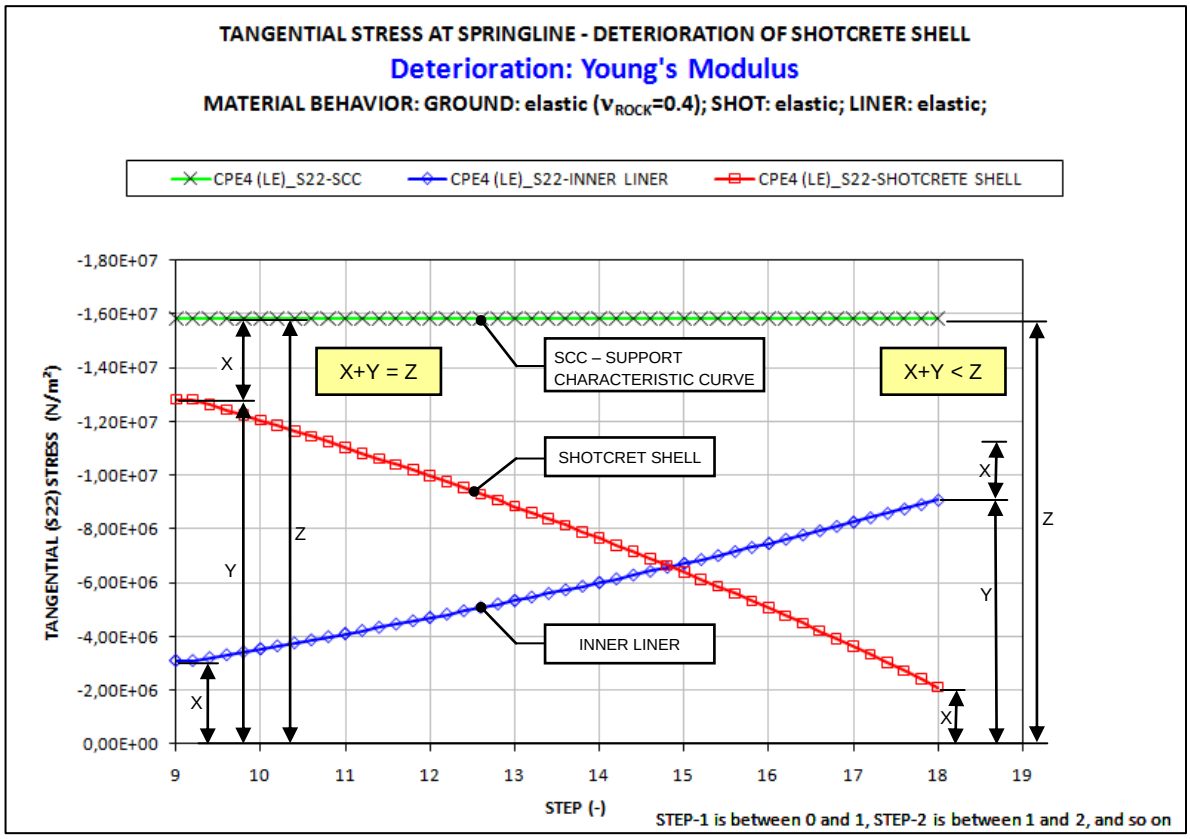

Fig. 34: Transfer of stresses from the shotcrete shell to the inner liner during deterioration of the shotcrete; deterioration caused by degradation of the Young's modulus of shotcrete; support characteristic curve is the sum of the stresses in the shotcrete shell and in the inner liner "Z=X+Y" after tunnel construction (step-9); a compare of the stresses in the shotcrete shell and the inner liner with the support characteristic curve shows, that after deterioration of the shotcrete (step-18), less stresses have to be carried by the support elements (shotcrete shell and inner liner) "Z>X+Y" than at step-9; results based on (C02);

Generally, an increase of the stresses in the inner liner due to the deterioration of the shotcrete shell is obtained. Furthermore, the stresses in the shotcrete shell decrease more than the stresses in the inner liner increase. This can be seen by a comparison of the stresses at step-9 and step-18. If the stresses of the inner liner (X) and the shotcrete shell (Y) at step-9 are summed, the stresses are equal to the stresses of the support characteristic curve (Z). If this is done in step-19, the stresses in the shotcrete shell plus the stresses in the inner liner are less than the stresses of the support characteristic curve ($Z > X + Y$).

3.2.2 Investigation of the effects of element types and of material behavior

Fig. 35 shows a comparison of the effects of different element types and of different material behaviors during the deterioration of the shotcrete:

- Case A: LE material behavior & CPE4 elements
- Case B: LE-PP (C) material behavior & CPE4 elements
- Case C: LE material behavior & CPE8R elements

The deterioration is simulated by a degradation of the Young's modulus.

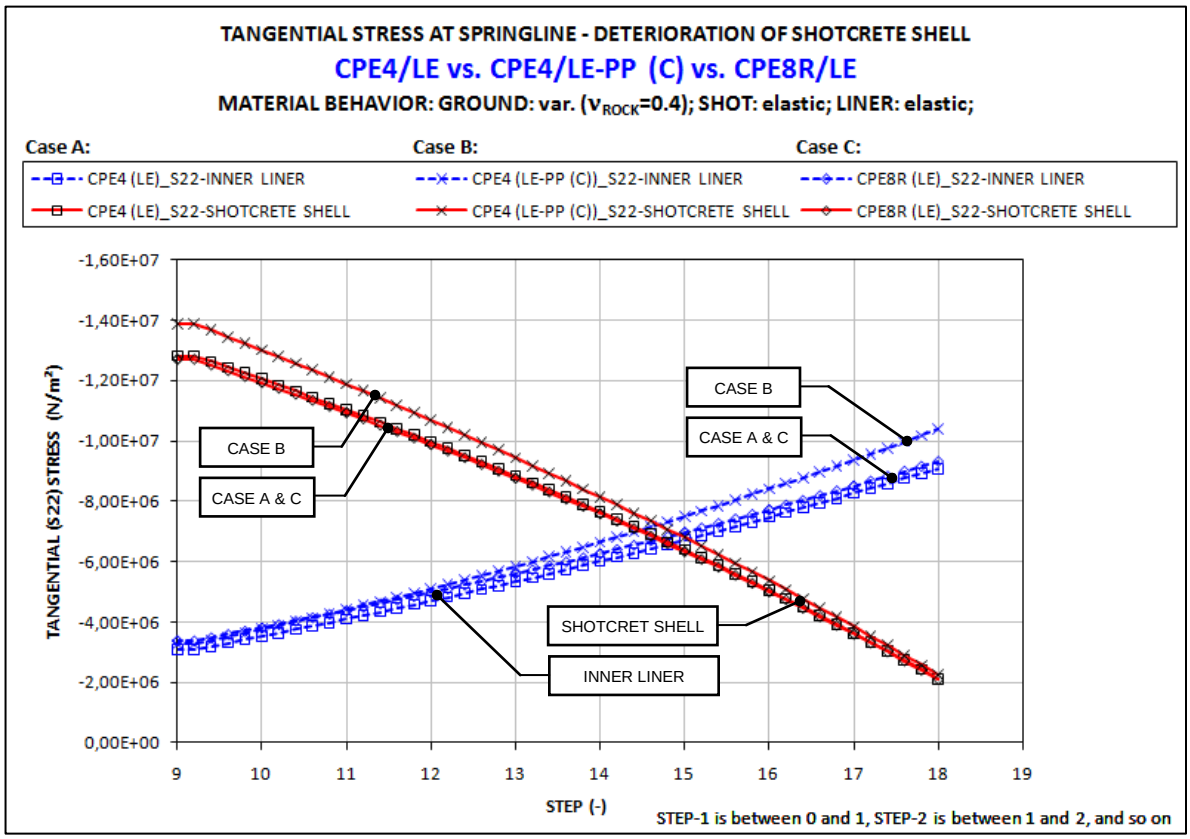

Fig. 35: Comparison of Cases A, B and C; tangential stresses in shotcrete shell and inner liner during deterioration of shotcrete; stresses at spring-line; deterioration caused by degradation of Young's modulus; results based on (C02+C08+C14);

Concerning the results of "Case B", the stresses in the shotcrete shell are higher at the beginning of the deterioration process (step-9) than the stresses in the shotcrete shell which are calculated using "Case A or C". The higher stresses in "Case B" are caused by additional plastic deformations of the ground during the construction of the tunnel (see chapter 3.1 and Fig. 30). Furthermore, one can observe that at the end of the deterioration process (step-18), all stresses in the shotcrete shell are approximately equal (Case A, B & C).

Concerning the load transfer from the shotcrete shell to the inner liner, one can conclude higher stresses in the inner liner at the end of the deterioration process (step-18) using a linearly elastic – perfectly plastic material behavior (Case B) instead of using a linear elastic material behavior (Case A & C).

Table 7 shows the values of the radial displacements at the spring-line for all three cases. The deterioration of the shotcrete, which is caused by degradation of the Young's modulus, starts at step-9 and ends at step-18. The absolute values for these steps are shown. The column "Δ" shows the relative displacements between step-9 and step-18. Slightly higher relative displacements can be obtained, using a LE-PP (C) material behavior, than using LE material behavior.

Table 7: Comparison of cases A, B and C; radial displacements of tunnel perimeter at spring-line before (step-9) and after (step-18); deterioration of shotcrete; degradation of E and f_C; inner liner is considered; results based on (C02+C08+C14)

ν_{GROUND} = 0.4	DISPLACEMENT – TUNNEL PERIMETER (m)		
	STEP-9	STEP-18	Δ
Case A: CPE4 (LE)	4.67E-02	4.75E-02	8.01E-04
Case B: CPE4 (LE-PP (C))	5.71E-02	5.80E-02	9.50E-04
Case C: CPE8R (LE)	4.65E-02	4.73E-02	8.14E-04

Considering the stress transfer in Fig. 35 and the results of Table 7, one can speculate that the released stresses of the shotcrete shell, which are caused by deterioration of the shotcrete, are redistributed to the surrounding ground and to the inner liner.

Fig. 36, Fig. 37 and Fig. 38 show the stresses along the circumference of the inner liner. These results are based on the deterioration of the Young's modulus of the shotcrete shell. The dashed lines are the stresses at the outer boundaries, and the solid lines are the stresses at the inner boundaries of the inner liner. These figures show three different stages of deterioration. The green square (□) lines are the stresses at 10% deterioration, the blue diamond (◊) lines are the stresses at 50% deterioration, and the red triangular (Δ) lines are the stresses at 90% deterioration.

Fig. 36 shows the stresses which are obtained by a model based on CPE4 elements and a linear elastic material behavior (Case A). Comparing the stress distributions in the inner liner at a deterioration of 10% with the stress distribution at a deterioration of 90%, one can conclude an increase of the thrusts at the spring-line as well as at the tunnel-crown. The increase of the thrust may be a little bit higher at the spring-line than at the tunnel-crown. Furthermore, one can conclude that the moments in the inner liner change slightly. (See also chapter 3.2.3)

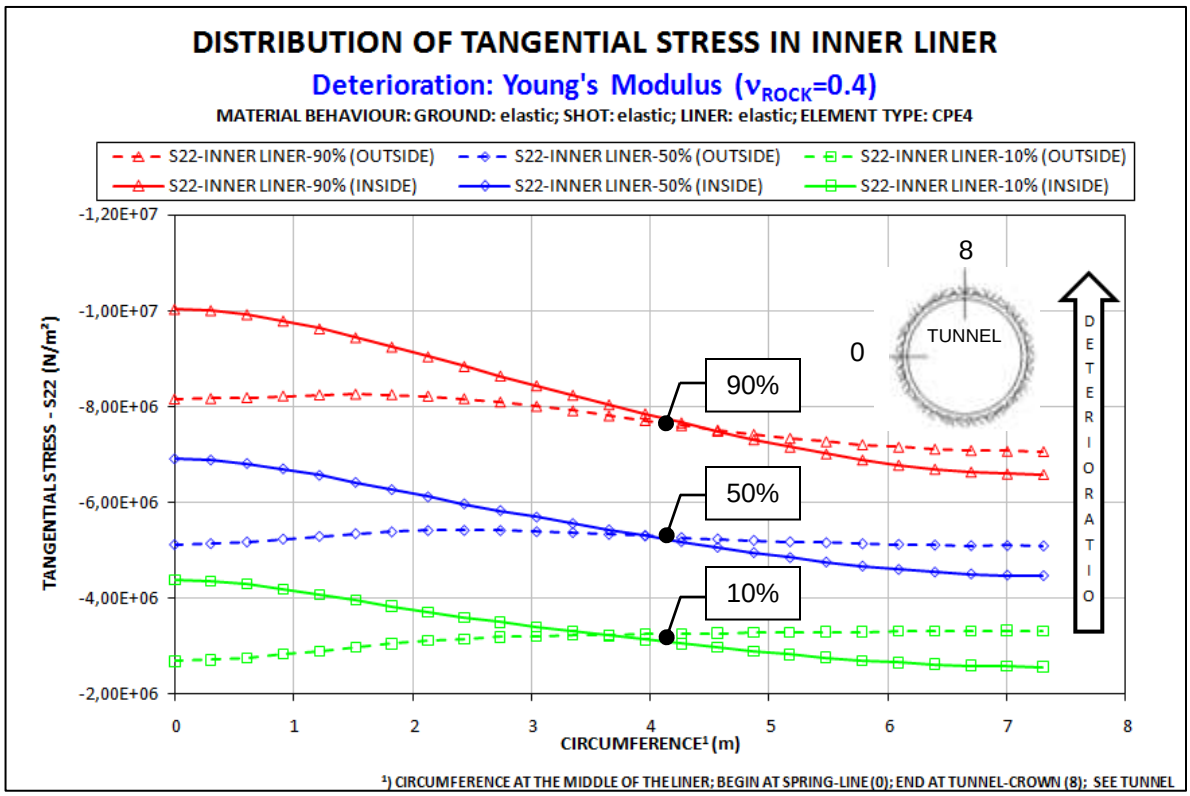

Fig. 36: Stresses at outside and inside along the circumference of the inner liner for several deterioration steps (10%, 50%, 90%); deterioration caused by degradation of Young's modulus; Case A (CPE4 elements, LE material behavior); results based on (C02)

Fig. 37 shows the stresses which are obtained with a model based on CPE4 elements and a linearly elastic – perfectly plastic material behavior (Case B). The difference between the stresses at the spring-line and at the tunnel-crown at a deterioration of 10% is smaller than at a deterioration of 90%. The maximum stress at a deterioration of 90% along the circumference of the liner changes two times from the inside to the outside of the liner. The change of the maximum stress can be explained by a change of the moment distribution. Additional investigations of this behavior have to be done to make more definite statements.

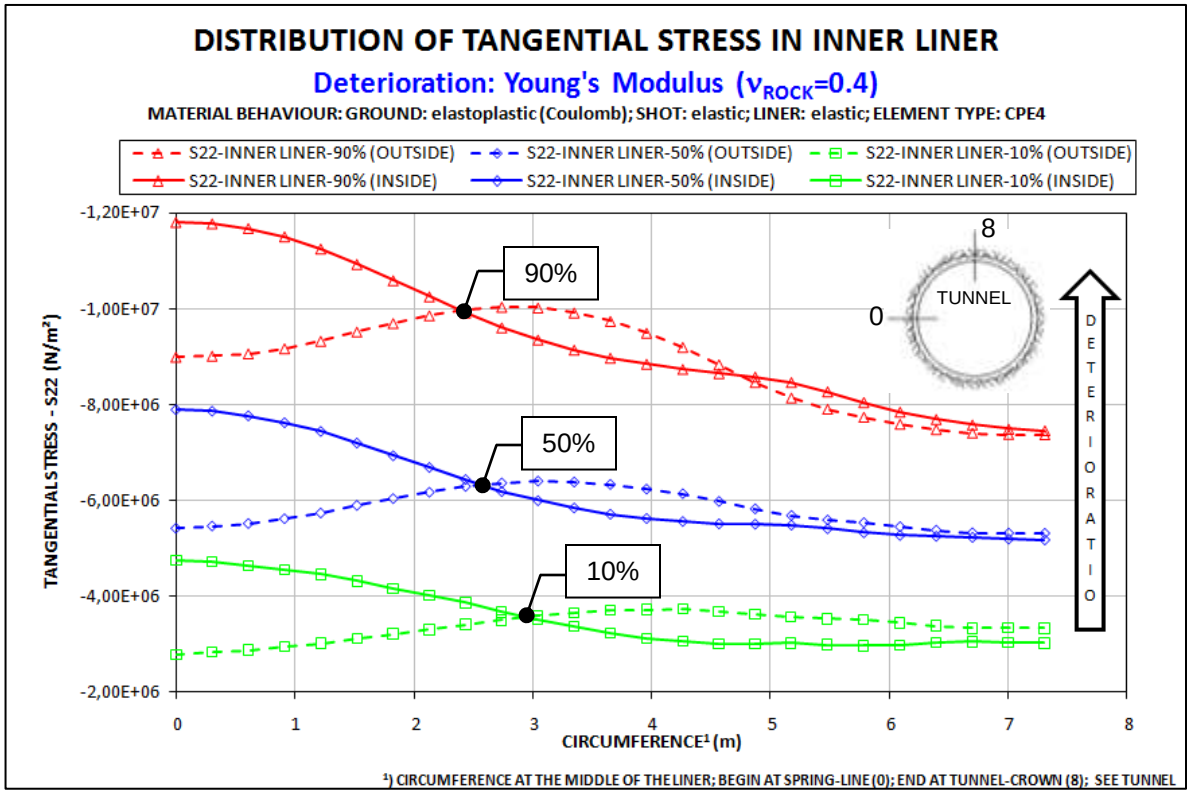

Fig. 37: Stresses at outside and inside along the circumference of the inner liner for several deterioration steps (10%, 50%, 90%); deterioration caused by degradation of Young's modulus; Case B (CPE4 elements, LE-PP material behavior); results based on (C08)

Fig. 38 shows the stresses, which are obtained by a model based on CPE8R elements and a linear elastic material behavior (Case C). The main difference between this (Case C) and the other investigations (Cases A and B) is in the use of 8-node elements instead of 4-node elements. The stresses along the inner liner, which are obtained from Case C are slightly higher than the stresses which are obtained from Case A.

Generally, the stress distribution based on a linear elastic material behavior is similar using 4-node elements or 8-node elements. Additional investigations of a linearly elastic – perfectly plastic material behavior should be performed.

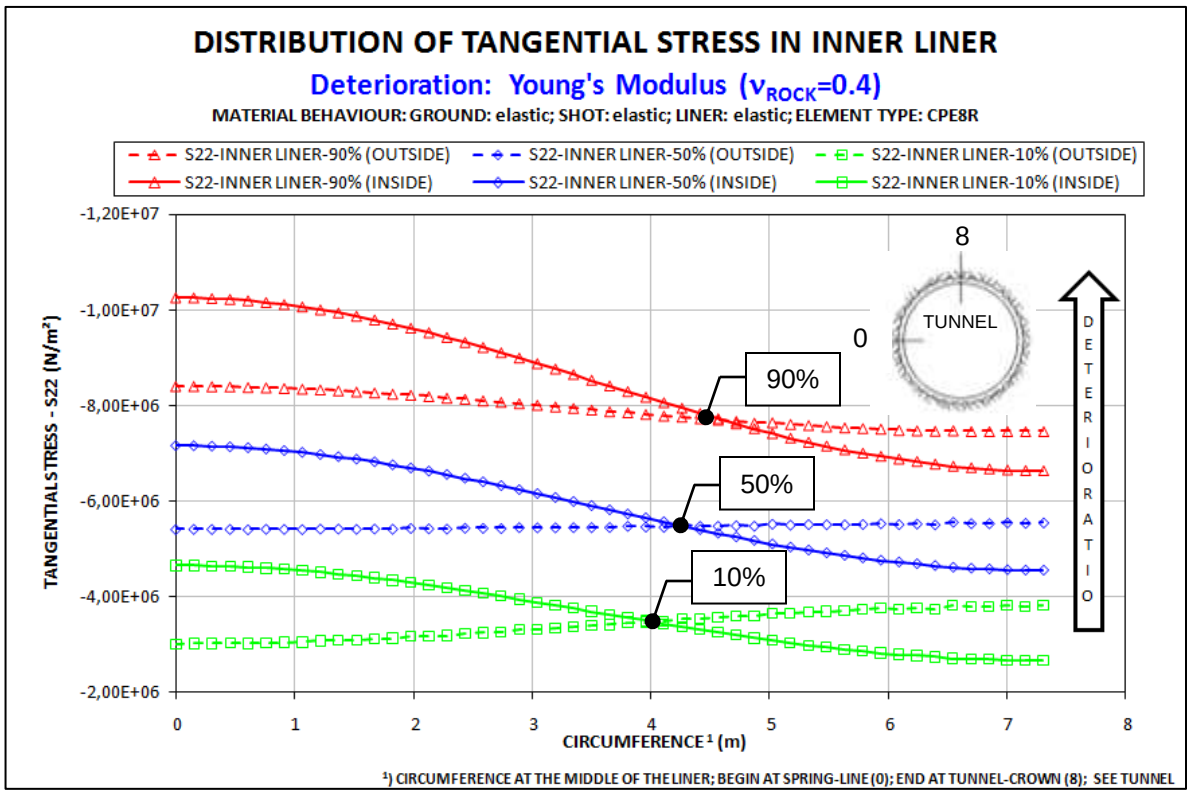

Fig. 38: Stresses at outside and inside along the circumference of the inner liner for several deterioration steps (10%, 50%, 90%); deterioration caused by degradation of Young's modulus; Case C (CPE8R elements, LE material behavior); results based on (C14)

3.2.3 Investigation of the effects of different deterioration processes of shotcrete

Only results for Case A (CPE4 elements, LE material behavior) are discussed here.

As mentioned in chapter 2.7, this investigation uses three different deterioration processes: First, the Young's modulus (E) is degraded, second, the compressive strength (f_C) is degraded, and third, the Young's modulus and the compressive strength (E & f_C) are degraded, simultaneously.

Following the classification of the three deterioration processes (based on Case A):

Case A-1:

- Deterioration of the Young's modulus (E)
- Fig. 39

Case A-2:

- Deterioration of the compressive strength (f_C)
- Fig. 40

Case A-3:

- Simultaneous deterioration of the Young's modulus and the compressive strength (E & f_C)
- Fig. 41

Fig. 42 illustrates that the stresses in Case 1 and Case 3 are exactly the same. In other words, the deterioration of shotcrete caused by lowering the compressive strength has no effect on the combined deterioration in Case 3. Thus, for Case 3 the decisive factor to simulate the deterioration of shotcrete is only the Young's modulus.

Now the question arises, can the compressive strength also become the decisive factor in Case 3? Fig. 43 illustrates that the stresses in the inner liner in Case 1 are always higher than the stresses in the inner liner in Case 2. Accordingly, the stresses in the shotcrete shell in Case 1 are never higher than the stresses in the shotcrete shell in Case 2. One can thus speculate that the compressive strength could become the decisive factor if the stresses in the inner liner in Case 1 are lower than in Case 2, or if the stresses in the shotcrete shell in Case 1 are higher than in Case 2. Additional investigations are necessary to prove this.

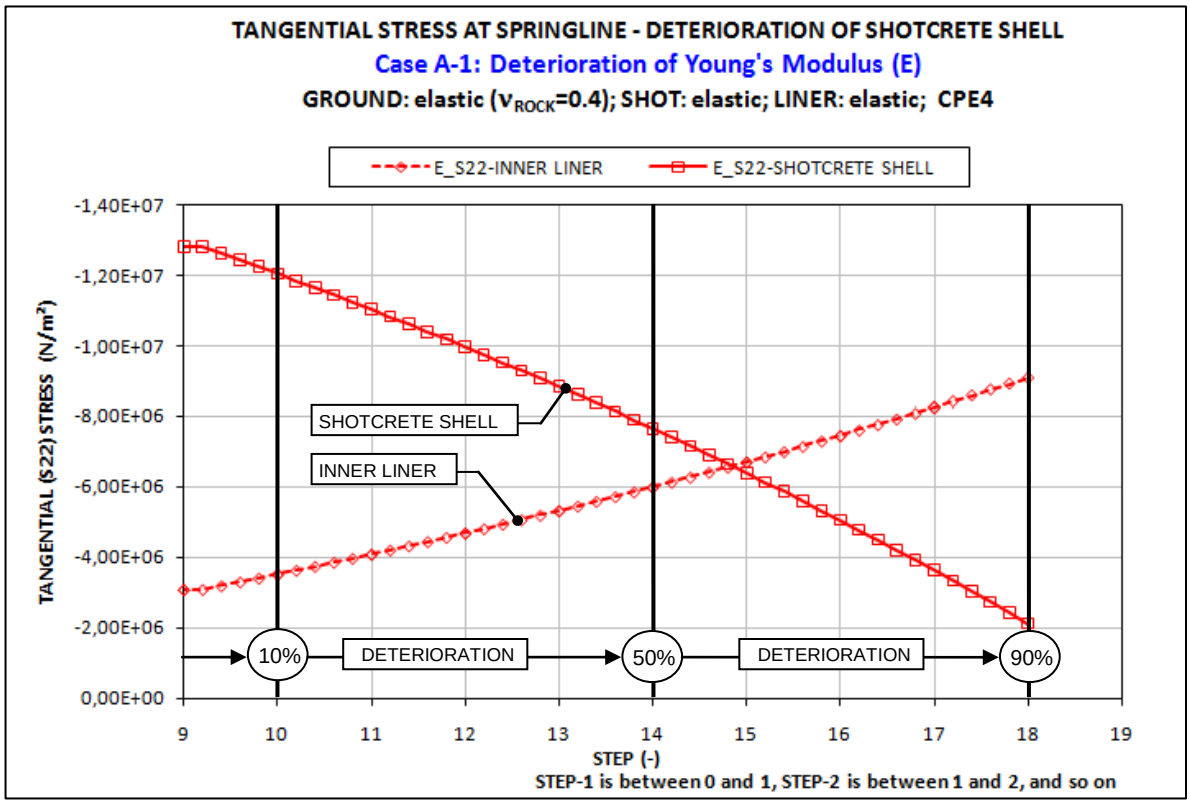

Fig. 39: Case A-1; stress transfer from shotcrete shell to inner liner, caused by deterioration of shotcrete; deterioration caused by degradation of Young's modulus; results based on (C02)

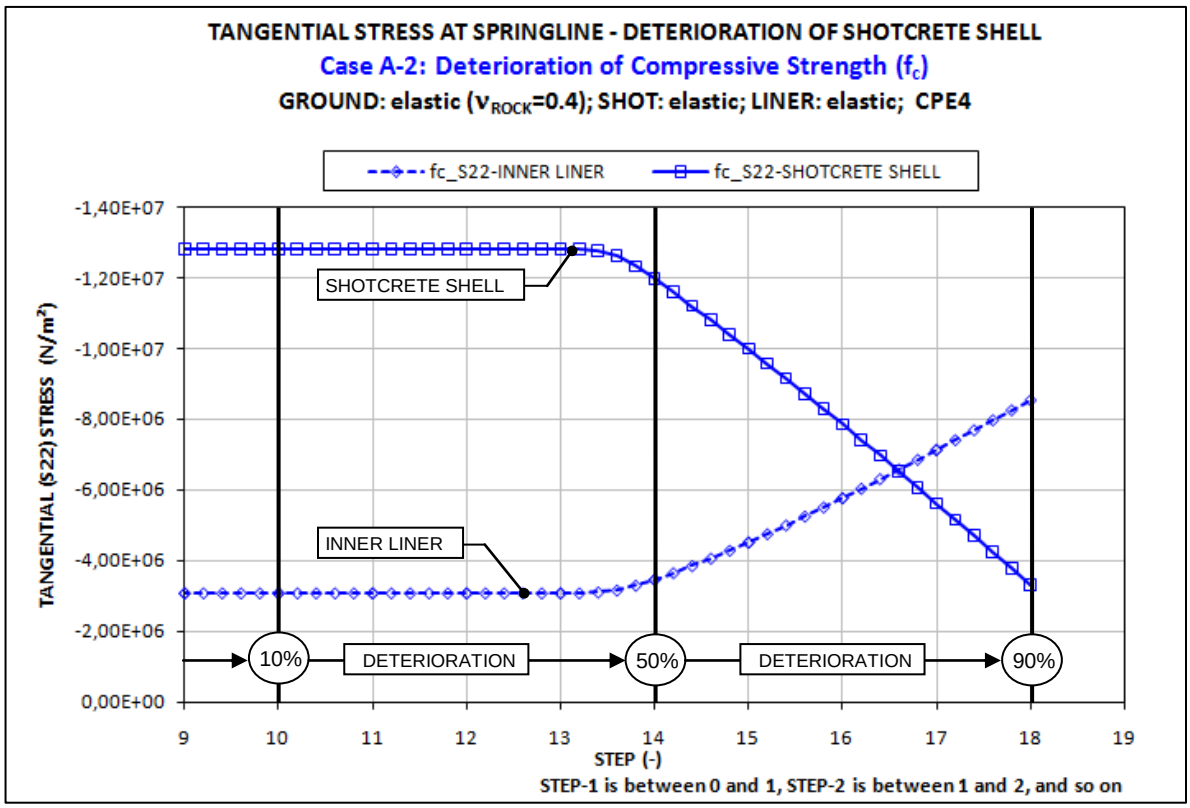

Fig. 40: Case A-1; stress transfer from shotcrete shell to inner liner, caused by deterioration of shotcrete; deterioration caused by degradation of compressive strength; results based on (C04)

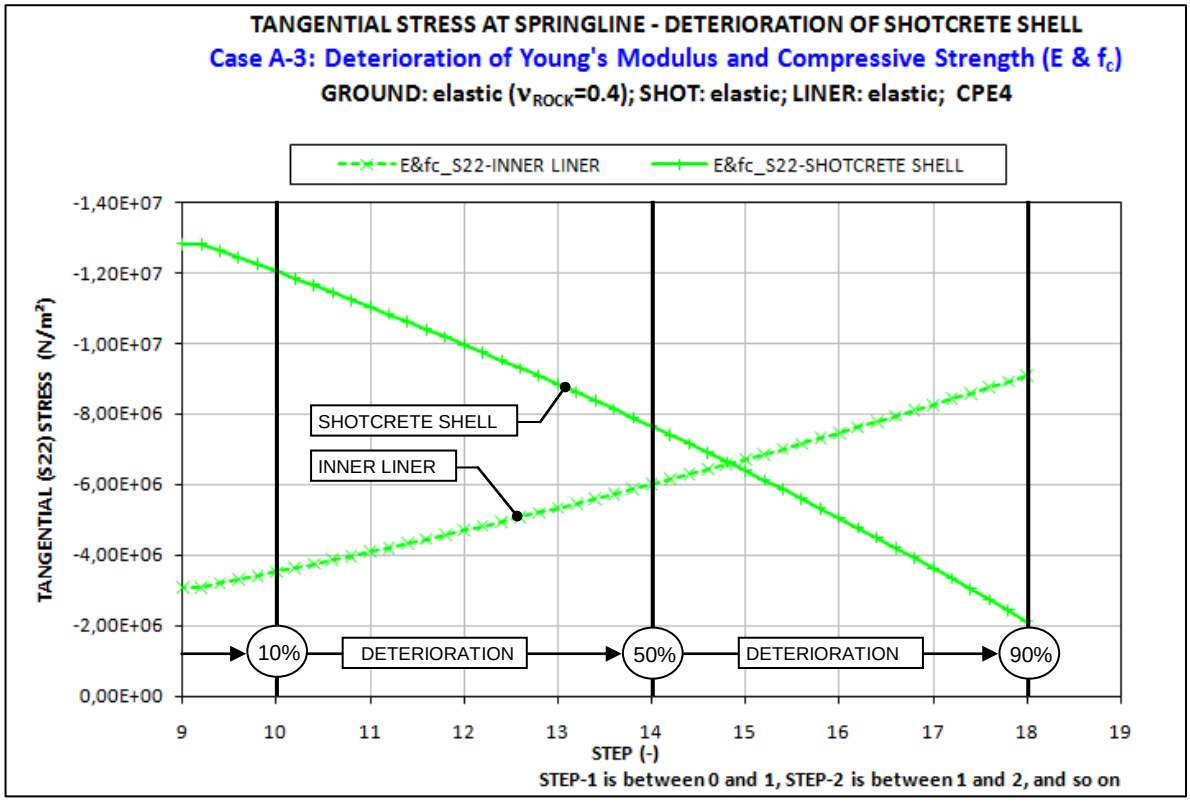

Fig. 41: Case A-1; stress transfer from shotcrete shell to inner liner, caused by deterioration of shotcrete; deterioration caused by degradation of E & f_C; results based on (C02)

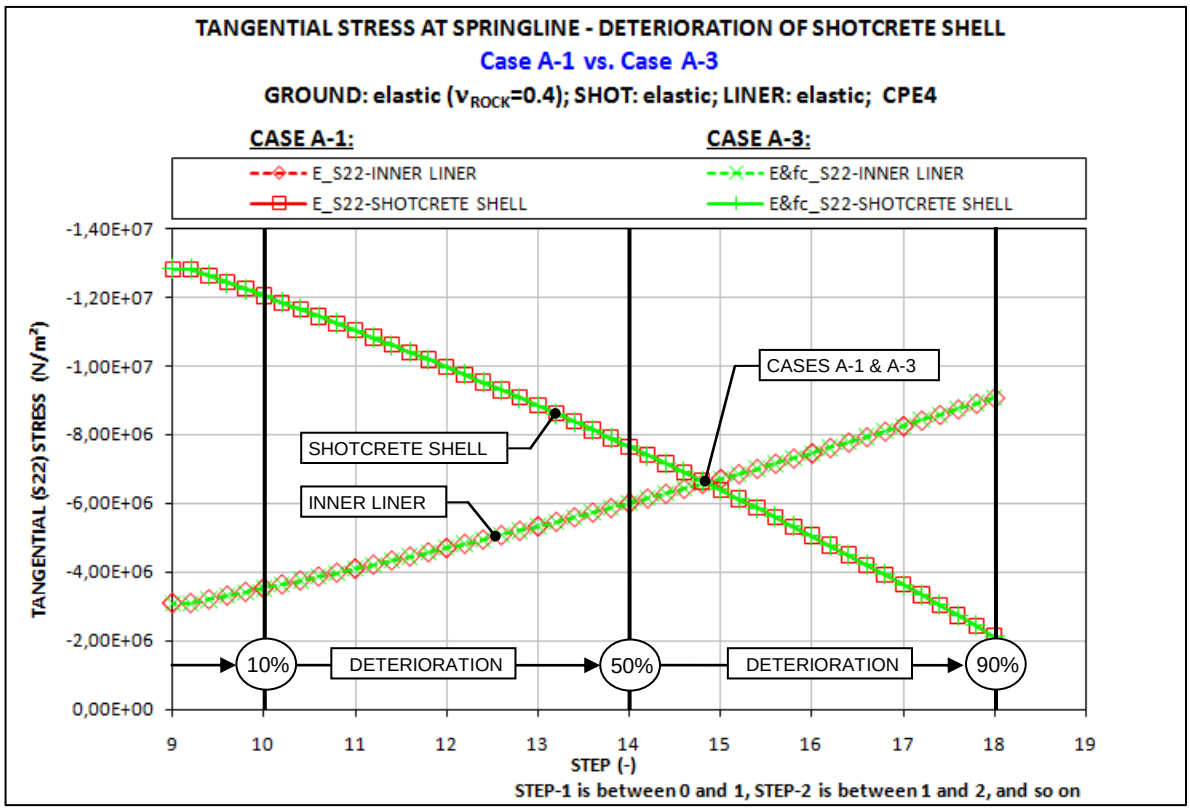

Fig. 42: Comparison of Cases A-1 and A-3; transfer of tangential stresses from shotcrete shell to inner liner caused by deterioration of the shotcrete; results based on (C02+C06)

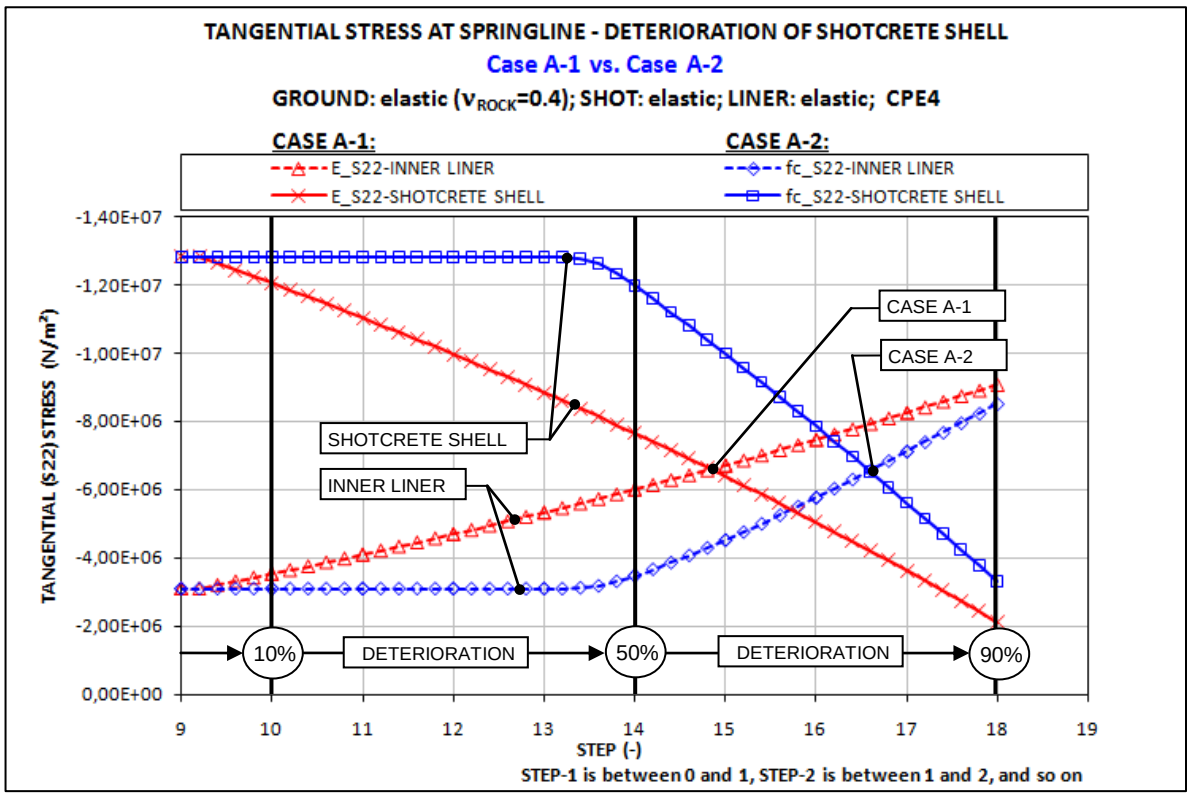

Fig. 43 Comparison of Cases A-1 and A-2; transfer of tangential stresses from shotcrete shell to inner liner caused by deterioration of the shotcrete; results based on (C02+C04)

Fig. 44 shows the corresponding displacements of the tunnel perimeter at the spring-line in these three cases. A behavior similar to the stresses in the inner liner was obtained. Considering Case A-2, between step-9 and step-14 the displacements are nearly zero and between 50% and 90% deterioration, the tunnel perimeter moves radially inward. The displacements of Cases A-1 and A-3 are the same. The tunnel perimeter moves over all steps at a constant rate radially inward (Cases A-1 and A-3).

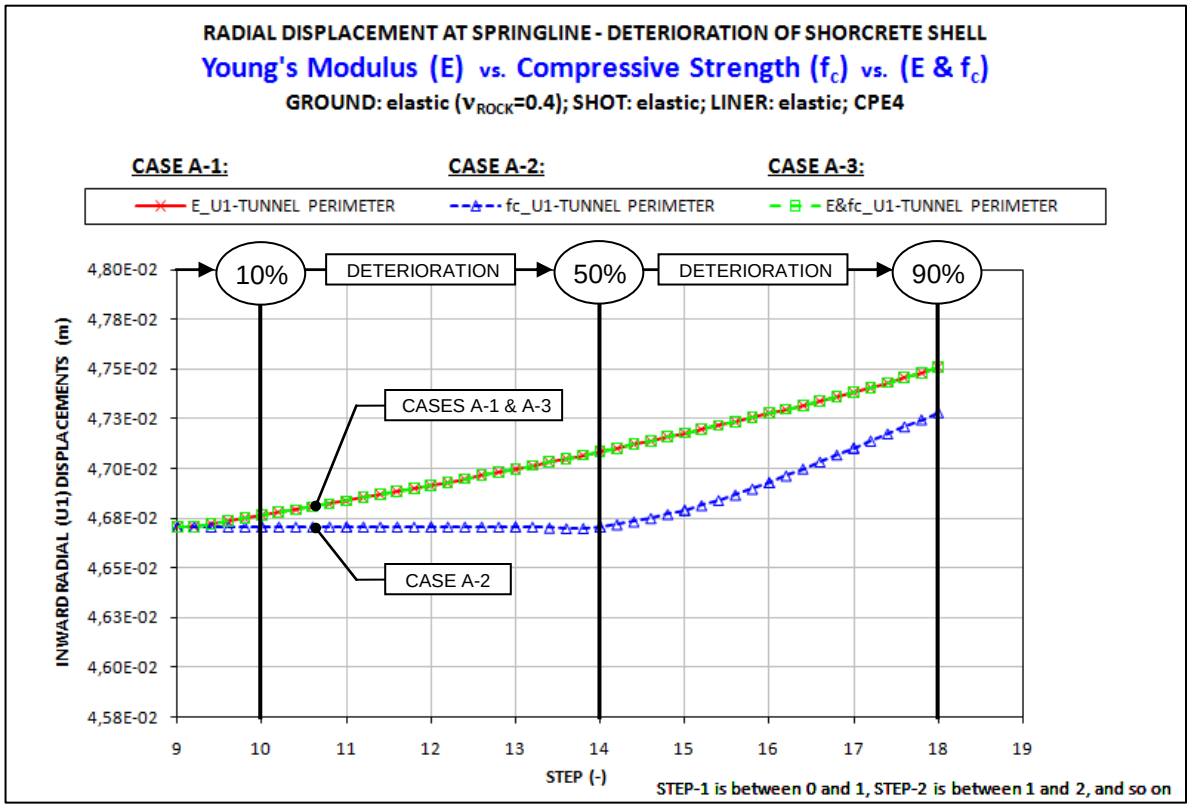

Fig. 44: Comparison of Cases A-1, A-2 and A-3; radial displacements at the spring-line caused by deterioration of shotcrete; positive displacements = inward movement; results based on (C02+C04+C06)

Stress distribution along the circumference of the shotcrete shell and the inner liner

Fig. 45 shows the stresses in the shotcrete shell along the circumference. These results are based on the combined system, ground plus shotcrete shell plus inner liner, and on the deterioration of the Young's modulus and compressive strength (Case A-3). First, a comparison of the stress distributions at deterioration levels of 10%, 50% and 90% is presented. Note that the deterioration of the combined case is equal to the deterioration of the Young's modulus (Case A-1 = Case A-3).

For a deterioration of 10%, greater stresses in the shotcrete shell were obtained at the spring-line than at the tunnel-crown. For a deterioration of 90%, the stresses in the shotcrete shell are at a lower level than at a deterioration of 10%, and the stresses at the

spring-line are approximately equal to the stresses at the tunnel-crown. Therefore, the stresses at the spring-line decrease more significantly than at the tunnel-crown.

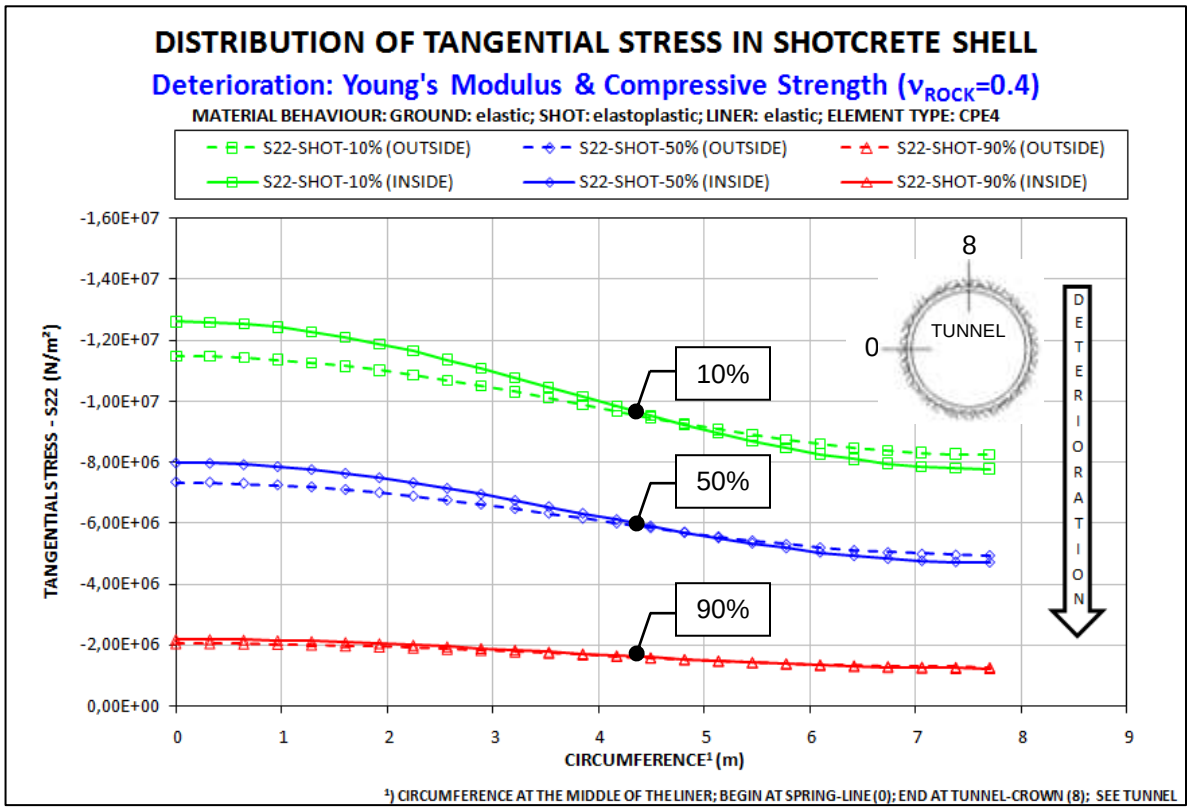

Fig. 45: Stresses at outside and inside along the circumference of the shotcrete shell for several deterioration steps (10%, 50%, 90%); deterioration caused by simultaneously degrading Young's modulus and compressive strength (Case A-3); (results equal to Case A-1); results based on (C06)

Fig. 46 shows the corresponding stresses along the circumference of the inner liner. For a deterioration of 10%, higher outside stresses were obtained at the tunnel-crown than at the spring-line. However, for a deterioration of 90% the outside stresses at the spring-line are higher than the outside stresses at the tunnel-crown. The stresses at the inside of the inner liner at the spring-line are always higher than at the tunnel-crown. Generally, during the deterioration of the shotcrete, a larger increase of the stresses in the inner liner was observed at the spring-line than at the tunnel-crown. Comparing the stresses at the inside and the outside of the inner liner at the spring-line, the stresses at the inside are higher than at the outside and at the tunnel-crown the outside stresses are higher than at the inside. An interpretation of these results follows in chapter 4.

Fig. 47 shows the stresses along the circumference of the shotcrete shell for the deterioration of the compressive strength. The stress distribution at a deterioration of 10% is similar to the 10% deterioration of the combined case (Fig. 45). The stress distribution in the shotcrete shell at a deterioration of 90% is uniform, i.e. the stresses at the spring-line are equal to the stresses at the tunnel-crown. The main decrease of the stresses in the shotcrete shell occurs between 50% and 90% deterioration.

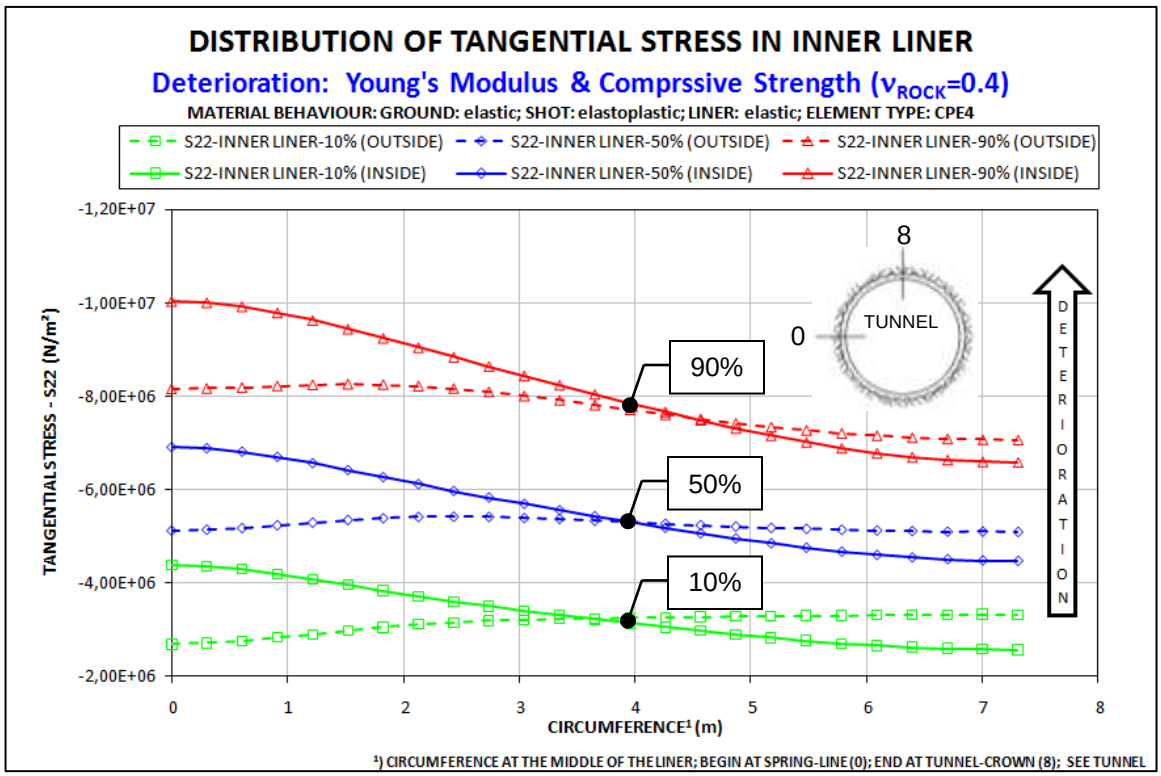

Fig. 46: Stresses at outside and inside along the circumference of the inner liner for several deterioration steps (10%, 50%, 90%); deterioration caused by simultaneously degrading Young's modulus and compressive strength (Case A-3); (results equal to Case A-1); results based on (C06)

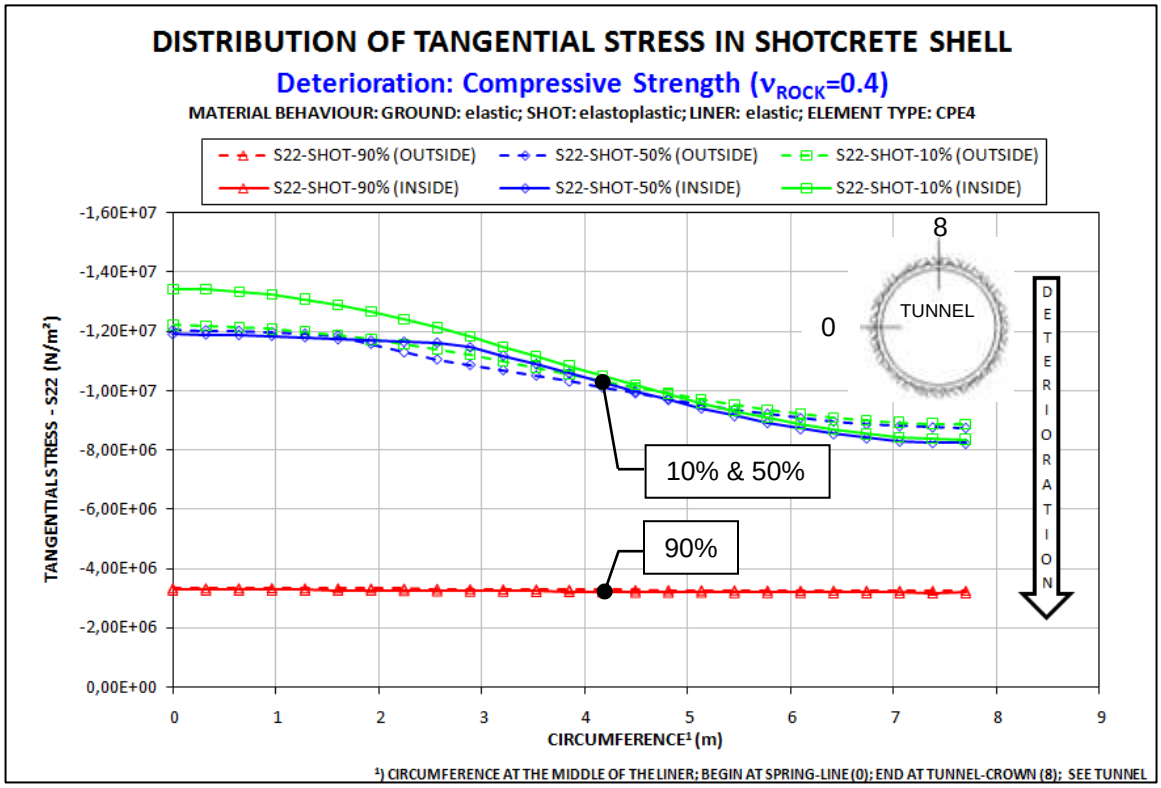

Fig. 47: Stresses at outside and inside along the circumference of the shotcrete shell for several deterioration steps (10%, 50%, 90%); deterioration caused by degradation of compressive strength (Case A-2); results based on (C04)

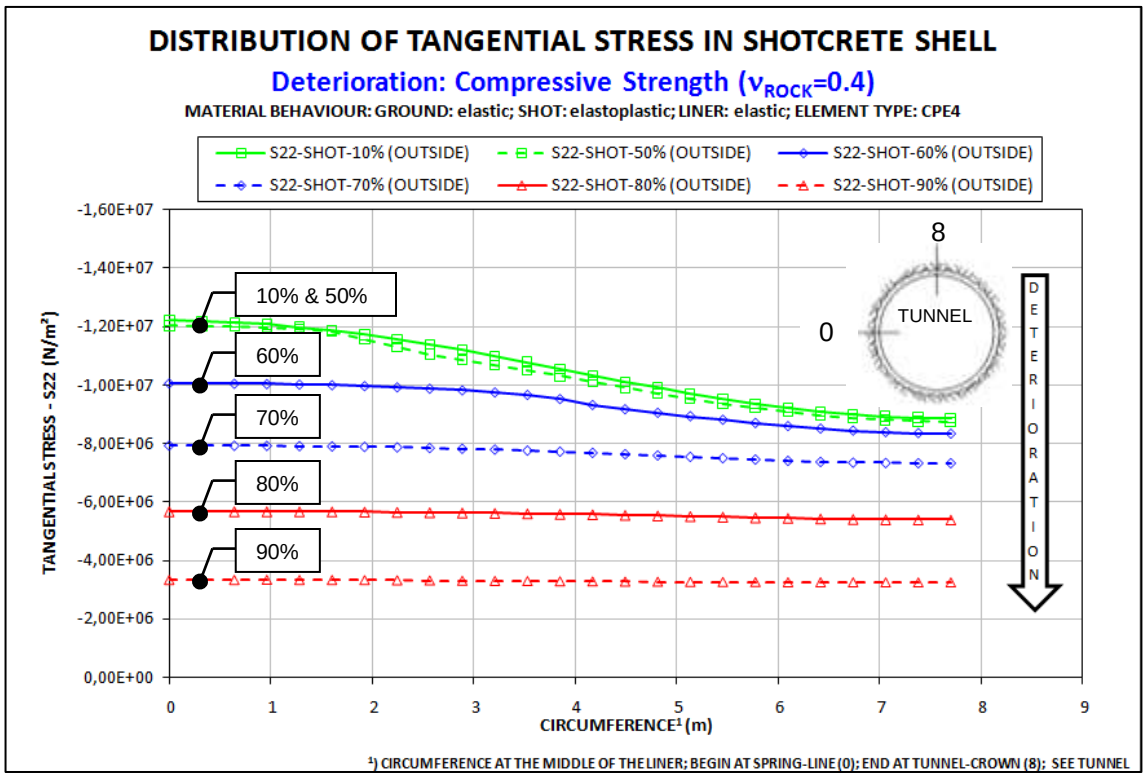

Fig. 48: Outside stresses along the circumference of the shotcrete shell for several deterioration steps (10%, 50%, 60%, 70%, 80%, 90%); deterioration caused by degradation of compressive strength (Case A-2); results based on (C04)

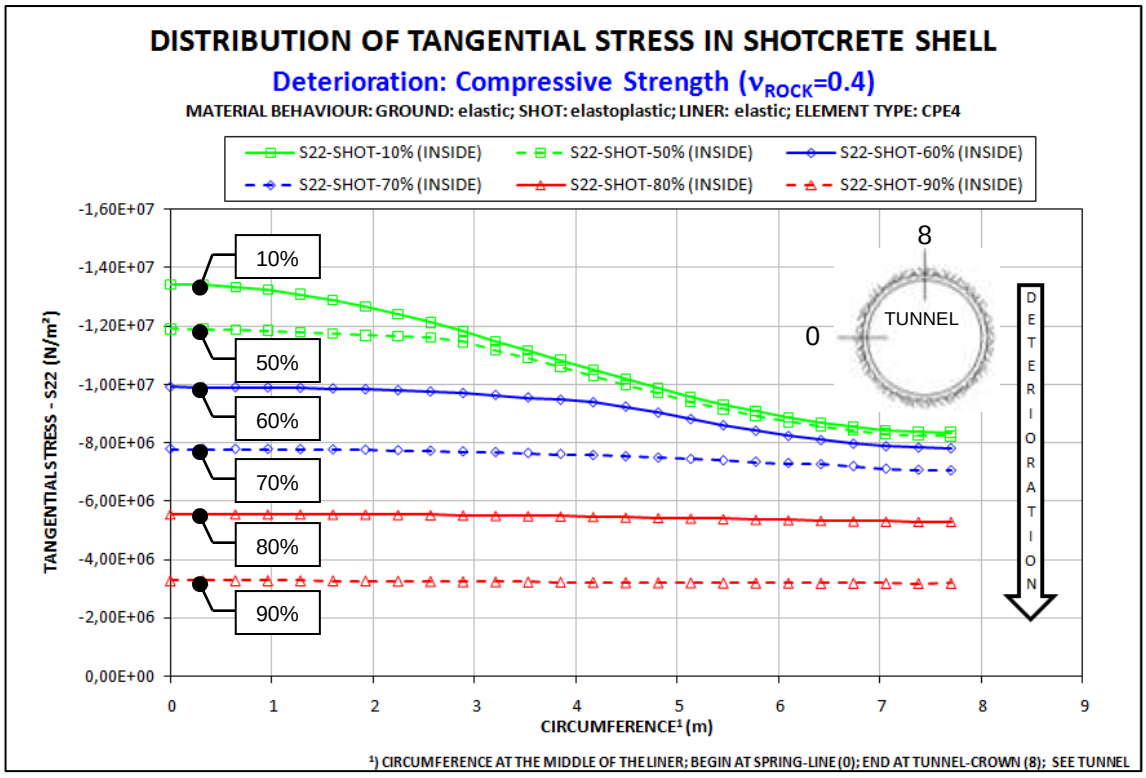

Fig. 49: Stresses at inside along the circumference of the shotcrete shell for several deterioration steps (10%, 50%, 60%, 70%, 80%, 90%); deterioration caused by degradation of compressive strength (Case A-2); results based on (C04)

Comparing Fig. 45 with Fig. 47 one can observe that an uniform stress distribution in the shotcrete shell is only reached by degradation of the compressive strength (Case A-2).

Fig. 48 and Fig. 49 investigate in the degradation of the compressive strength in steps of 10%, from 50% to 90% deterioration. Specifically, the stress distribution at the outside of the shotcrete shell is shown in Fig. 48, and the stress distribution at the inside of the shotcrete shell is shown in Fig. 49.

Fig. 50 shows the stresses along the circumference of the inner liner. These results are based on the deterioration of the compressive strength. Between 10% and 50% deterioration of the shotcrete shell, nearly no rise of the stresses in the inner liner can be observed. To investigate the stress distribution between 50% and 90% deterioration in more detail, Fig. 51 shows the stresses at the outside of the inner liner, and Fig. 52 shows the stresses at the inside of the inner liner. Note that the deterioration between 50% and 90% is shown in steps of 10%.

From zero deterioration to a deterioration of 50%, the stresses on the outside of the inner liner at the spring-line are less than at the tunnel-crown (Fig. 51). At a deterioration of 60%, the stresses at the spring-line are approximately equal to the stresses at the tunnel-crown. At a deterioration of 70% the stresses at the spring-line are greater than the stresses at the tunnel-crown. Note that after a deterioration of 70% the stresses increase at the spring-line by the same amount as at the tunnel-crown. In other words, a more significant increase of the stresses at the spring-line, compared to the tunnel-crown, can only be observed in the beginning of the deterioration process.

The stresses at the inside of the inner liner at the spring-line are always greater than at the tunnel-crown (Fig. 52). Similar to the stresses at the outside of the liner, a greater increase of the stresses at the spring-line can be observed at the beginning of the deterioration process.

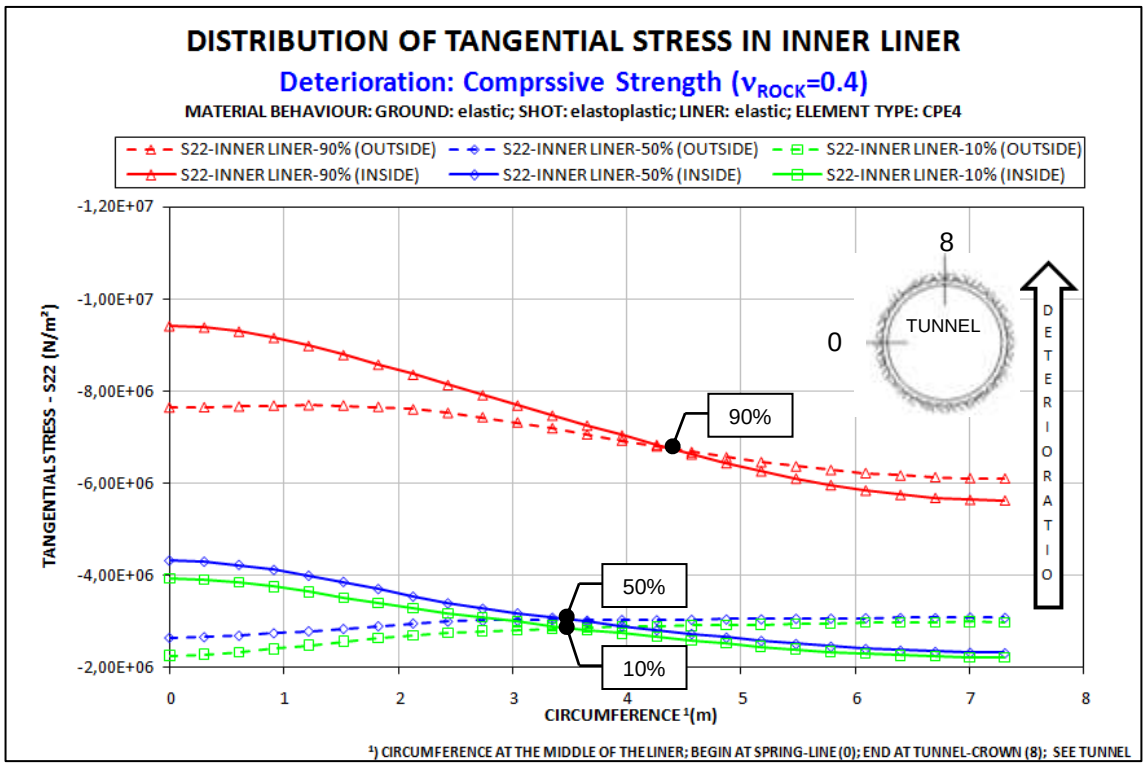

Fig. 50: Stresses at outside and inside along the circumference of the inner liner for several deterioration steps (10%, 50%, 90%); deterioration caused by degradation of compressive strength (Case A-2); results based on (C04)

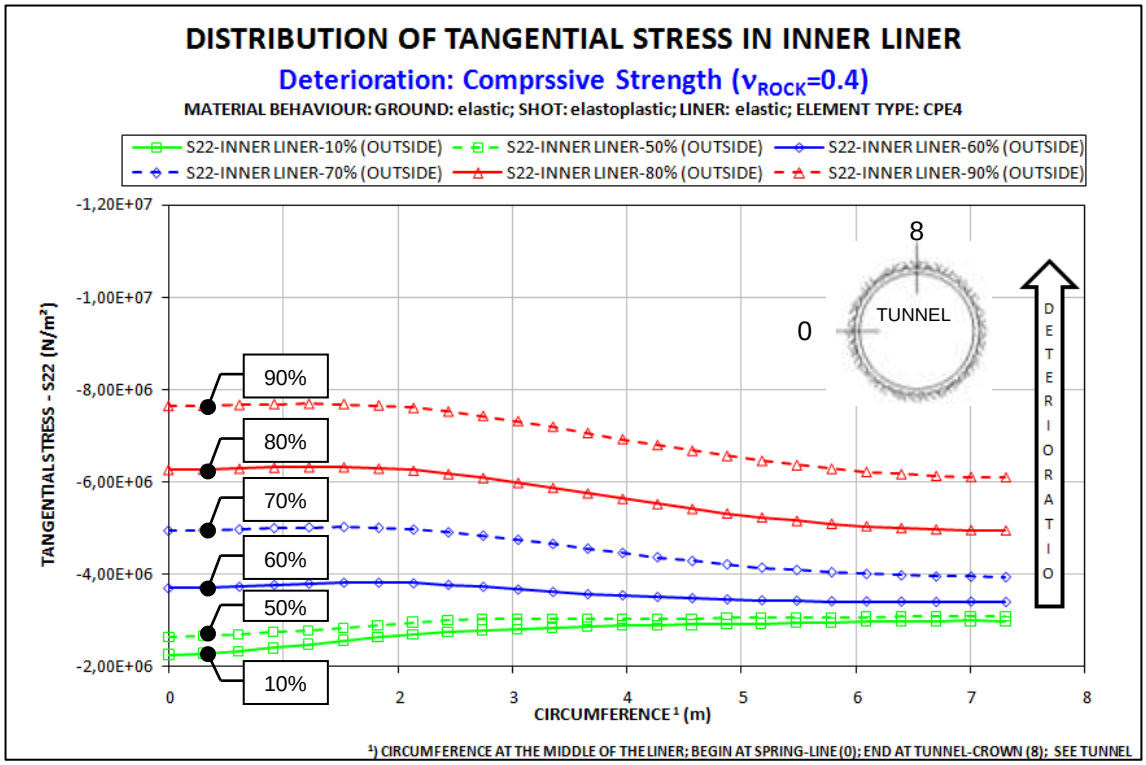

Fig. 51: Stresses at outside along the circumference of the inner liner for several deterioration steps (10%, 50%, 60%, 70%, 80%, 90%); deterioration caused by degradation of compressive strength (Case A-2); results based on (C04)

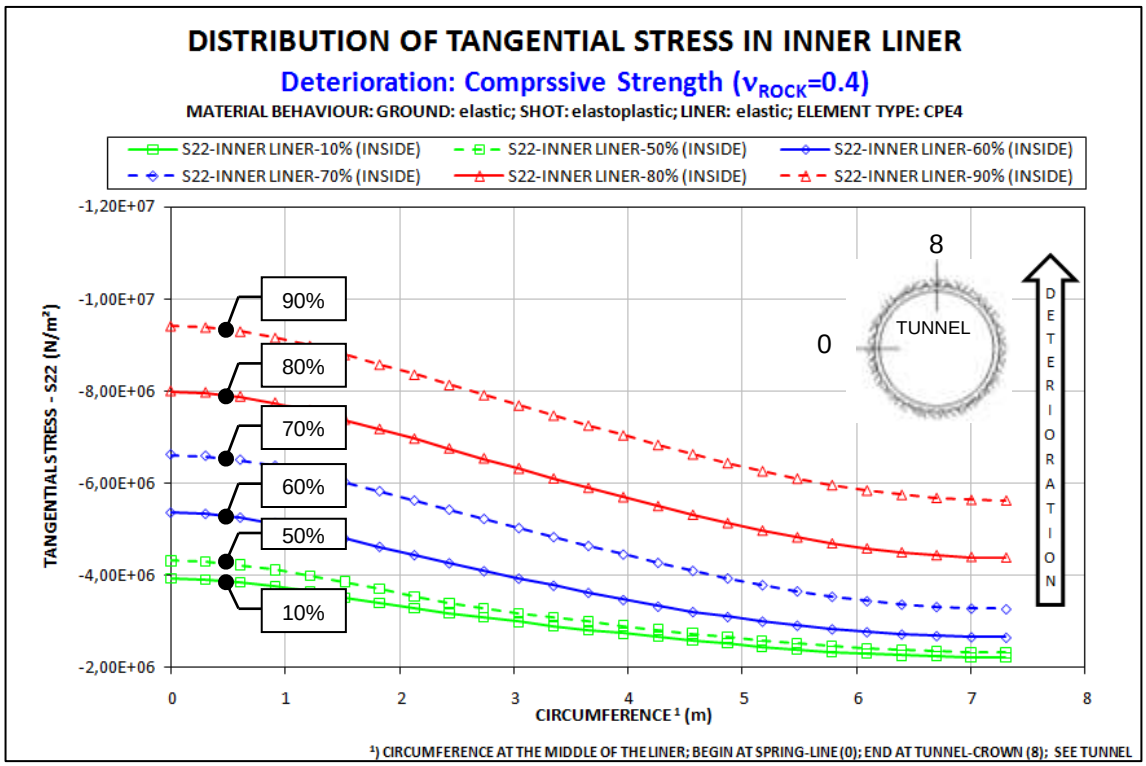

Fig. 52: Stresses at inside along the circumference of the inner liner for several deterioration steps (10%, 50%, 60%, 70%, 80%, 90%); deterioration caused by degradation of compressive strength (Case A-2); results based on (C04)

Thrusts and moments:

Based on the stress distributions along the shotcrete shell and inner liner the thrusts and moments along the circumference of the support elements (shotcrete shell and inner liner) are investigated. The same three deterioration levels as above (10%, 50% and 90%) are considered. All graphs which are subsequently represented are based on a deterioration of the shotcrete caused by degradation of the Young's modulus (Case A-1). Furthermore, a combined system of ground plus shotcrete shell plus inner liner is assumed for all results. Fig. 53 & Fig. 54 represent the thrusts and moments along the circumference of the shotcrete shell, followed by Fig. 55 & Fig. 56 which show the distribution of the thrusts and moments along the inner liner.

Fig. 53 illustrates the distribution of the thrusts in the shotcrete shell during deterioration of the shotcrete. After tunnel construction, the thrusts at the spring-line are higher than at the tunnel-crown. During the deterioration of shotcrete, a higher decrease of the thrusts can be observed at the spring-line than at the tunnel-crown.

Fig. 55 shows the distribution of the thrusts in the inner liner during deterioration of the shotcrete. After the tunnel construction, the thrusts at the spring-line and the tunnel-crown are approximately equal. During the deterioration of the shotcrete, the thrusts at the spring-line increase more than the thrusts at the tunnel-crown.

Comparing the thrusts at the spring-line in the shotcrete shell (Fig. 53) at a deterioration of 10% and the thrusts at the spring-line in the inner liner (Fig. 55) at a deterioration of 90%, one can note higher thrusts in the inner liner after the deterioration of 90% than in the shotcrete shell after a deterioration of 10%. Thus, one can speculate that after deterioration of the shotcrete, the inner liner has to carry more load than the shotcrete shell did after tunnel construction, but one has to be aware that the shotcrete shell has a thickness of 20cm and the inner liner has a thickness of 30cm. Thus, the stresses at the spring-line in the shotcrete shell (Fig. 45) after tunnel construction are higher than the stresses at the spring-line in the inner liner after deterioration (Fig. 38).

Fig. 54 illustrates the distribution of the moments in the shotcrete shell during deterioration of the shotcrete. After tunnel construction, the moments at the spring-line are higher and have another sign than the moments at the tunnel-crown. During deterioration, the moments at the spring-line as well as the moments at the tunnel-crown get reduced.

Fig. 56 shows the distribution of the moments in the inner liner during deterioration of the shotcrete. After the tunnel construction, the moments at the spring-line are higher and have another sign than the moments at the tunnel-crown. During deterioration of the shotcrete, one can observe slightly increasing of the moments in the inner liner at the spring-line as well as slightly decreasing of the moments in the inner liner at the tunnel-crown.

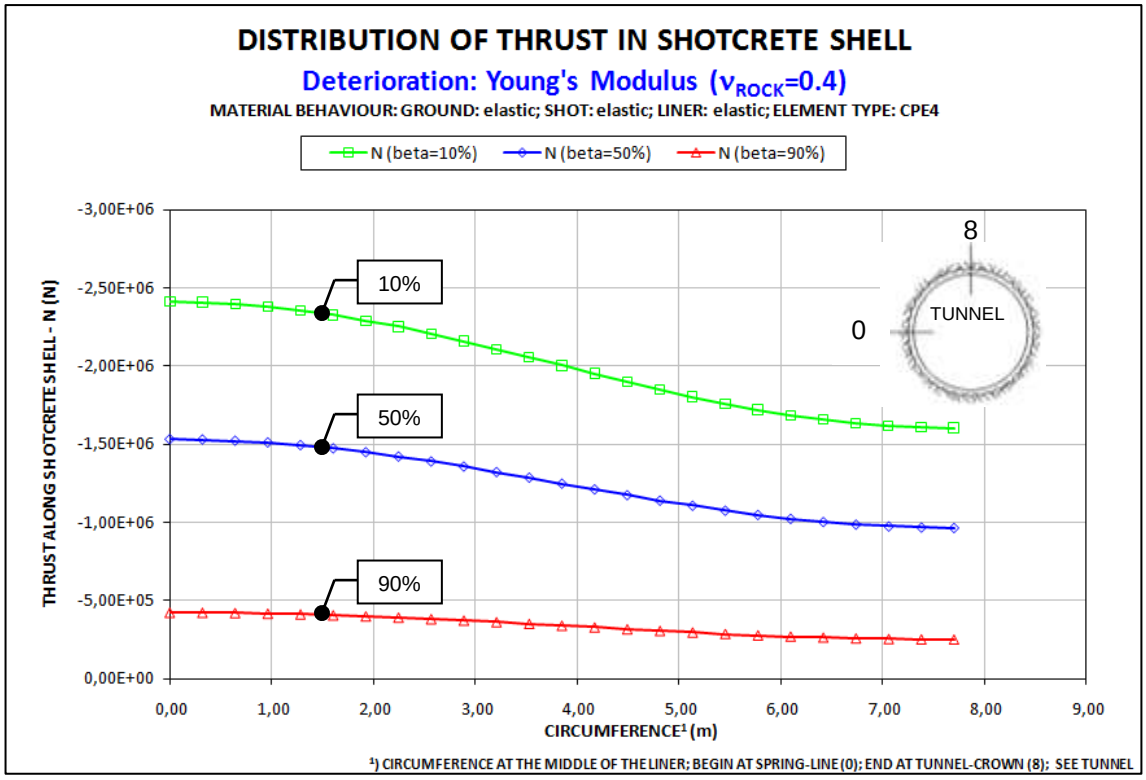

Fig. 53: Thrust along the circumference of the shotcrete shell for several deterioration steps (10%, 50%, 90%); deterioration caused by degradation of Young's modulus (Case A-1); results based on (C02)

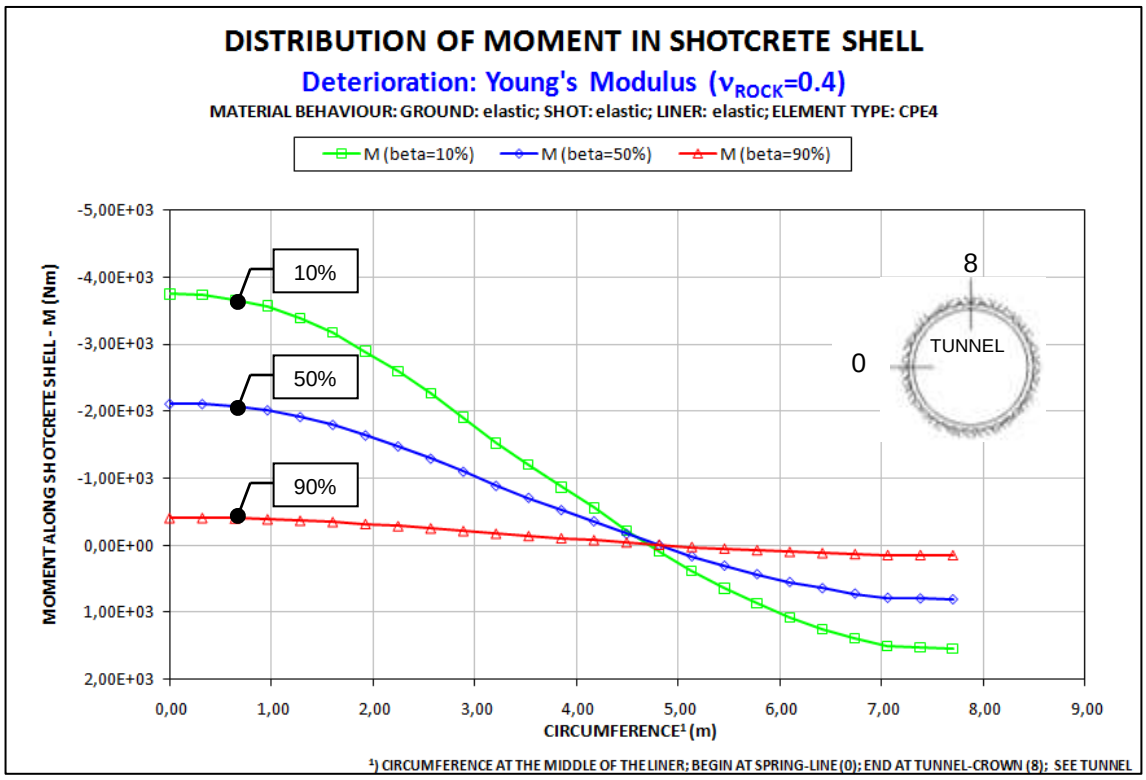

Fig. 54: Moments along the circumference o the shotcrete shell for several deterioration steps (10%, 50%, 90%); deterioration caused by degradation of Young's modulus (Case A-1); results based on (C02)

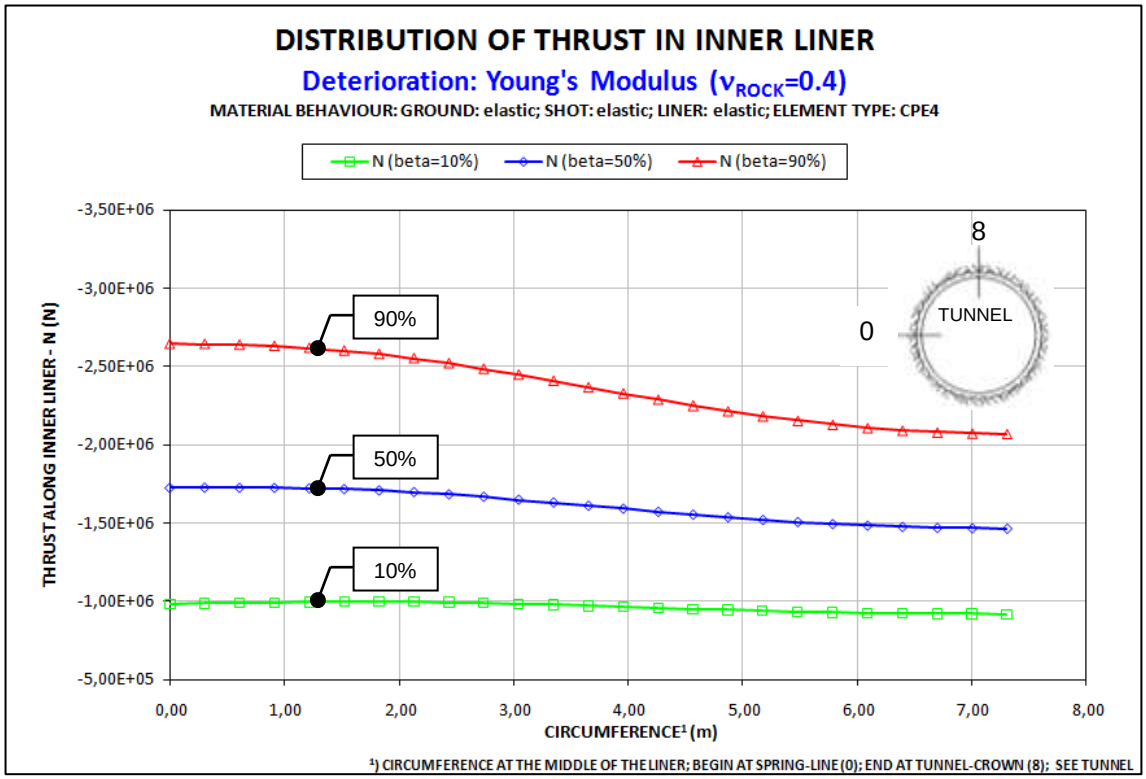

Fig. 55: Thrust along the circumference of the inner liner for several deterioration steps (10%, 50%, 90%); deterioration caused by degradation of Young's modulus (Case A-1); results based on (C02)

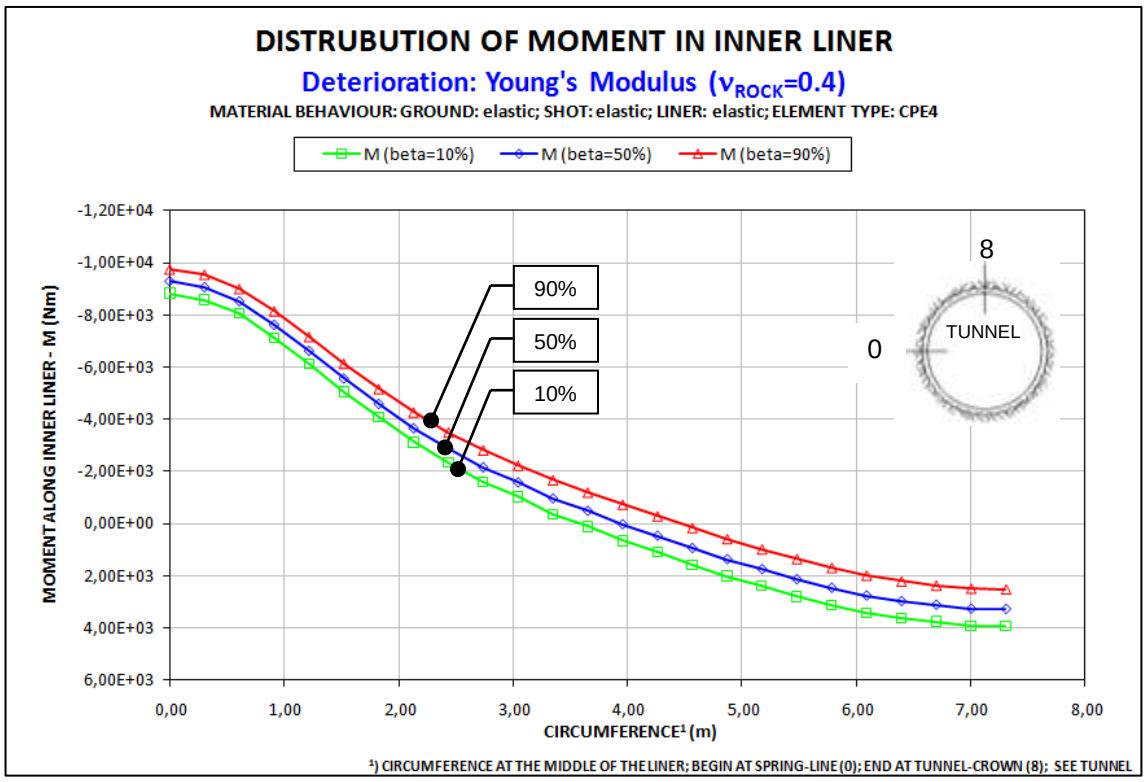

Fig. 56: Moments along the circumference o the inner liner for several deterioration steps (10%, 50%, 90%); deterioration caused by degradation of Young's modulus (Case A-1); results based on (C02)

4 CONCLUSION

4.1 Summary of Research Approach

The aim of the research was to build a model for Finite Element simulating the deterioration of the shotcrete shell and to find out how this affects the inner liner.

Simulation of the tunnel construction

Pre-displacements and support-delay are considered by the Load Reduction Method. The simulation of the placement of support elements can be done with four different methods, the Model Change Method, the Dummy Node Method, the Changing Stiffness Method and the Four Calculation Method. For this investigation the Four Calculation Method was chosen for the following reasons:

- Possibility for contact formulations between support elements is provided (i.e. Coulomb friction)
- Realistic behavior in terms of tangential stresses of the support elements can be obtained

(For details see chapter 2.5.4 and chapter 2.6.5)

Simulation of the effects of deterioration of shotcrete

Using this model (Four Calculation Method) in which stresses are introduced into the initial- and final support, a parametric study has been carried out. The investigation of the deterioration of the shotcrete shell was done by degradation of several material parameters such as the Young's modulus and the compressive strength.

The combinations of Finite Element types, material behavior and deterioration parameters were used:

- 4-node Finite Elements (CPE4) plus linear elastic material behavior (LE)
    - Deterioration of shotcrete by degradation:
        - Young's Modulus (E)
        - compressive strength (f_C)
        - Young's Modulus with compressive strength simultaneously (E & f_C)
- 4-node Finite Elements (CPE4) plus linearly elastic – perfectly plastic material behavior with a Coulomb failure criterion (LE-PP (C))
    - Deterioration of shotcrete by degradation:
        - Young's Modulus (E)
        - compressive strength (f_C)
        - Young's Modulus with compressive strength simultaneously (E & f_C)

- 8-node Finite Elements with reduced integration (CPE8R) plus linear elastic material behavior (LE)
    - Deterioration of shotcrete by degradation:
        - Young's Modulus (E)
        - compressive strength (f_C)
        - Young's Modulus with compressive strength simultaneously (E & f_C)

4.2 Interpretation and discussion

The major conclusions of this investigation are as follows:

Simulation of the tunnel construction:

To ensure load on the inner liner after the simulation of the tunnel construction process is finished (Step 8), the liner is included on a load reduction factor of β = 95%. (Fig. 57)
As a consequence of considering of the combined system "ground plus shotcrete shell plus inner liner" lower stresses in the shotcrete are obtained compared to only considering a combined system of "ground plus shotcrete shell" ("SCC" in Fig. 57).

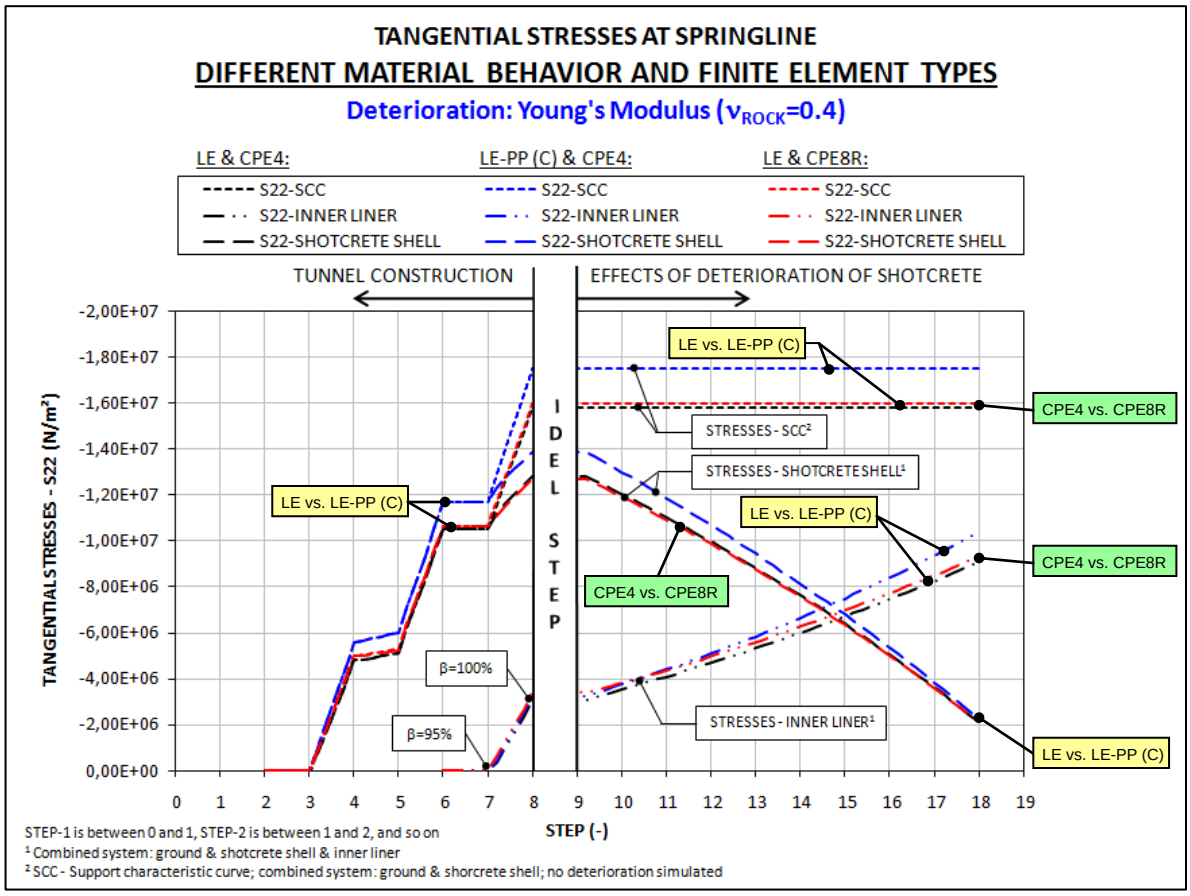

Fig. 57: Overview – tangential stresses at spring line in inner liner and shotcrete shell during the "tunnel construction" process and the "deterioration" process; deterioration caused by degrading the Young's modulus; different material behaviors and finite element types are compared; results based on (C02+C08+C14)

Simulation of the effects of deterioration of shotcrete

The effect of deteriorating material properties, E and f_C, was investigated separately and in combination. Thus, three different cases are considered.

Fig. 58 shows the load transfer of tangential stresses from shotcrete shell to inner liner for these three cases:

Case A-1: Deterioration of the Young's modulus (E)
Case A-2: Deterioration of the compressive strength (f_C)
Case A-3: Simultaneous deterioration of the Young's modulus and the compressive strength (E & f_C)

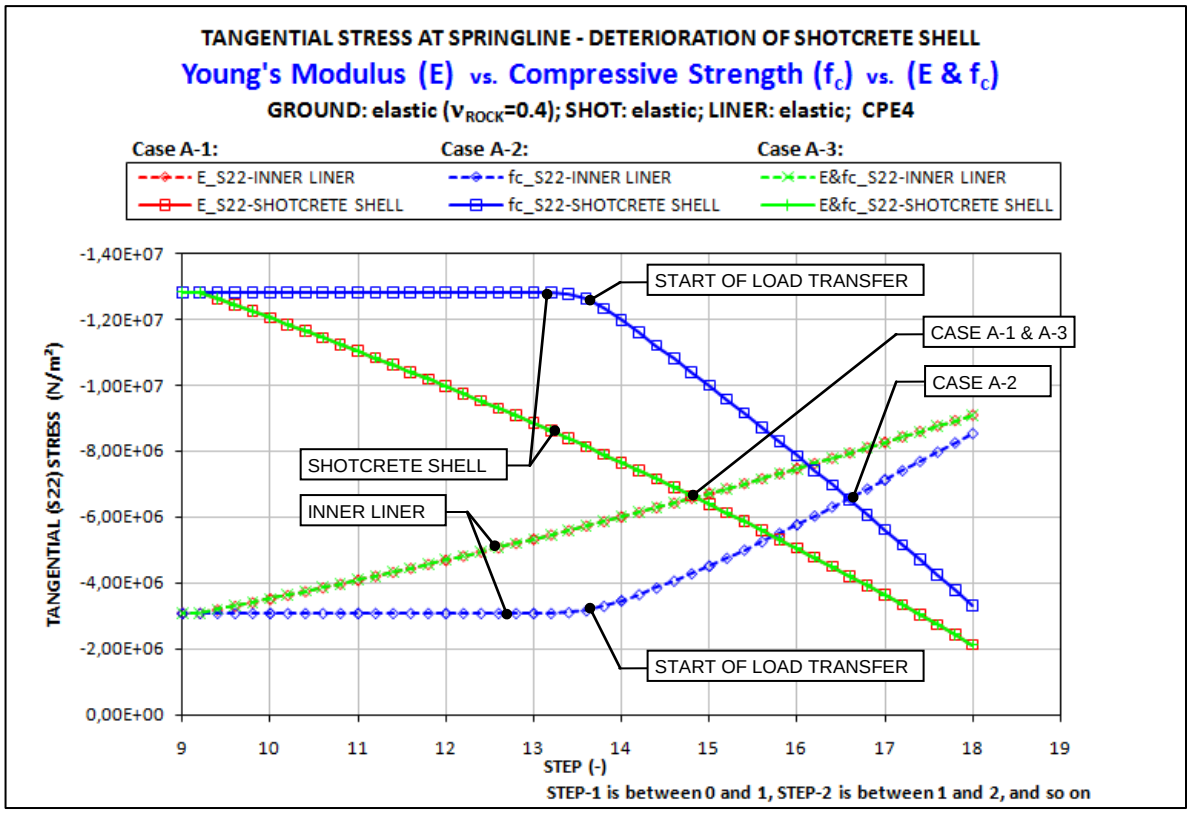

Fig. 58: Comparison of Cases A-1, A-2 and A-3; transfer of tangential stresses from shotcrete shell to inner liner caused by deterioration of the shotcrete; results based on (C02+C04+C06)

Exactly the same results were obtained from the combination (Case A-3) as from the deterioration of Young's modulus separately (Case A-1). Comparing the deteriorations which are caused by the degradation of E and f_C, one can observe that using f_C as deterioration-factor, the load transfer starts later and at a higher rate than using E as deterioration-factor. However, during deterioration, the stresses in the inner liner, which are caused by degrading the compressive strength of the shotcrete (Case A-2) are never higher than the stresses in the inner liner, which are caused by degrading the Young's modulus of the shotcrete (Case A-1). Moreover, the stresses in the shotcrete shell, which

are caused by degrading the compressive strength of shotcrete (Case A-2) are never higher than the stresses in the shotcrete shell, which are caused by degrading the Young's modulus of the shotcrete (Case A-1). Thus, one can speculate if the stresses in the inner liner or in the shotcrete shell, which are caused by degrading the compressive strength of the shotcrete (Case A-2) are higher than the stresses, which are caused by degrading the Young's modulus of the shotcrete (Case A-1), the compressive strength become the decisive factor for the combined case (Case A-3) and so the stresses of the combined case are exactly the same as the stresses, which are obtained by degrading the compressive strength (Case A-3 = Case A-2). Additional investigations are necessary to prove this.

The key features of the comparison of the deterioration-factors are:

- A superposition[4] in kind of stresses of the two deterioration factors, E and f_C, cannot be observed.
- Using the same deterioration-rate, the load-transfer, which is caused by the deterioration of the compressive strength, is faster than the load transfer, which is caused by the deterioration of the Young's modulus.
- The load transfer, which is caused by a deterioration of f_C can start with a delay[5].

Fig. 59 and Fig. 60 show the stress distribution along the circumference of the inner liner during deterioration of the shotcrete. Fig. 59 illustrates the stress distribution in the inner liner, which is caused by degrading the Young's modulus of the shotcrete and Fig. 60 shows the stress distribution in the inner liner, which is caused by degrading the compressive strength of the shotcrete. At 90% deterioration of the shotcrete both stress distributions (the one, which is caused by degrading the Young's modulus and the other one, which is caused by degrading the compressive strength) in the inner liner are approximately similar. The stresses in the inner liner at 90% deterioration of the shotcrete (Fig. 59), which is caused by degrading the Young's modulus, are slightly higher than the stresses in the inner liner at 90% deterioration of the shotcrete (Fig. 60), which are caused by degrading the compressive strength.

[4] Summation of stresses "(Case A-1) + (Case A-2) = (Case A-3)" cannot be observed.
[5] See Fig. 58: Load transfer, which is caused by degrading f_C starts between step-13 and step-14

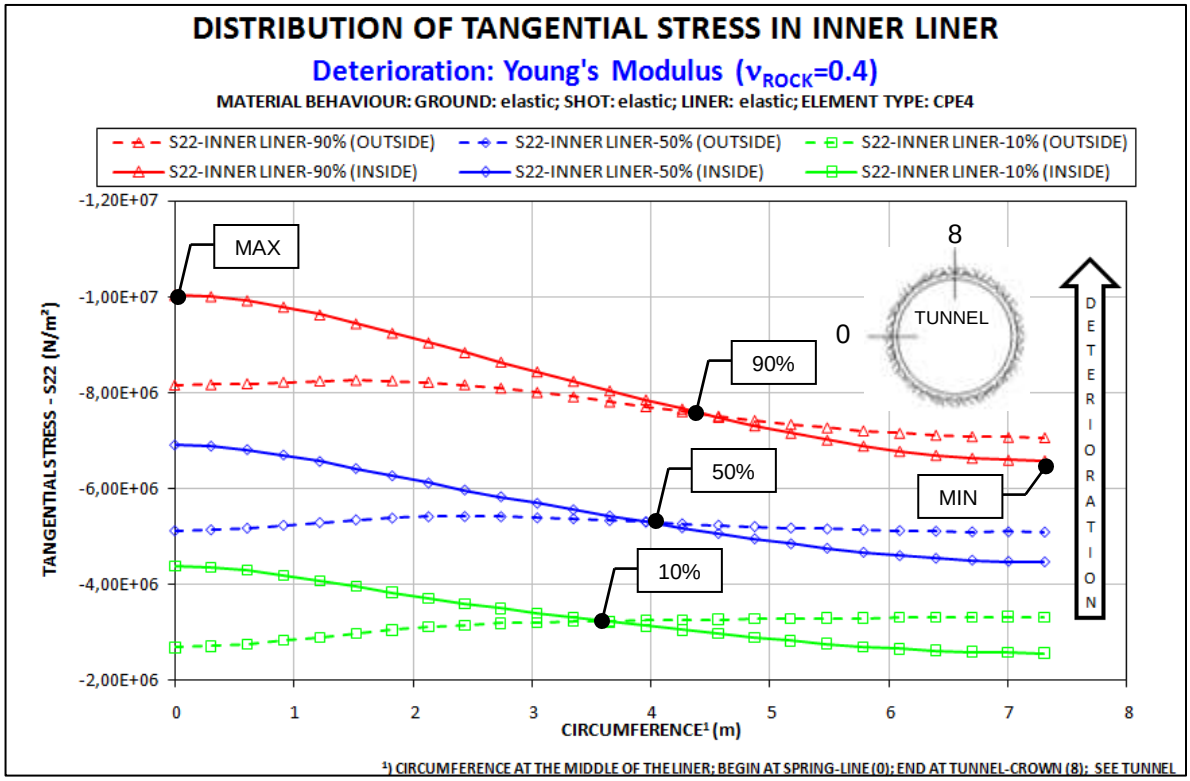

Fig. 59: Stresses at outside and inside along the circumference of the inner liner for several deterioration steps (10%, 50%, 90%); deterioration caused by degrading Young's modulus (Case A-1); results based on (C02)

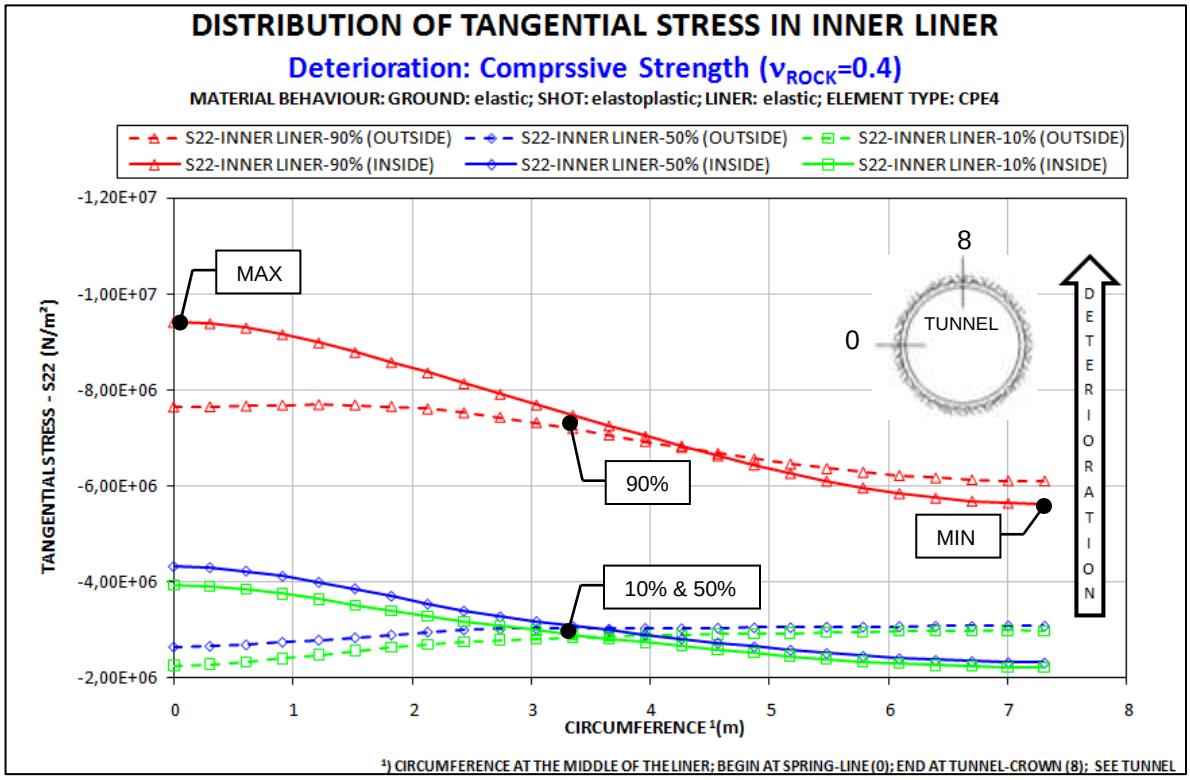

Fig. 60: Stresses at outside and inside along the circumference of the inner liner for several deterioration steps (10%, 50%, 90%); deterioration caused by degrading compressive strength (Case A-2); results based on (C04)

Generally, lateral earth-pressure-coefficients of K < 1.0 lead to tangential compressive-stresses in the liner, which are higher at the spring-line than at the tunnel-crown. In both cases (Case A-1 (Fig. 59) & Case A-2 (Fig. 60)), the maximum stresses after deterioration of the shotcrete are observed at the spring-line at the inner liner interior. Accordingly, the minimum stresses for both cases (Case A-1 & Case A-2) are observed at the tunnel-crown at the inner liner interior.

Fig. 61 compares the absolute values of the relative increase of the stresses in the inner liner with the absolute values of the relative decrease of the stresses in the shotcrete shell. The stresses were obtained at deterioration levels of 10% and 90% of the shotcrete. All investigated calculations (C01 to C18, see Table 5) are included in this scattergram. A linear relationship for all calculations can be observed, i.e. the increases of the stresses in the inner liner and decreases of the stresses in the shotcrete shell have a linear relationship.

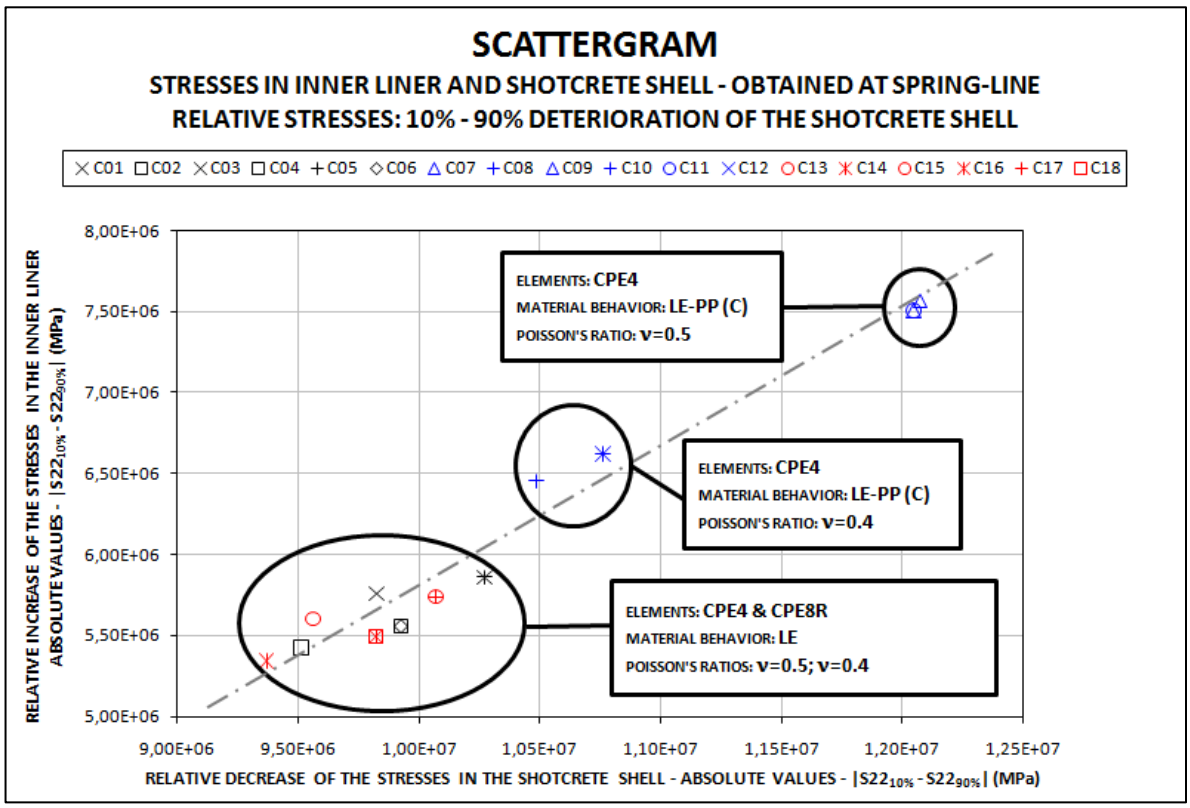

Fig. 61: Scattergram, absolute values of relative stresses in shotcrete shell and inner liner at a deterioration level of 10% and 90%; results based on (C01 to C18, see Table 5);

Other aspects

Fig. 57 illustrates that changing element types (“CPE4” vs. “CPE8R”) has only insignificant effects on the stresses in the support elements (shotcrete shell and inner liner) and Fig. 62 presents that changing element types (“CPE4” vs. “CPE8R”) has only insignificant effects in the displacements of the tunnel perimeter.

Furthermore, in Fig. 57 can be seen that changing material behavior (“LE” vs. “LE-PP (C)”) of the ground is affecting the stresses in the support elements. The best way to explain these effects is to consider the radial displacements of the tunnel perimeter at the spring-line during the “tunnel construction” and the “deterioration” processes (Fig. 62).

The main difference is that plastic deformation occurs during the “tunnel construction” process (Fig. 62), which caused higher tangential stresses in the shotcrete shell after the “tunnel construction” process (step-8, Fig. 57) using “LE-PP (C)” material behavior than using “LE” material behavior. Furthermore, one can observe that at the end of the “deterioration” process (step-18, Fig. 57), all stresses in the shotcrete shell are approximately similar (“LE” & “LE-PP (C)).

Concerning the stresses in the inner liner at the end of the “deterioration” process (step-18, Fig. 57), one can observe higher stresses using a linearly elastic – perfectly plastic material behavior instead of using a linear elastic material behavior. (Note that after the “tunnel construction” process, the stresses in the inner liner, which are obtained using a linear elastic material behavior, are approximately similar to the stresses which are obtained using a linearly elastic – perfectly plastic material behavior.)

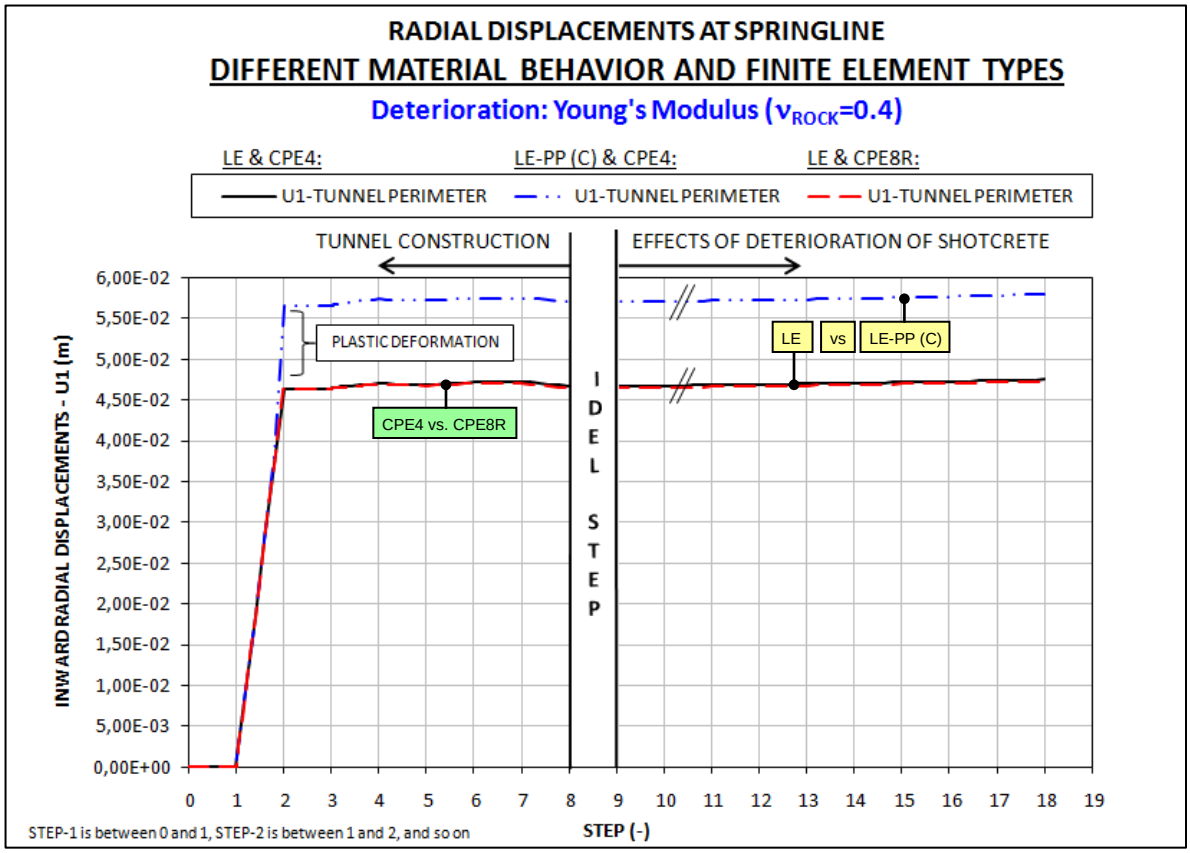

Fig. 62 Overview – inward radial displacements at the spring line of the tunnel perimeter during the “tunnel construction” process and the “deterioration” process; deterioration caused by degrading the Young’s modulus; different material behaviors and finite element types are compared; results based on (C02+C08+C14)

4.3 Recommendations for future work

Several potential areas of research can enhance the investigation of the deterioration of shotcrete presented in this thesis:

Deterioration of different components of the tunnel support system

It is very likely that not only the shotcrete is affected by deterioration. Also the contact between the ground and the shotcrete shell and the contact between the shotcrete shell and the inner liner can be affected. Further, the properties of the ground around the opening may change due to weathering. The material properties and load-bearing thickness of the inner liner might be reduced by environmental effects such as de-icing and salt corrosion. All of this should be considered in the main degradation processes and their effects on long-term stability of tunnels.

Variation of other parameters

The parametric study can be expanded to consider, for instance, different ground parameters and overburden as well as different thicknesses of the shotcrete shell and of the inner liner. Also varying the load reduction factors to simulate pre-displacements and support-delay might be useful.

Further developments of the numerical methods

The Four Calculation Method allow one to consider “contact friction” but not for divergent deformation behavior (Fig. 63). The Changing Stiffness Method can handle “contact friction” for divergent and convergent deformation behavior, but allow one not to obtain realistic behaviors in terms of displacements and in terms of stresses of the support elements during the simulation of the tunnel construction. Hence, these two methods have to be consequently further developed.

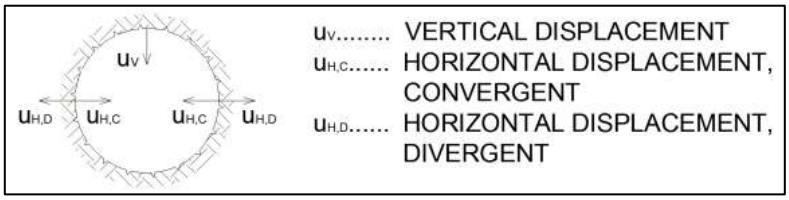

Fig. 63: Convergent and divergent deformation behavior

Improving the background knowledge about deterioration

Most importantly, the natural properties should be tested. Specimens of the support elements and the ground should be tested as or immediately after the tunnel is constructed, as well as after a time period of operation. It is also important that the specimens are obtained at the same locations and that the geology of the surrounding ground is known.

III. List of References

Bathe, K.-J. (1996). *Finite Elemente Procedure*. Ney Jersy: Prentice-Hall, Inc.

Baudendistel, M. (1979). Zum Entwurf von Tunnel mit großem Ausbruchsquerschnitt. *Rock Mechanics*, *8*, 75-100.

Bolton, M. D. (1986). The strength and dilatancy of sands. *Geotechnique*, *36*(1), 65-78.

Brinkgreve, R. B. J., & Veermeer, P. A. (2002). *PLAXIS 3D Tunnel, Version 8: General Information, Tutorial Manual, Reference Manual, Material Model Manual, Scientific Manual, Validation and Verification Manual* (8th ed.). Lisse/Abdingdon/Exton(PA)/Tokyo: A.A. Balkema Publishers.

Brosch, F. J. (1990). Anisotropy of dilation, 3-D stress state and the talobre friction cone. *Rock Mechanics and Rock Engineering*, *23*(2), 113-121.

DS 853. (2007). Richtlinie 853; Eisenbahntunnel planen, bauen und instand halten. Frankfurt am Main: Deutsche Bahn AG.

Einstein, H. H., Bobet, A., & Aristorenas, G. (1995). *Feasibility Study Opalinuston - Text and Appendix 1* (p. 234). Cambridge, MA: Massachusetts Institute of Technology.

Golser, H. (2008). BBT SE: Technischer Bericht, Geomechanische Planung, Zusammenfassende Darstellung. Retrieved from http://www.bmvit.gv.at/verkehr/eisenbahn/verfahren/bbt/bbt3b/index.html.

Golser, H., & Schubert, W. (2003). Application of numerical simulation at the tunnel site. In G. Beer (Ed.), *Numerical Simulation in Tunnelling* (pp. 427-474). Wien: Springer-Verlag.

Hibbitt, H. D., Karlson, K., & Sorenson, S. (2007). *ABAQUS Version 6.7: CAE User's Manual, Analysis User's manual, Example Problems Manual, Keyword Reference Manual, Theory Manual, User Subroutines Reference Manual*. Rhode Island: HKS Inc.

Laabmayr, F., & Swoboda, G. (1978). Beitrag zur Weiterentwicklung flachliegender Tunnelbauwerke im Lockergestein. In H. Lessmann (Ed.), *Moderner Tunnelbau bei der Münchner U-Bahn* (pp. 55-71). Wien - New York: Springer-Verlag.

Laabmayr, F., & Swoboda, G. (1986). Grundlagen und Entwicklung bei Entwurf und Berechnung im seichtliegenden Tunnel - Teil 1. *Felsbau*, *4*(3), 138-143.

Lombardi, G. (1973). Dimensioning of Tunnels Linings with regards to Construction Procedure. *Tunnels & tunnelling*, *5*(4), 340-351. Progressive Media Markets, Ltd.

Marcher, T., & Jiricny, F. (2004). Interaction of primary lining and final lining of a NATM tunnel with respect to relevant long-term effects. *Winter Workshop of Rock Mass Mechanic*. Poland.

Meißner, H. (1996). Tunnelbau unter Tage, Empfehlungen des Arbeitskreises "Numerik in der Geotechnik" der Deutschen Gesellschaft für Erd- und Grundbau e.V. *Numerik in der Geotechnik*.

Möller, S. (2006). *Tunnel induced settlements and structural forces in linings*.

Möller, S. C., Krajewski, W., & Wawrzyniak, C. (2010). Bemessung von Tunnelbauwerken in bindigem Boden - Erfahrung mit unterschiedlichen Stoffgesetzen. *Felsbau magazin*, *1*, 70-79.

Pacher, F. (1964). Deformationsmessungen in Versuchstollen als Mittel zur Erforschung des Gebirgsverhalten und zur Bemessung des Ausbaues. *Felsmech Ingenieursgeol Suppl IV*, 149-161.

Panet, M. (1976). *la mècanique des roches - appliquèe aux ouvrages du gènie civil* (p. 235). Lyon: Association Amicale des Ingènieurs.

Panet, M. (1978). Stability Analysis of a Tunnel driven in a Rock Mass in tracking account of the Post-Failure Behavior. *Rock Mechanics*, *Vol. 8*(1), 209-223.

RVS 9.32. (2004). Tunnel - Statisch Konstruktive Richtlinien, Geschlossene Bauweise im Lockergestein unter Bebauung. Wien.

Sandrone, F., & Labiouse, V. (2009). Analysis of the evolution of road tunnels equilibrium conditions with a convergence–confinement approach. *Rock Mechanics and Rock Engineering*, *43*(2), 201-218.

Schwartz, C. W., & Einstein, H. H. (1980). *Improved Design of Tunnel Supports: Volume 1 - Simplified Analysis for Ground-Structure Interaction in Tunneling* (p. 450). Cambridge, MA: Massachusetts Institute of Technology.

Zachow, R. (1995). Dimensionierung zweischaliger Tunnel im Fels auf der Grundlage von in-situ-Messungen. *Forschungsergebnisse aus dem Tunnel- und Kavernenbau der Universität Hannover*. Hannover: Rokahr R. B.

ÖVBB. (2004). Richtlinie Spritzbeton. Wien.